

TSUNAMI HAZARD ANALYSIS FOR GÜLLÜK BAY

A THESIS SUBMITTED TO  
THE GRADUATE SCHOOL OF NATURAL AND APPLIED SCIENCES  
OF  
MIDDLE EAST TECHNICAL UNIVERSITY

BY

SENA ACAR

IN PARTIAL FULFILLMENT OF THE REQUIREMENTS  
FOR  
THE DEGREE OF MASTER OF SCIENCE  
IN  
CIVIL ENGINEERING

JANUARY 2015



Approval of the thesis:

**TSUNAMI HAZARD ANALYSIS FOR GÜLLÜK BAY**

submitted by **SENA ACAR** in partial fulfillment of the requirements for the degree of **Master of Science in Civil Engineering Department, Middle East Technical University** by,

Prof. Dr. Gülbin Dural Ünver  
Dean, Graduate School of **Natural and Applied Sciences** \_\_\_\_\_

Prof. Dr. Ahmet Cevdet Yalçiner  
Head of Department, **Civil Engineering** \_\_\_\_\_

Prof. Dr. Ahmet Cevdet Yalçiner  
Supervisor, **Civil Engineering Department, METU** \_\_\_\_\_

**Examining Committee Members:**

Prof. Dr. Ayşen Ergin  
Civil Eng. Dept., METU \_\_\_\_\_

Prof. Dr. Ahmet Cevdet Yalçiner  
Civil Eng. Dept., METU \_\_\_\_\_

Prof. Dr. Ayşen Dener Akkaya  
Statistics Dept., METU \_\_\_\_\_

Assoc. Prof. Dr. Utku Kanoğlu  
Engineering Sciences Dept., METU \_\_\_\_\_

Assist. Prof. Dr. Gülizar Özyurt Tarakcıoğlu  
Civil Eng. Dept., METU \_\_\_\_\_

**Date: 26.01.2015**

.....

**I hereby declare that all information in this document has been obtained and presented in accordance with academic rules and ethical conduct. I also declare that, as required by these rules and conduct, I have fully cited and referenced all material and results that are not original to this work.**

Name, Last name : Sena Acar

Signature :

## **ABSTRACT**

### **TSUNAMI HAZARD ANALYSIS FOR GÜLLÜK BAY**

Acar, Sena

M.Sc., Department of Civil Engineering

Supervisor: Prof. Dr. Ahmet Cevdet Yalciner

January 2015, 113 pages

The deterministic and probabilistic tsunami hazard analysis is one of the primary issues for disaster management and the determination mitigation strategies. Güllük bay (Turkey) located in southern Aegean Sea is selected as the study region to evaluate the effects of probable tsunami waves in the region. The critical structures in Güllük bay are aquaculture facilities, commercial port, marinas, airport and small size waterfront structures at touristic centers. The seismic and non-seismic sources are processed using the available data. The estimated rupture parameters of seismic sources and dimensional parameters of non-seismic sources are used in simulations in deterministic approach. The seismic data based on seismic monitoring between 1950-2014 is used and the earthquake magnitudes which may occur in 100, 500, 1000 years return periods are computed statistically by extreme value analysis in probabilistic approach. The related rupture parameters have been determined due to the rupture parameters measured in past earthquakes in the region.

Tsunami simulations due to selected rupture parameters of different return periods are performed by using tsunami numerical code NAMI DANCE. The near shore tsunami parameters (maximums of water elevations, current velocities, momentum fluxes, discharge fluxes, flow depth) are computed. Simulation results for each tsunami scenario are compared, discussed and presented in regard to tsunami hazard analysis for Güllük bay.

Keywords: Tsunami, Güllük bay, NAMI DANCE, Tsunami Hazard Analysis, Extreme Value Statistics, Deterministic, Probabilistic.

## ÖZ

### GÜLLÜK KÖRFEZİ'NDE TSUNAMİ RİSK ANALİZİ

Acar, Sena

Yüksek Lisans, İnşaat Mühendisliği Bölümü

Tez Yöneticisi: Prof. Dr. Ahmet Cevdet Yalçın

Ocak 2015, 113 sayfa

Deterministik ve olasılıksal tsunami risk analizi, afet yönetimi ve hasarların azaltılmasına yönelik stratejiler belirlenirken gerekli olan birincil konular arasında yer almaktadır. Olası tsunami etkilerinin değerlendirilmesi için Ege Denizi'nin güneyinde yer alan Güllük Körfezi (Türkiye) çalışma alanı olarak seçilmiştir. Güllük Körfezi'ndeki kritik yapılar; su ürünleri tesisleri, ticari liman, marinalar, hava alanı ve turistik bölgelerde yer alan küçük kıyı yapılarıdır. Mevcut veriler kullanılarak sismik ve sismik olmayan tsunami kaynakları değerlendirilmiştir. Sismik tsunami kaynakları için tahmin edilen fay kırılma parametreleri ile sismik olmayan tsunami kaynaklarının boyutlu parametreleri deterministik yaklaşım simülasyonlarında kullanılmıştır. Olasılıksal yaklaşımda, ekstrem değer analizi ile 1950-2014 yılları arasında ölçülmüş deprem büyüklükleri kullanılarak; 100, 500 ve 1000 yıllık dönüş periyotlarındaki deprem büyüklükleri istatistiksel olarak hesaplanmıştır. Bölgedeki eski depremlerin ölçülen değerleri kullanılarak ilgili fay kırılma parametreleri belirlenmiştir.

NAMI DANCE sayısal tsunami kodu kullanılarak seçilen fay kırılma parametreleri kullanılarak tsunami simülasyonları yapılmıştır. Yakın kıyı parametreleri (en büyük su yükseklikleri, anlık hızlar, momentum akışları, debi akışları, su derinlikleri) hesaplanmıştır. Güllük Körfezi'ndeki tsunami risk analizi için bütün tsunami senaryolarının simülasyon sonuçları karşılaştırılmış, tartışılmış ve sunulmuştur.

Anahtar kelimeler: Tsunami, Güllük Körfezi, NAMI DANCE, Tsunami Risk Analizi, Ekstrem Değer İstatistikleri, Deterministik, Olasılıksal.



To my beloved family and  
To people who make me feel loved...

## **ACKNOWLEDGEMENTS**

I would like to express my very great appreciation to supervisor Prof. Dr. Ahmet Cevdet Yalçınır not only for his wide knowledge background and experiences he shared but also for his invaluable support, encouragement and patience throughout thesis studies.

I feel so lucky to meet and work with the staff of the Coastal Engineering Research Center. I would also like to extend my thanks to all staff that they present me a great perspective on coastal issues, and they make me feel as a part of Coastal and Harbor Engineering's lovely family.

Special thanks to my parents for their priceless love, encouragement, support and patience. My special thanks are extend to the people that make me feel loved and great.

This thesis study is partially supported by European Union Projects, ASTARTE (Assessment, Strategy and Risk Reduction for Tsunamis in Europe).

## TABLE OF CONTENTS

ABSTRACT .....	V
ÖZ .....	VII
ACKNOWLEDGEMENTS .....	X
TABLE OF CONTENTS .....	XI
LIST OF TABLES .....	XIII
LIST OF FIGURES .....	XV
CHAPTERS	
1 INTRODUCTION.....	1
2 LITERATURE REVIEW.....	3
3 METHODOLOGY .....	13
4 TSUNAMI HAZARD ANALYSIS FOR GÜLLÜK BAY .....	17
4.1 Description of the Study Region .....	17
4.2 Data Processing for Güllük Bay .....	21
4.3 Tsunami Numerical Modeling.....	23
4.3.1 Estimation of seismic tsunami sources for Güllük bay (deterministic approach) .....	25
4.3.2 Simulations of probable seismic tsunami source case .....	31
4.3.3 Estimation of probable non-seismic tsunami sources for Güllük bay	35
4.3.4 Simulations of probable non-seismic tsunami sources case .....	39
4.4 Estimation of seismic tsunami sources according to 100, 500 and 1000 years return periods for Güllük bay (probabilistic approach) .....	58
4.4.1 Extreme value statistics .....	61
4.4.2 Poisson Distribution.....	65
4.4.3 Determination of rupture parameters for seismic source (s18- z22) according to 100, 500 and 1000 years return periods.....	68

4.4.4	Simulations of probable seismic tsunami sources according to 100, 500 and 1000 years return periods.....	75
5	DISCUSSION OF RESULTS AND CONCLUSIONS .....	95
6	REFERENCES.....	101
7	APPENDIX A .....	111

## LIST OF TABLES

### TABLES

<b>Table 4.1:</b> Boundary coordinates of nested domains in Güllük bay for seismic source case .....	23
<b>Table 4.2:</b> Boundary coordinates of nested domains in Güllük bay for non-seismic source case .....	23
<b>Table 4.3:</b> Tsunami Source Parameters (TRANSFER Work Packages, 2009).....	27
<b>Table 4.4:</b> The Estimated Rupture Parameters and Initial Sea State of Selected Tsunami Source s18-Z22 .....	29
<b>Table 4.5:</b> The Estimated Rupture Parameters and Initial Sea State of Selected Tsunami Source s07-Z11-1 .....	30
<b>Table 4.6:</b> The Estimated Rupture Parameters and Initial Sea State of Selected Tsunami Source s10-Z12-1 .....	30
<b>Table 4.7:</b> The Estimated Rupture Parameters and Initial Sea State of Selected Tsunami Source s11-Z12-2 .....	30
<b>Table 4.8:</b> The Estimated Rupture Parameters and Initial Sea State of Selected Tsunami Source s12-Z14 .....	31
<b>Table 4.9:</b> The Estimated Rupture Parameters and Initial Sea State of Selected Tsunami Source s35 .....	31
<b>Table 4.10:</b> The Estimated Rupture Parameters and Initial Sea State of Non-seismic Source Scenario-1 (Caldera Collapse of Santorini) .....	38
<b>Table 4.11:</b> The Estimated Rupture Parameters and Initial Sea State of Non-seismic Source Scenario-2 (Caldera Collapse of Columbus) .....	38
<b>Table 4.12:</b> The Estimated Rupture Parameters and Initial Sea State of Non-seismic Source Scenario-3 (Caldera Eruption of Columbus) .....	38
<b>Table 4.13:</b> X-Y coordinates and depths of selected numerical gauge points .....	49
<b>Table 4.14:</b> Computed near shore tsunami parameters for "Didim-Tekağaç" .....	51

<b>Table 4.15:</b> Computed near shore tsunami parameters for "Fish farms" .....	53
<b>Table 4.16:</b> Computed near shore tsunami parameters for "Güllük" .....	55
<b>Table 4.17:</b> Computed near shore tsunami parameters for "Yalıkavak" .....	57
<b>Table 4.18:</b> Characteristics of distribution functions for extreme value analysis...	63
<b>Table 4.19:</b> Constants $\alpha$ , $\beta$ of unbiased plotting position formula .....	64
<b>Table 4.20:</b> Magnitude-frequency analysis according to Gutenberg–Richter law..	66
<b>Table 4.21:</b> Probable earthquake magnitudes with 100, 500 and 1000 years return periods according to Poisson distribution .....	67
<b>Table 4.22:</b> Empirical relationships between $M_w$ and $\log(L, W, A)$ .....	69
<b>Table 4.23:</b> Computed rupture parameters ( $L, W, u$ ) from $M_w$ with different empirical relationships .....	70
<b>Table 4.24:</b> Domain B with its boundary coordinates for probabilistic approach ..	71
<b>Table 4.25:</b> The estimated rupture parameters for seismic source (s18-z22) according to 100, 500 and 1000 years return periods .....	74
<b>Table 4.26:</b> The estimated rupture parameters and initial sea state of seismic tsunami source (s18-z22) according to 100 years return period .....	74
<b>Table 4.27:</b> The estimated rupture parameters and initial sea state of seismic tsunami source (s18-z22) according to 500 years return period .....	75
<b>Table 4.28:</b> The estimated rupture parameters and initial sea state of seismic tsunami source (s18-z22) according to 1000 years return period .....	75
<b>Table 4.29:</b> Computed near shore tsunami parameters for "Didim Tekağaç" .....	87
<b>Table 4.30:</b> Computed near shore tsunami parameters for "Fish Farms" .....	89
<b>Table 4.31:</b> Computed near shore tsunami parameters for "Güllük" .....	91
<b>Table 4.32:</b> Computed near shore tsunami parameters for "Yalıkavak".....	93
<b>Table 5.1:</b> Summary table of tsunami hazard analysis with maximum positive wave amplitudes for numerical gauge points according to selected tsunami sources .....	97
<b>Table 5.2:</b> Summary table of tsunami hazard analysis with maximum current velocities for numerical gauge points according to selected tsunami sources.	97
<b>Table A.1:</b> Rupture parameters of historical earthquakes in project region (Kalafat et al., 2009).....	109

## LIST OF FIGURES

### FIGURES

<b>Figure 3.1:</b> Flowchart of modeling stages.....	13
<b>Figure 4.1:</b> Location of the study region with Google Earth satellite images .....	18
<b>Figure 4.2:</b> Some of critical locations for tsunami hazard analysis in Güllük bay .	19
<b>Figure 4.3:</b> Fish farms located in Güllük bay ( <a href="http://www.cevrehukuk.com">http://www.cevrehukuk.com</a> ) .....	20
<b>Figure 4.4:</b> Nested domains in Güllük bay for seismic source case .....	22
<b>Figure 4.5:</b> Nested domains in Güllük bay for non-seismic source case .....	22
<b>Figure 4.6:</b> General view of topography and bathymetry of the Eastern Mediterranean Sea, distribution of earthquake epicenters since 1900 and main fault zones in Eastern Mediterranean region (Black dots represent the earthquake with the magnitude between 4 and 6; Red Stars indicate the earthquakes with the magnitude of greater than 6. ellipsoids show the possible tsunami generation regions) (Yalciner et al., 2008).....	26
<b>Figure 4.7:</b> Sea states at different time steps ( $t=30, 60, 120, 150, 180$ and $240$ min) in Domain D according to seismic source (s18-z22) .....	33
<b>Figure 4.8:</b> Tsunami parameters due to tsunami source s18-z22 according to simulation duration of 240 min .....	34
<b>Figure 4.9:</b> Generation of a caldera eruption/collapse due to volcanic eruption ....	36
<b>Figure 4.10:</b> Location of volcanic arc on Google Earth satellite images.....	37
<b>Figure 4.11:</b> Sea states at different time steps ( $t=60, 90, 120, 150, 180$ and $240$ min) in Domain D according to caldera collapse of Santorini.....	40
<b>Figure 4.12:</b> Tsunami parameters due to 300m caldera collapse of Santorini according to simulation duration 300 min .....	41
<b>Figure 4.13:</b> Sea states at different time steps ( $t=60, 90, 120, 150, 180$ and $240$ min) in Domain D according to caldera collapse of Columbus.....	43

<b>Figure 4.14:</b> Tsunami parameters due to 100m caldera collapse of Columbus according to simulation duration 300 min .....	44
<b>Figure 4.15:</b> Sea states at different time steps (t=60, 90, 120, 150, 180 and 240 min) in Domain D according to caldera eruption of Columbus.....	46
<b>Figure 4.16:</b> Tsunami parameters due to 100m caldera eruption of Columbus according to simulation duration 300 min .....	47
<b>Figure 4.17:</b> Locations of selected numerical gauge points in Domain D.....	49
<b>Figure 4.18:</b> Wave characteristics for gauge point "Didim-Tekağaç" .....	50
<b>Figure 4.19:</b> Wave characteristics for gauge point "Fish Farms" .....	52
<b>Figure 4.20:</b> Wave characteristics for gauge point "Güllük" .....	54
<b>Figure 4.21:</b> Wave characteristics for gauge point "Yalıkavak".....	56
<b>Figure 4.22:</b> Location of plates and seismic dynamisms in Turkey .....	58
<b>Figure 4.23:</b> Seismic activity in Turkey and surrounding area.....	60
<b>Figure 4.24:</b> Epicenters of the earthquakes with the magnitudes $M > 3$ and in southern part of Aegean Sea between 1950-2014 years (+ symbols show $3 < M < 3.99$ , x symbols show $4 < M < 4.99$ , • symbols show $5 < M < 5.99$ , red star symbols show $M > 7$ ).....	60
<b>Figure 4.25:</b> Results of extreme value statistics for probable earthquake magnitudes ( $M_w$ ) in the study region with different return periods .....	65
<b>Figure 4.26:</b> Gutenberg-Richter relationship for earthquake magnitude ( $M_w$ ).....	66
<b>Figure 4.27:</b> Tsunami parameters due to tsunami source s18-z22 with $45^\circ$ rake angle according to simulation duration of 240 min .....	72
<b>Figure 4.28:</b> Tsunami parameters due to tsunami source s18-z22 with $-45^\circ$ rake angle according to simulation duration of 240 min .....	73
<b>Figure 4.29:</b> Sea states at different time steps (t=30, 60, 120, 150, 180 and 240 min) in Domain B according to s18-z22 with 100 years return period .....	77
<b>Figure 4.30:</b> Tsunami parameters due to tsunami source s18-z22 according to 100 years return period for simulation duration of 240 min.....	78
<b>Figure 4.31:</b> Sea states at different time steps (t=30, 60, 120, 150, 180 and 240 min) in Domain B according to s18-z22 with 500 years return period .....	80
<b>Figure 4.32:</b> Tsunami parameters due to tsunami source s18-z22 according to 500 years return period for simulation duration of 240 min.....	81



<b>Figure 4.33:</b> Sea states at different time steps (t=30, 60, 120, 150, 180 and 240 min) in Domain B according to s18-z22 with 1000 years return period.....	83
<b>Figure 4.34:</b> Tsunami parameters due to tsunami source s18-z22 according to 1000 years return period for simulation duration of 240 min .....	84
<b>Figure 4.35:</b> Wave characteristics for gauge point "Didim-Tekağaç" .....	86
<b>Figure 4.36:</b> Wave characteristics for gauge point "Fish Farms" .....	88
<b>Figure 4.37:</b> Wave characteristics for gauge point "Güllük" .....	90
<b>Figure 4.38:</b> Wave characteristics for gauge point "Yalıkavak" .....	92



## CHAPTER 1

### INTRODUCTION

The term "Tsunami" started to be known in various languages soon after the Japanese calls regarding to damages of Great Meiji Tsunami occurred in 1896. Structure of this word formed of "tsu" and "nami" words where "tsu" means giant, "nami" means wave in Japanese. A tsunami is a huge wave (or series of waves) generated by an undersea earthquake, volcanic eruption, landslide. In undersea earthquake based tsunami generation mechanism, energy of the rupture is transferred to the water particles and causes rise in the sea level over the affected area. Transmission of the energy generates and propagates tsunami from source location as long waves.

Earthquake and tsunami history indicates that the dense population, coastal utilization, marine protected and marine aquaculture areas are vulnerable under tsunami motion. Ports, harbors and marinas are some of the vulnerable plants under tsunamis as well as coastal ecosystems and aquaculture areas. However all coastal facilities are the critical and those must be resilient against natural hazards in order to facilitate recovery operations.

2004 Indian Ocean tsunami was one of the deadliest and largest natural hazard all over the world. 'Tsunami risk reduction' issue has come into prominence after this disaster (Lovholt et al., 2014). Since 2004, six megathrust tsunamis happened in Indonesia, Samoa, Chile and Japan in 2006, 2007, 2009, 2010 and 2011. An undersea earthquake with magnitude 9.0 occurred in Pacific coast of Tohoku, Japan in 2011. The earthquake is named as "Great East Japan Earthquake" by being the most powerful earthquake ever recorded in Japan and fifth most powerful

earthquake in the world since 1900. Transmission of the energy caused giant tsunami waves that reached 40 meters in Miyako. The tsunami caused nuclear explosions primarily in Fukushima Daiichi Nuclear Power Plant Complex. There has thousands of death/injuries, collapsing of many buildings, structural damages on roads and railways with total economic loss of US\$235 billion according to the World Bank's estimation. This cost makes the Great East Japan Earthquake as the costliest natural disaster in the world from past to present.

Overall world, tsunamis mostly occur in Pacific Ocean. Despite tsunamis in oceans and open seas, there are great number of tsunami records in the Mediterranean and Aegean Sea due to undersea earthquakes, landslides and volcanic eruptions in this region.

The purpose of this thesis is numerical modeling of tsunami with accurate bathymetry/topography data and estimated rupture parameters by using NAMI DANCE tsunami simulation tool in Güllük bay (Turkey) to analyze behavior of tsunami. Tsunami inundation maps provide visualization of hazard zones and development of mitigation strategies according to these maps.

Surfer 12 software is used as data processing and mapping tool, NAMI DANCE code is used as computational tool in this thesis. The input data were collected from different sources. Analysis of estimated tsunamis in Güllük bay was done by convenient computational tools. Study region will be directly affected from tsunamis in Aegean Sea and Mediterranean. Inundation maps with maximum wave amplitudes and risk management in the study region will be the final product of this thesis.

Chapter 2 includes literature survey. Purpose of this thesis and methodology are explained in Chapter 3. Data processing and estimation of rupture parameters with related simulation results are given in Chapter 4. Chapter 4 includes analysis and discussion of numerical modeling results. Thesis is ended with general evaluation and conclusion with Chapter 5.

## CHAPTER 2

### LITERATURE REVIEW

Tsunami inundation modeling can be mainly divided into three parts as i) analytical investigations on tsunamis ii) numerical simulation of tsunamis iii) preparation of inundation maps.

A remarkable amount of increase is seen in tsunami hazard analysis and inundation mapping studies after the 2004 Indian Ocean Tsunami. Site-specific studies with modeling of run-up are done in local based. Studies should be developed in global scale. Lovholt et al. (2011) completed a first global tsunami hazard study with effects on population. Main purpose of the study is to develop an easy and strong model that can obtain consistent and reliable maximum water elevations in the tsunami affected zones. Plane wave linear hydrostatic transect simulations are mainly based on this method with validation of the standard run-up model results. The global hazard study is focused on megathrust earthquakes to reveal effects of the largest events. Non-seismic based tsunamis are not included. Inundation maps are prepared according to selected tsunami scenarios and findings from literature. Number of people that affected from tsunami are specified according to inundation maps by using the Landscan population data set.

Flouri et al. (2011) includes seismic-based tsunami hazard analysis for the Greek island of Rhodes in the southeast Aegean Sea. MOST software is used in simulations with accurate bathymetry and topography data for analysis of inundation in the study region. Worst case scenarios are developed according to seismic events. Simulation results include maximum water elevation, maximum flow depth, inundation zones for the study region with time periods of 100, 500 and

1000 years. Visualization of the inundation are done with combination of the modeling results and satellite images in two-dimensional plane.

Geist and Lynett (2014) indicates the importance of the tsunami hazard assessment with results of largest natural hazards 2004 Indian Ocean and 2011 Japan tsunamis. Probabilistic tsunami hazard assessment (PTHA) should provide estimation of all tsunami generation mechanisms. Although, earthquake-based tsunami sources were estimated initially, recent studies consider submarine landslide tsunami sources in PTHA. Correlation between landslide area and landslide volume with mean return period is not an easy task due to lack of information. These uncertainties and wide range of landslide failure types reduce the accuracy of tsunami generation mechanism. Further studies should be done to enhance and solve these problems in PTHA methods.

Balas and Ergin (2000) indicates that tsunami risk should be included for coastal structures in addition to wave characteristics, tidal range, storm surge, wave set-up, surf beat and structural system parameters. REBAD (Reliability Model) is built up to evaluate risk assessment according to tsunami for breakwaters. SORM (Second Order Reliability Method) was applied to observe the safety of Haydarpaşa Port (Sea of Marmara, Turkey). Tsunami waves have a larger return period according to storm waves with high level of risk. Failure of structure does not seem to occur according to tsunami effect for Haydarpaşa port. However, tsunami risk may be very important according to occurrence probability of a large seismic tsunami source.

Probabilistic tsunami inundation maps were developed firstly by Gonzalez et al. (2009). Probabilistic tsunami hazard assessment (PTHA) correlates tsunami modeling and probabilistic seismic hazard assessment (PSHA). The methodology is applied to Seaside, Oregon with the estimation of 100 and 500 years occurrence probability of maximum wave amplitudes. According to evaluations for 100 and 500 year tsunami, PTHA gives representative results for risk management. PTHA provides a technique for identification of tsunami hazard probabilities, then it may be combined with vulnerability and degree of hazards of tsunami risk.

Numerical modeling of tsunamis has very important role not only on visualization of generation, propagation, coastal amplification, inundation of tsunamis but also generating the supportive database of inundation for the disaster management. Basic equations for numerical simulations are dispersive (Boussinesq type) and nondispersive (nonlinear form of shallow water equations) equations that are used in numerical studies (Tinti, 1994; Synolakis, 1994; Imamura, 1995; Titov, 1994; Yalciner et al., 2001).

There are numerous numerical models which solves tsunami behavior from source to targets. Some of these tools are described in the following. Some of these tools are: TSUNAMI CEA/DASE, TsunamiClaw, Coulwave, COMCOT, UBO-TSUF&UBO-TSUF-VB, UBO-TSUF, TSUNAMI-SKREDP, 1HD, H2D, DPWAVES, GLOBOUSS, C3 Tsunami Model, MOST, TUNAMI N1, N2 and NAMI DANCE. Information about these numerical codes are taken from the Deliverable D5.8 of EU Funded TRANSFER Project Work Package 5. (TRANSFER, 2009).

TSUNAMI CEA/DASE<sup>©</sup> is developed by *Atomic Energy Commissariat (CEA)* and *France's Geophysical Laboratory (LDG)* for research and operational objects. The model is fully tested and certified. Nonlinear shallow water equations and finite difference method are used in the model. Okada elastic displacement and any surface deformation can be generated. FORTRAN language is used in development of the model. The model is used in tsunami scenarios in French Polynesia, Pacific Ocean, Indian Ocean and Mediterranean Sea.

TsunamiClaw<sup>©</sup> is developed by *University of Washington (USA)*. Nonlinear shallow water equations, finite volume, Riemann solvers as numerical themes and 2D+1 rectangular mesh with adaptive rectification are used in the model. Wetting and drying is allowed. Multi segment fault model and any surface deformation are the source for the model. The model can use six nested levels and mesh with adaptive refinement can be observed. Fortran 77 is used as programming language

and operating systems are Unix, Linux. The model is used for tsunami propagation and inundation in Sumatra.

Coulwave<sup>®</sup> is developed by *Texas A&M University (USA)* and validation of the model is done with benchmark problems. Finite volumes, fourth order, implicit, domain decomposition of Boussinesq equations, MPS numerical schemes and cartesian mesh type are used in the model. Wetting and drying is allowed. Breaking of waves can be obtained in the model. Fortran 90 is used as programming language with a command driven/batch run user interface. Inundation Science and Engineering Cooperative and TRANSFER partners are used the model. The physical and numerical tsunami simulations for Seaside, Oregon are compared using the Lidar-measured laboratory beach and Coulwave and STOC numerical models to see the effect of macro-roughness and sharp topographic changes.

COMCOT<sup>®</sup> is developed by *Cornell University (USA)*. The model is tested and validated by benchmark problems with analytical, experimental and field data. Shallow water wave equations, finite difference method and leap-frog scheme method are used in the model. Selection of coordinate system (cartesian or spherical) is allowed and nested grids are used in the model. Submarine landslide, seismic fault and any surface deformation can be used as the source of tsunami generation. The model is efficient and accurate. Selection of tsunami generation mechanism is an advantageous feature for the model. FORTRAN 90 is used as programming language. The model is used for modeling of wave generation, propagation, run-up and inundation.

UBO-TSUFD and UBO-TSUFD-VB<sup>®</sup> are developed by *Università di Bologna, Dip. di Fisica, Settore Geofisica (Italy)*. Shallow water wave equations are used in the model. Rectangular constant grid domain with cartesian and geographical coordinates are combined with finite difference and leap frog scheme methods as numerical scheme. Bathymetric effects are corrected by computing multi-fault vertical co-seismic displacements using Okada's equations. FORTRAN 90/95 is used as programming language. The model is applied in tsunami scenarios in



Sumatra tsunami (2004), Java tsunami (2006), the Mediterranean Sea, the Indian Ocean.

UBO-TSUFE<sup>©</sup> is also developed by *Università di Bologna, Dip. di Fisica, Settore Geofisica (Italy)*. Shallow water wave equations are used in the model. Finite element method and two step time integration methods are used as the numerical scheme. Constant boundary grid domain are combined with triangular components and cartesian coordinate system. The model computes multi-fault vertical co-seismic displacements using Okada's equations for the case of a seismic source.

UBO-TSUIMP<sup>©</sup> computes impulses due to particle movements. In the model, energy loss due to the interactive relation between the boundaries and sea bottom is obtained. Coriolis effect is also included. The model is applied in tsunami scenarios in the Mediterranean Sea (tsunami scenarios in the Adriatic Sea for historical data, Ionian Sea, Tyrrhenian Sea, Izmit bay (1999) seismic-based tsunami, tsunami scenarios in the Gulf of Corinth), in the Indian Ocean (Sumatra (2004), Java (2006) etc.).

TSUNAMI-SKREDP<sup>©</sup> is developed by *Norwegian Geotechnical Institute (NCG) (Norway)*. The model is fully tested (grid refinement, feature assessments, comparison of the results with different codes) and certified. Shallow water wave equations are used in the model. Finite difference, second order, explicit methods are used as the numerical scheme. Initial sea level changes, defined tsunami generation source mechanisms as landslides and earthquakes or source data files are the main input for the model. FORTRAN 77 is used as programming language with a Norwegian user interface. The model is applied in North East Atlantic, Arctic Ocean, Norwegian Fjords, Mediterranean, Indian Ocean, South China Sea, hydropower purposed reservoirs in Norway, the Philippines.

1HD<sup>©</sup> is developed by *Department of Mathematics, University of Oslo/ICG (Norway)*. The model is fully tested (grid refinement, feature assessments, comparison of the results with different codes, check against benchmark problems

and analytical solutions). Boussinesq equations and full potential theory are used as equation type. Finite difference and element method, boundary integral method, Eulerian and Lagrangian coordinates are used as numerical schemes and combined with adaptable mesh grid. In the model, grid resolution assessment is necessary. Dispersive and non-linear effects are included in generation and propagation of tsunami. FORTRAN 77 is used as programming language, Unix, Linux are operating systems with mixed language user interface. The model is used in tsunami scenarios in North East Atlantic, Arctic Ocean, Norwegian Fjords, Indian Ocean, Mediterranean by University of Oslo, NGI and ICG.

H2D<sup>©</sup> is developed by *Universidad de Cantabria (Spain)*. Shallow water wave equations are used in the model. Finite difference and implicit alter direction methods are used as numerical scheme. Upwind are used for the advective methods. Cartesian coordinate system is combined with rectangular quadratic cells as grid type. Gaussian hump is the generation model. Coriolis, nonlinear advection, bottom friction, horizontal eddy viscosity, wetting and drying are regarded in the model. FORTRAN 77 is used as programming language. The model is applied in Mediterranean Sea, Algerian, Alboran Sea.

DPWAVES<sup>©</sup> is developed by *Norwegian Geotechnical Institute, ICG*. Validation of the model is done for basin oscillations and solitary waves. Implicit second order finite element method are used as numerical scheme with adaptive mesh grid. Wetting and drying is not allowed in the model. Adaptive meshes provide flexibility. Diffpack (C++) is used as programming language, Unix, Linux are operating systems. The model is applied in Indian Ocean, Paleo Barents Sea for research purposes, and Norwegian Fjords for risk assessment by NGI.

GLOBOUSS<sup>©</sup> is developed by *Department of Mathematics, University of Oslo/ICG (Norway)*. The model is tested (grid refinement, comparison of the results with different codes, analytical solutions). Boussinesq equations with Coriolis effects are used in the model. Finite differences method, implicit method and ADI iteration method for implicit equations are combined with Arakawa C grid, geographical and

Cartesian coordinates. Wetting and drying is not allowed in the model. The code is sufficient for dispersive transoceanic propagation. FORTRAN 77 is used as programming language, Unix, Linux are operating systems with an English user interface. The model is applied in wide range of oceanic areas by University of Oslo, NGI and ICG.

C3 model is developed by *Universidad de Cantabria (Spain)*. Validation of the model is done by using benchmark problems. Shallow water wave equations are used in the model. Finite difference method with leap-frog scheme method and finite volume method applied in inundation zones, and these numerical schemes are combined with Cartesian/spherical coordinate system and embedded grids. Wetting and drying is allowed in this model. Okada 1985 is selected as generation model for co-seismic tsunamis. C3 model includes most profitable properties of COMCOT model and TSUNAMICLAW model. The model is using hybrid finite difference-finite volume method that provides efficient and accurate results. FORTRAN 90 is used as programming language, Windows, Linux are the operating systems. Input data files can be entered to the model. The model is applied in the Cadiz test area as part of TRANSFER project.

MOST (Method of Splitting Tsunamis) is developed by *National Oceanographic Atmospheric Administration NOAA/Pacific Marine Environmental Laboratory*. The model is used for tsunami prediction in real time for the Pacific Ocean. 246 tsunami model scenarios for unit sources are involved in the model which represent active subduction zones around Pacific Ocean. It stores all simulation data for each unit solution, including amplitudes and velocities for each offshore location (Titov, 2005).

Estimated seismic source parameters and measured tsunami data are used to define pre-computed generated and propagated tsunami database. The model compares scenarios and observed database, and selects best matched linear combination. This property enables estimation of tsunami parameters in deep water which can be used as source of a tsunami in inundation for a specified region.

Tsunami propagation and inundation are analyzed for two huge tsunamis occurred in Sunda in 1797 and 1833 with MOST model by Borrero et al. (2006). Inundation distance are found as relevant with bathymetry and topography according to Synolakis et al. (2009). Presented inundation maps for Southern California are prepared by MOST model in their articles.

Numerical Analysis Model for Investigation of Near-field tsunamis No.1., TUNAMI-N1<sup>©</sup> is developed by Prof. Fumihiko Imamura et al. in *Disaster Control Research Center in Tohoku University (Japan)* in 1991 as a part of Tsunami Inundation Modeling Exchange (TIME) Project using FORTRAN programming language. The model is improved to TUNAMI-N2<sup>©</sup> which defines the tsunami source parameters by using seismic rupture characteristics and solves nonlinear shallow water equations and compute/analyze generation, propagation and coastal amplification of tsunamis due to the inputted rupture parameters and or tsunami sources. The model computes all necessary parameters to analyze behavior of tsunami in shallow and inundation zones. The water elevations and depth averaged velocities at selected time intervals in the study domain and time series of these parameters at selected locations are the main outputs of TUNAMI-N2<sup>©</sup>. In the computation the bottom friction is also considered. The solution is performed for the irregular shaped bathymetry by using finite difference method which provides sufficient accuracy in simulation results. TUNAMI-N2 is used in lots of studies such as Shuto, Goto and Imamura (1990), Goto and Ogawa (1992), Imamura (1995), Goto et al. (1997), Yalciner et al. (2001, 2002).

NAMI DANCE is developed in C<sup>++</sup> programming language with same computational procedure used in TUNAMI-N2 by Russian and Turkish scientists. Non-linear form of shallow water wave equations are used in the model to obtain simulation results in shorter time with less error. Finite difference method and leap-frog scheme method are used as numerical scheme. The model can compute propagation of the wave in all locations even on shallow water or on land for a specified region.

TUNAMI-N3 is developed by *Disaster Control Research Center, Tohoku University (Japan)* and *Ocean Engineering Research Center, Middle East Technical University (METU) (Turkey)*. Nonlinear form of shallow water wave equations are used in the model. Finite difference method and leap frog scheme method are used as numerical scheme. Faults ruptures are based on Okada, Manshinha & Smyle during generation of the model. Tsunami generation, propagation and run-up in nested grid domains are the main features of the model. FORTRAN is used as programming language, Dos, Windows or UNIX are the operating systems for the model. The model has been used in wide range of oceans and seas in worldwide such as Sumatera Tsunami (1833), Krakatau Tsunami (1883), Sumatera Tsunami (1935), Flores Tsunami (1992), East Java Tsunami (1994), Toli-toli Tsunami (1996), Biak Tsunami (1996), North Banggai Tsunami (2000), Aceh Tsunami (2004), South Java Tsunami (2006), Caribbean Sea and tsunami scenarios for Fethiye and Pylos, Haydarpassa harbor, Güllük bay.

In this thesis, tsunami hazard analysis for Güllük bay (southwest of Turkey) according to estimated seismic and non-seismic sources with deterministic and probabilistic approach are explained in the following sections.



## CHAPTER 3

### METHODOLOGY

Modeling of a tsunami and inundation mapping process need accurate, reliable data and computational tools. Bathymetry/topography data and rupture parameters are the necessary data for modeling. In addition to those data, validation and verification of computational tools also must be done. Computational tool models the tsunami by using the input data. Analysis results of the numerical modeling are the base data for inundation mapping. Flow chart of the methodology is shown in Figure 3.1.

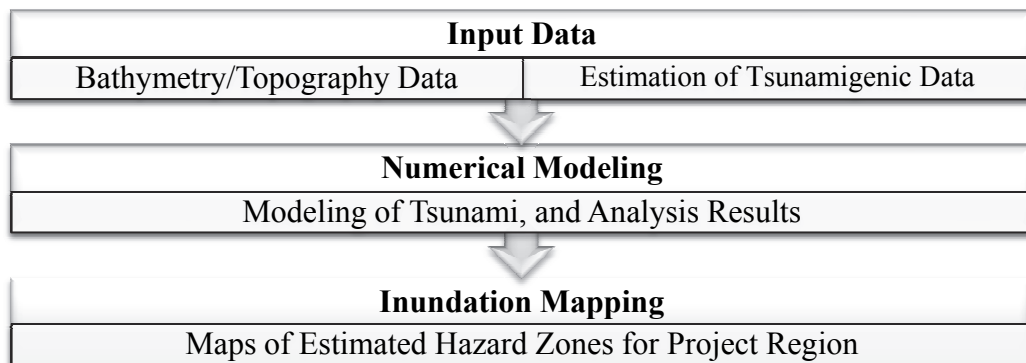


**Figure 3.1:** Flowchart of modeling stages

Following phases were followed during the thesis:

Phase 1: Literature survey on the historical tsunamis

- i) The historical time that tsunami reports and records covered
- ii) Reliability of the historical documents should be evaluated. Verification of this information can be done from the respective publications or catalogues.

iii) Using the collected data of historical events, run-up heights and inundation distances should be estimated.

#### Phase 2: Processing of the data

Reliability of the bathymetric and topographic data with highest resolution is the most important parameter in accurate modeling. Data should be collected from satellite images, navigational charts, field measurements (if available), existing maps. Additional digitization would be needed to perform in order to improve the quality of the shoreline data. By merging all available data in essential data format, the digital form of the bathymetry/topography data for a study region must be obtained.

#### Phase 3: Estimation of tsunami source data for deterministic approach

Tsunamis are generated by several types of mechanisms such as landslides, seismic activities, volcanic activities and other types of energy input the water medium. Type of the tsunami generation mechanisms and their characteristics must be determined at the first stage. This is not an easy task and needs cooperation between professionals from different disciplines in order to reduce the uncertainties in the source parameters. Near field and far field submarine faults, submarine landslide features and volcanic activities must be examined in order to select the credible worst case tsunami scenario(s) for the study region in deterministic approach.

#### Phase 4: Estimation of tsunami source data for probabilistic approach

The data of earthquake magnitudes and ruptures is obtained from the instrumental database of seismic monitoring. This data is used in statistical analysis for probabilistic approach. Extreme value statistics is performed to determine the extreme values of the earthquake magnitudes in regard to selected return periods. Rupture parameters are also defined according to their relations with magnitude.



#### Phase 5: Computation of the tsunami source parameters

Using the estimated rupture parameters the related tsunami sources must be computed. Numerical modeling tool can directly compute the tsunami source, if not user must compute and define the tsunami source by the help of estimated rupture parameters. The tsunami source of selected scenarios must be shown with figures.

#### Phase 6: Selection of nested domains for numerical modeling of tsunami

Nested study domains that represents the study region must be determined. Grid size of each domain must be determined according to the capacity of software and hardware. Bathymetry and topography data of each domain in sufficient accuracy and their required digital format must be used in numerical tools. The shoreline data used in the model must fit well with the real shoreline is one of the main requirements.

#### Phase 7: Simulation and computation of estimated tsunami parameters

Initial condition of the numerical modeling tool is the tsunami source. It is computed from rupture parameters (from Phase 4). Tsunami source and the bathymetry/topography data (from Phase 6) are used in numerical tools to simulate tsunami behavior from generation to coastal regions. The main tsunami parameters at the study region are computed for each simulation.

#### Phase 8: Preparation of inundation map for the study region

The temporal changes of these parameters are plotted for selected locations (critical structures). The spatial distributions of maximums of these tsunami parameters (from Phase 7) are also plotted for each simulation in the study region. The inundation maps developed from the distributions of maximum elevations in the region and maximum flow depth at land (inundation areas). The hazard zones in the study regions can be determined from these maps. Those are also used as one of

the input to risk assessment, development of mitigation strategies and disaster management.

## CHAPTER 4

### TSUNAMI HAZARD ANALYSIS FOR GÜLLÜK BAY

In this chapter, brief information about study region, data processing, estimation of seismic and non-seismic tsunami sources according to deterministic approach and tsunami modeling simulations are given. This chapter includes the first three parts which given in methodology.

#### 4.1 Description of the Study Region

Güllük bay is located in southeast of Aegean Sea of Turkey. The location of the study region is given in Figure 4.1. Güllük bay is formed basically by four large natural coves and many small bays and inlets. Local industries are mainly based on fish farming for sea bass and bream, and the export of bauxite from the recently relocated harbor on the outskirts of Güllük. Furthermore, Güllük bay is one of the seven largest gulfs and bays on the west coast of Turkey and contributes about 80% of countries' aquaculture production. Public port and nearby private piers in Güllük bay has a capacity of handling over 5 million tons of cargo per year. Milas Bodrum Airport is located at the end of Güllük bay on a low elevation area. Figure 4.2 shows some of the main critical regions in Güllük bay.

The bay and the surroundings have attracted special attention recently due to the negative environmental impact, such as high levels of turbidity, landscape modification, or rapid biodiversity change. Subsequently, the general public awareness on the conservation of the natural environment has been increasing,

arguing that all of these most likely originated from the increasing number of fish farming and aquaculture plants.

The fish farms are vulnerable against external effects mainly against storm, long wave action and sudden change of water temperature and concentration of suspended sediment. When long waves are considered any low level tsunami may even be destructive to the coastal utilities and aquaculture. According the historical information the area is subjected to tsunamis generated by seismic and volcanic sources. Since the tsunami and aquaculture has not been studied previously, the risk level of aquaculture facilities under the tsunami motion is uncertain. Within this direction, the tsunami effects mainly on the aquaculture industry and on coastal structures and settlements shall be studied. The general layout of fish farms (aquaculture facilities) is shown in Figure 4.3.

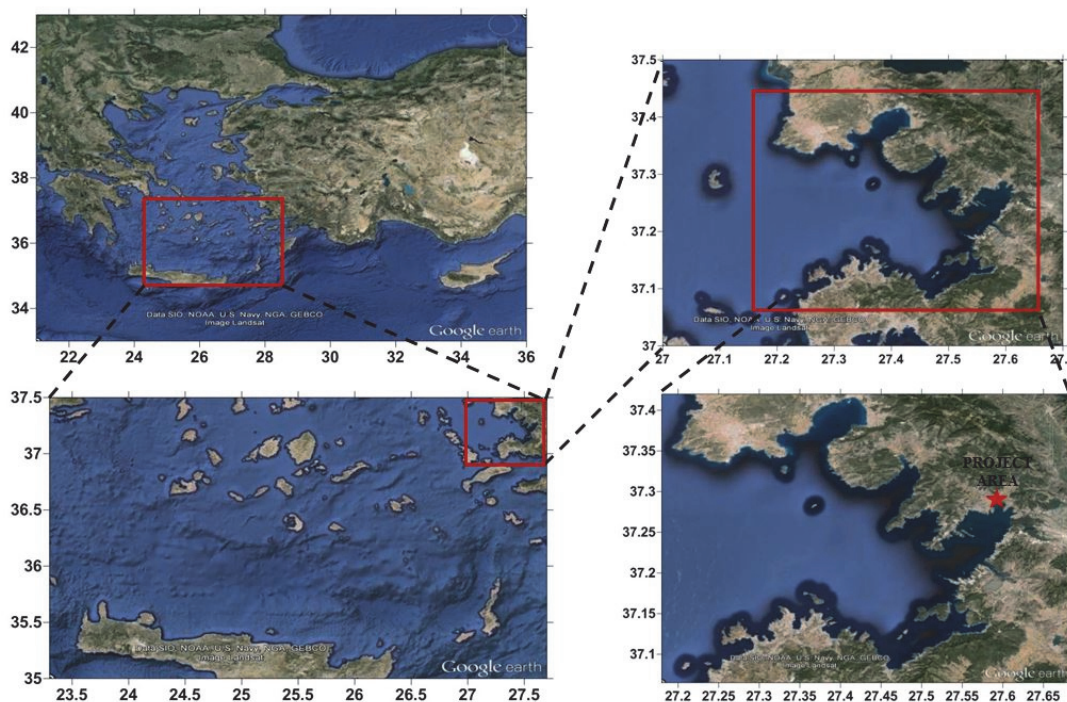


**Figure 4.1:** Location of the study region with Google Earth satellite images



Panaromic view of Güllük bay



Commercial port in Güllük bay



Milas Bodrum Airport on the low land area at the end of Güllük bay



Small inlet at Bogazici Village in Güllük bay



Fish farms in Güllük bay

**Figure 4.2:** Some of critical locations for tsunami hazard analysis in Güllük bay



**Figure 4.3:** Fish farms located in Güllük bay (<http://www.cevrehukuk.com>)

The boundary coordinates of the study region (Güllük bay) are determined as 35 E, 23.3 N and 37.5 E, 35 N in GCS\_WGS84 coordinate system.

Historical tsunamis may guide the modeler to select and input the tsunami scenarios. Historical documents and geological investigations have shown that earthquakes, submarine landslides, volcanic eruptions and tsunamis were common disastrous events occurred in Mediterranean and Aegean Sea for many years.

In this thesis, seismic and non-seismic tsunami sources are investigated and used in numerical modeling in regard to tsunami hazard analysis for Güllük bay. Seismic tsunami sources and related simulations are given in Section 4.3.1 and 4.3.2, non-seismic tsunami sources and related simulations are given in Section 4.3.3 and 4.3.4.

## 4.2 Data Processing for Güllük Bay

In this study the high resolution bathymetry is processed using the available data from the local and international sources. Collection of bathymetry/topography data with 30 sec (900m grid size) resolution from GEBCO<sup>®</sup> (General Bathymetric Chart of the Oceans) of the British Oceanographic Data Centre. Collection of topography data with 30m resolution from ASTER satellite from the web site at <http://gdex.cr.usgs.gov/gdex/>.

The available data is sufficiently accurate at the bay. The resolution of the bathymetry data is 30m at land and 900m in the sea. In order to improve quality of the shoreline data in the region of Güllük bay, additional digitization has been performed and those are merged into the available XYZ data.

After combining all data, the gridded data sets for different domains are developed by using commercial software SURFER<sup>®</sup> version 12. Kriging method was used to obtain nested domain's contours. Kriging method fits a mathematical function to a specified number of points with autocorrelation. This feature gives more accurate results during interpolation process.

The grid size of largest domain named Domain B was chosen as 270m. The boundary of smaller domain should contain in the previous larger domain and the smaller domain's grid size should have one-third of the previous larger domain in NAMI DANCE nested domain analysis. As a result of this principal, the grid sizes of Domains C and D are 90m and 30m respectively.

There has two different nested domain sets for seismic and non-seismic tsunami sources. Nested domains for seismic case and non-seismic case are represented in Figure 4.4 and Figure 4.5, respectively. The boundary coordinates of these domains are given in Table 4.1 and Table 4.2, respectively.

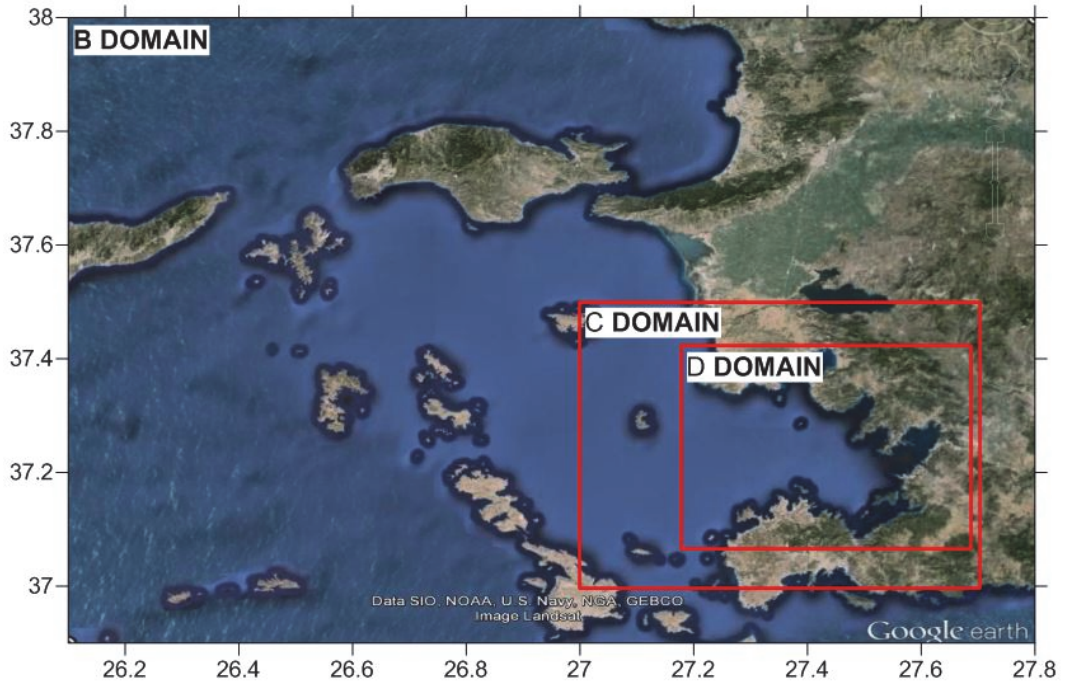


**Figure 4.4:** Nested domains in Gulluk bay for seismic source case

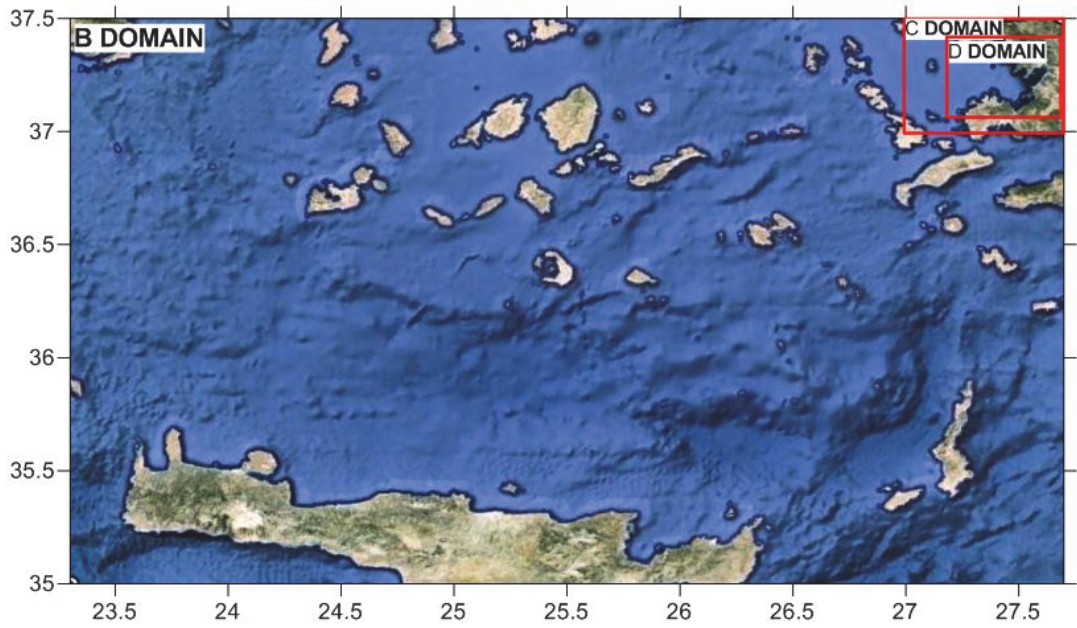


**Figure 4.5:** Nested domains in Gulluk bay for non-seismic source case



**Table 4.1:** Boundary coordinates of nested domains in Güllük bay for seismic source case

Domain Name	Left Longitude (°)	Right Longitude (°)	Bottom Latitude (°)	Top Latitude (°)	Resolution (m)
<b>B</b>	26.1 E	27.8 E	36.9 N	38.0 N	270
<b>C</b>	27 E	27.7 E	37 N	37.5 N	90
<b>D</b>	27.18 E	27.685 E	37.065 N	37.42 N	30

**Table 4.2:** Boundary coordinates of nested domains in Güllük bay for non-seismic source case

Domain Name	Left Longitude (°)	Right Longitude (°)	Bottom Latitude (°)	Top Latitude (°)	Resolution (m)
<b>B</b>	23.3 E	27.7 E	35 N	37.5 N	270
<b>C</b>	27 E	27.7 E	37 N	37.5 N	90
<b>D</b>	27.18 E	27.685 E	37.065 N	37.42 N	30

### 4.3 Tsunami Numerical Modeling

Numerical modeling with the estimation of tsunami sources provide computation and visualization of generation, propagation and inundation of tsunamis. Tsunami simulation will be more accurate and reliable with validated and verified numerical modeling tool and reliable data (rupture parameters, bathymetry/topography data). Numerical modeling tools solve similar equations with different techniques for tsunami simulation. Non-linear shallow water equations with friction term are widely used equation in tsunami modeling. Those equations are given below:

$$\frac{\partial \eta}{\partial t} + \frac{\partial M}{\partial x} + \frac{\partial N}{\partial y} = 0 \quad (1)$$

$$\frac{\partial M}{\partial t} + \frac{\partial}{\partial x} \left( \frac{M^2}{D} \right) + \frac{\partial}{\partial y} \left( \frac{MN}{D} \right) + gD \frac{\partial \eta}{\partial x} + \frac{k}{2gD^2} M \sqrt{(M^2 + N^2)} = 0 \quad (2)$$

$$\frac{\partial N}{\partial t} + \frac{\partial}{\partial x} \left( \frac{MN}{D} \right) + \frac{\partial}{\partial y} \left( \frac{N^2}{D} \right) + gD \frac{\partial \eta}{\partial y} + \frac{k}{2gD^2} N \sqrt{(M^2 + N^2)} = 0 \quad (3)$$

$\eta$ : water surface elevation,

$M, N$ : discharge fluxes in  $x$  and  $y$  direction respectively,

$D$ : water depth,

$h$ : undisturbed basin depth,

$k$ : bottom friction coefficient

Tsunami models solve Nonlinear form of Shallow Water Equations by using selected tsunami scenarios such as i) the credible worst case scenario(s) in deterministic approach and ii) selected scenarios with selected probabilities that should create maximum runup and inundation in the offshore. The maps of tsunami parameters are the main outputs of the tsunami numerical models. In this thesis, worst case scenarios and probabilistic scenarios with different return periods are identified and simulated. The results are used in tsunami hazard analysis. In simulations the tsunami numerical model NAMI DANCE is used.

NAMI DANCE is developed in C<sup>++</sup> programming language with same computational procedure used in TUNAMI-N2 by Russian and Turkish scientists (<http://namidance.ce.metu.edu.tr/pdf/>)

In the first step, the parameters of different tsunami (seismic, volcanic, landslide based or other) sources should be defined. Locations and characteristics of seismic and non-seismic tsunami sources that can affect Güllük region are identified. This is not an easy task, and much discussion is needed with experts for evaluating and considering uncertainties. In the following section the estimation of tsunami source parameters are presented.

#### **4.3.1 Estimation of seismic tsunami sources for Güllük bay (deterministic approach)**

Co-seismic tsunamis are triggered by rupture of fault plane. The rupture parameters are epicenter of the earthquake, focal depth, dimensions of the fault plane, slip displacement, strike, dip and rake angles.

Location of the sources of historical tsunamis are not definite. But the available information of tsunami history can guide the researchers to estimate the probable source locations. The current seismological data of seismic monitoring can certainly help the researchers to estimate the locations of the probably large magnitude earthquakes and hence the probable locations of the tsunami sources. These rupture parameters of the earthquakes at the locations of these sources can be evaluated and credible worst case scenarios can be determined.

Cita et al. (1996), Yalciner et al. (2008) and Papadopoulos et al. (2009) documented seismic events according to their geological investigations. Yalciner et al. (2008) includes seismic tsunami sources that can produce a tsunami in Mediterranean and Aegean Sea. These regions are shown in Figure 4.6, rupture parameters of these regions are shown in Table 4.3.

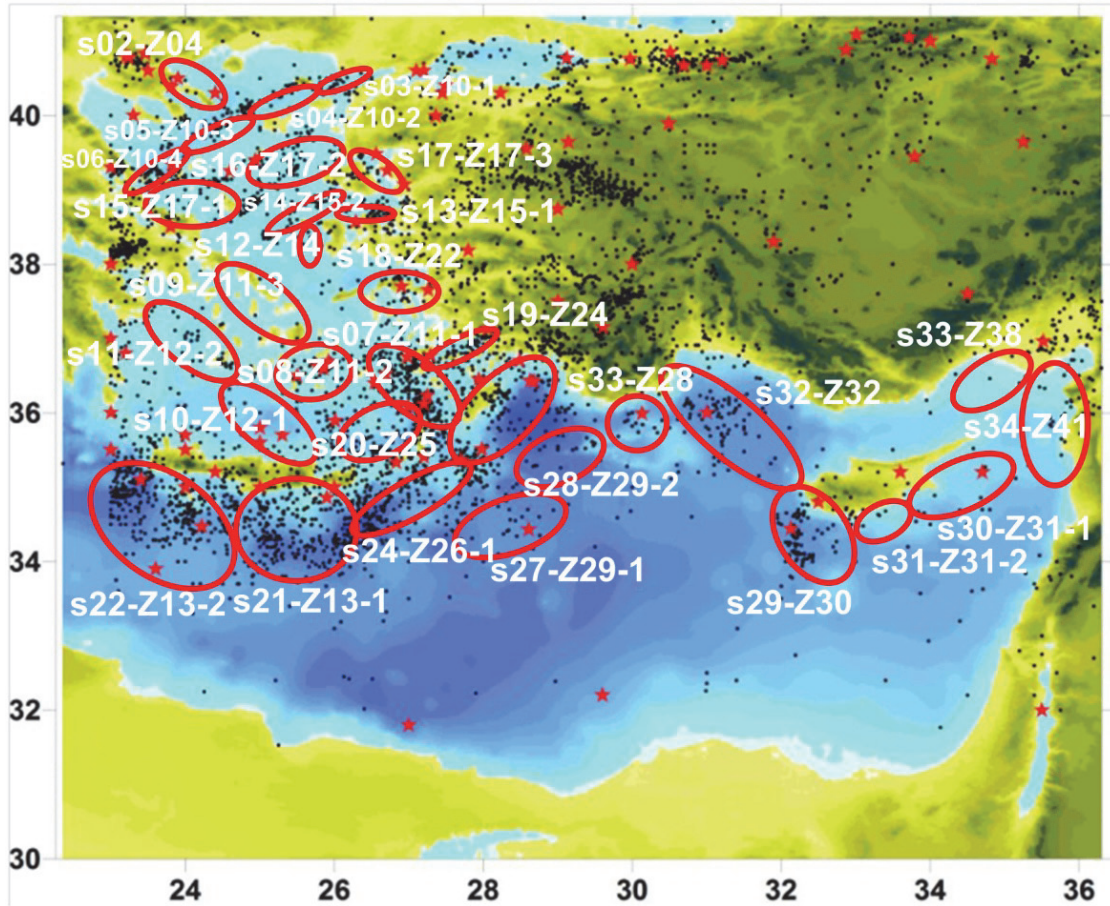


**Figure 4.6:** General view of topography and bathymetry of the Eastern Mediterranean Sea, distribution of earthquake epicenters since 1900 and main fault zones in Eastern Mediterranean region (Black dots represent the earthquake with the magnitude between 4 and 6; Red Stars indicate the earthquakes with the magnitude of greater than 6. ellipsoids show the possible tsunami generation regions) (Yalciner et al., 2008)

**Table 4.3: Tsunami Source Parameters (TRANSFER Work Packages, 2009)**

Name	Type	Epicenter	Dip (°)	Rake (°)	Strike (°)	Depth (km)	Max (+)ve amp (m)	Max (-)ve amp (m)	L (km)	W (km)	U (m)
s01-365	Not defined	23.45E 35.3N	10	110	315	25	8.1	-0.9	100	90	20
s02-Z04	Not defined	23.78E 40.83N	45	45	140	10	1.2	-0.2	90	12	6
s03-Z10-1	Strike-slip	26.40E 40.40N	45	45	245	10	2.1	-0.4	70	15	8
s04-Z10-2	Strike-slip	25.95E 40.15N	45	45	235	10	2.1	-0.4	85	15	8
s05-Z10-3	Strike-slip	25.15E 39.75N	45	45	235	10	2.1	-0.4	85	15	8
s06-Z10-4	Strike-slip	24.50E 39.20N	45	45	200	10	2.1	-0.4	70	15	8
s07-Z11-1	Not defined	27.68E 36.10N	45	45	330	40	1	-0.1	120	40	6
s08-Z11-2	Not defined	25.32E 36.48N	45	45	60	30	0.9	-0.1	85	40	6
s09-Z11-3	Not defined	24.60E 38.00N	45	45	150	30	1.1	-0.2	145	30	6
s10-Z12-1	Not defined	25.76E 35.39N	45	45	330	40	0.9	-0.1	145	30	6
s11-Z12-2	Not defined	24.70E 36.45N	45	45	330	40	0.9	-0.1	145	30	6
s12-Z14	Normal	25.70E 37.97N	45	45	5	20	1.3	-0.2	65	30	6
s13-Z15-1	Normal	26.20E 38.69N	45	45	85	15	1.1	-0.2	55	15	6
s14-Z15-2	Normal	25.25E 38.53N	45	45	60	15	1.1	-0.2	95	15	6
s15-Z17-1	Strike-slip and normal faults	23.70E 39.02N	45	45	120	10	1.9	-0.3	100	30	6
s16-Z17-2	Strike-slip and normal faults	25.00E 39.40N	45	45	80	10	1.4	-0.2	100	15	6
s17-Z17-3	Strike-slip and normal faults	27.12E 38.91N	45	45	330	10	1.3	-0.1	105	15	6
s18-Z22	Normal	26.36E 37.64N	45	45	95	20	1.4	-0.2	95	30	6
s19-Z24	Strike slip and normal faults	28.18E 37.09N	45	45	240	40	0.3	-0.1	95	10	6
s20-Z25	Normal	26.17E 35.69N	45	45	60	40	1.2	-0.2	115	50	6
s21-Z13-1	Not defined	26.41E 34.21N	10	110	265	50	1.3	-0.7	155	60	6
s22-Z13-2	Not defined	24.80E 34.32N	10	110	280	50	1.3	-0.8	190	60	6
s23-Z13-3	Not defined	22.99E 35.13N	10	110	310	50	1.1	-0.7	110	60	6

**Table 4.3 (continued)**

Name	Type	Epicenter	Dip (°)	Rake (°)	Strike (°)	Depth (km)	Max (+)ve amp (m)	Max (-)ve amp (m)	L (km)	W (km)	U (m)
s24-Z26-1	Normal and left-lateral Strike slip fault	27.88E 35.33N	10	110	240	50	1.3	-0.7	170	60	6
s25-Z26-2	Normal and left-lateral strike slip fault	29.00E 36.66N	10	110	210	50	1.3	-0.8	175	60	6
s26-Z28	Strike-slip	29.77E 35.69N	45	45	60	40	0.9	-0.1	75	40	6
s27-Z29-1	Strike-slip + cascade	27.78E 34.20N	45	45	60	40	1.1	-0.2	135	40	6
s28-Z29-2	Strike-slip + cascade	28.48E 35.16N	45	45	60	40	1	-0.2	125	40	6
s29-Z30	Strike-slip + cascade	32.98E 33.83N	10	110	330	40	1.1	-0.2	150	40	6
s30-Z31-1	Not defined	33.79E 34.68N	10	110	60	40	1.1	-0.2	140	40	6
s31-Z31-2	Not defined	33.09E 34.33N	45	45	60	40	0.9	-0.1	75	40	6
s32-Z32	Strike slip+ cascading	32.10E 35.40N	10	110	305	20	1.6	-0.2	155	40	6
s33-Z38	left-lateral strike slip fault	34.41E 36.13N	45	45	45	40	1	-0.1	105	40	6
s34-Z41	left-lateral strike slip fault and normal	35.70E 35.07N	45	45	5	40	1.1	-0.1	175	40	6
s35	Not defined	28.46E 34.45N	27	99	294	7.5	1.8	-0.2	125	63	3.65
s36	Not defined	28.43E 36.07N	10	110	184	7.5	0.2	-1.5	185	50	2.9
s37	Not defined	28.39E 35.82N	25	90	303	7.5	1.3	-0.3	90	45	2.7
s38	Not defined	28.4E 35.5N	10	110	55	7.5	2.4	-0.7	190	90	5

Seismic sources that can affect Güllük region are selected from Table 4.3. The rupture parameters and the visualization of initial wave are given for each selected tsunami source between Tables 4.4 and 4.9. Among these sources, the tsunami source s18-z22 can be determined as one of the most effective tsunami source for Güllük bay in tsunami hazard analysis.

In order to evaluate the reliability of estimated rupture parameters of tsunami source S18-z22, the current seismic measurements and rupture parameters are obtained from different data sources. The seismic data is obtained from Boğaziçi University Kandilli Observatory and Earthquake Research Institute's (KOERI) web site <http://www.koeri.boun.edu.tr>. The data extracted from KOERI for Güllük bay is given in Section 4.4. The epicenter and strike angle are selected for tsunami source s18-z22 according to KOERI's data. It has been observed that the already defined other rupture parameters (dimensions of fault, surface displacement, focal depth, dip and rake angles) were in the same order of magnitude given in Kalafat et al., 2009. Therefore same parameters as given in Table 4.3 are selected. Hence the source parameters of s18-z22 is revised and given in Table 4.4.

**Table 4.4:** The Estimated Rupture Parameters and Initial Sea State of Selected Tsunami Source s18-Z22

Estimated Rupture Parameters $M=7.6$			
Epicenter of fault axis	26.592E 37.26N	Dip angle (deg.)	45
Strike angle (deg. CW)	66	Rake angle (deg.)	45
Focal depth (km)	20	Displacement (m)	8
Length of fault (km)	95	Width of fault (km)	30
Maximum (+)ve amp. (m)	1.83	Minimum (-)ve amp. (m)	-0.17

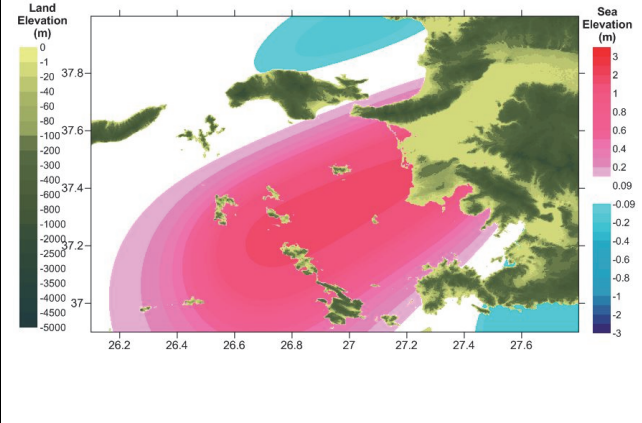


**Table 4.5:** The Estimated Rupture Parameters and Initial Sea State of Selected Tsunami Source s07-Z11-1

Estimated Rupture Parameters $M=7.8$			
Epicenter of fault axis	27.68E 36.1N	Dip angle (deg.)	45
Strike angle (deg. CW)	330	Rake angle (deg.)	45
Focal depth (km)	40	Displacement (m)	6
Length of fault (km)	120	Width of fault (km)	40
Maximum (+)ve amp.(m)	1	Minimum (-)ve amp. (m)	-0.1

**Table 4.6:** The Estimated Rupture Parameters and Initial Sea State of Selected Tsunami Source s10-Z12-1

Estimated Rupture Parameters $M=7.8$			
Epicenter of fault axis	25.7E 35.39N	Dip angle (deg.)	45
Strike angle (deg. CW)	330	Rake angle (deg.)	45
Focal depth (km)	40	Displacement (m)	6
Length of fault (km)	145	Width of fault (km)	30
Maximum (+)ve amp.(m)	0.9	Minimum (-)ve amp. (m)	-0.1

**Table 4.7:** The Estimated Rupture Parameters and Initial Sea State of Selected Tsunami Source s11-Z12-2

Estimated Rupture Parameters $M=7.8$			
Epicenter of fault axis	24.7E 36.45N	Dip angle (deg.)	45
Strike angle (deg. CW)	330	Rake angle (deg.)	45
Focal depth (km)	40	Displacement (m)	6
Length of fault (km)	145	Width of fault (km)	30
Maximum (+)ve amp.(m)	0.9	Minimum (-)ve amp. (m)	-0.1



**Table 4.8:** The Estimated Rupture Parameters and Initial Sea State of Selected Tsunami Source s12-Z14

Estimated Rupture Parameters $M=7.4$			
Epicenter of fault axis	25.7E 37.97N	Dip angle (deg.)	45
Strike angle (deg. CW)	5	Rake angle (deg.)	45
Focal depth (km)	20	Displacement (m)	6
Length of fault (km)	65	Width of fault (km)	30
Maximum (+)ve amp.(m)	1.3	Minimum (-)ve amp. (m)	-0.2

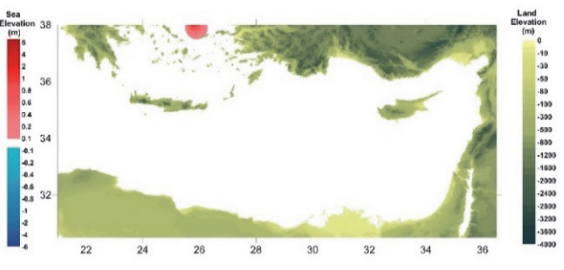
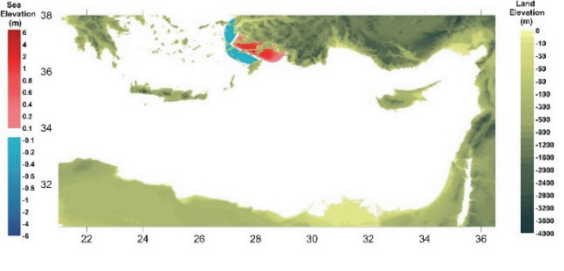


**Table 4.9:** The Estimated Rupture Parameters and Initial Sea State of Selected Tsunami Source s35

Estimated Rupture Parameters $M=8.0$			
Epicenter of fault axis	28.46E 36.45N	Dip angle (deg.)	27
Strike angle (deg. CW)	294	Rake angle (deg.)	99
Focal depth (km)	7.5	Displacement (m)	3.65
Length of fault (km)	125	Width of fault (km)	63
Maximum (+)ve amp.(m)	1.8	Minimum (-)ve amp. (m)	-0.2



#### 4.3.2 Simulations of probable seismic tsunami source case

Estimated tsunami source and accurate bathymetric/topographic data are input data for numerical modeling tool. 240 min tsunami simulation gives time histories of water surface fluctuations, wave amplitudes at every grid point, inundation and runup on the shore for nested Domains B, C and D. Wave characteristics such as water elevation, current velocity, flux, Froude number are plotted for selected numerical gauge points, and Surfer<sup>®</sup> version 12 is used to take snapshots of any time for nested domains.

In this section, tsunami simulation is done for seismic source (s18-z22) that can be the most effective source for Güllük region. Source is presented in a frame with its fault parameters and the plot of initial wave occurred due to the rupture (see Table 4.4). Simulation duration is selected as 4 hours. This time is sufficient to see the maximum effects of potential tsunamis in Güllük bay. 270m, 90m and 30m nested grid sizes in Domain B, C and D are used as bathymetric/topographic data. Nested domains are presented in Figure 4.4, and boundary coordinates of these domains are given in Table 4.1.

Tsunami parameters (the distribution of maximum and minimum water surface elevations, the distribution of arrival time of first wave, the maximum current velocity, the maximum flow depth and momentum flux on land) and the output data at selected numerical gauge points are presented for the simulated source. Sea level changes at different time steps are visualized to identify wave's generation, propagation and reach the coast for selected tsunami scenario. Location of the numerical gauge points are given in Figure 4.17, coordinates and depths of the numerical gauge points are given in Table 4.13.

### **Propagation of tsunami according to seismic source (s18-z22)**

Wave propagation of the tsunami due to seismic source (s18-z22) is simulated for the simulation duration 240 min. The computed sea states at different time steps ( $t=30, 60, 120, 150, 180$  and 240 min) in Domain D are represented in Figure 4.7.

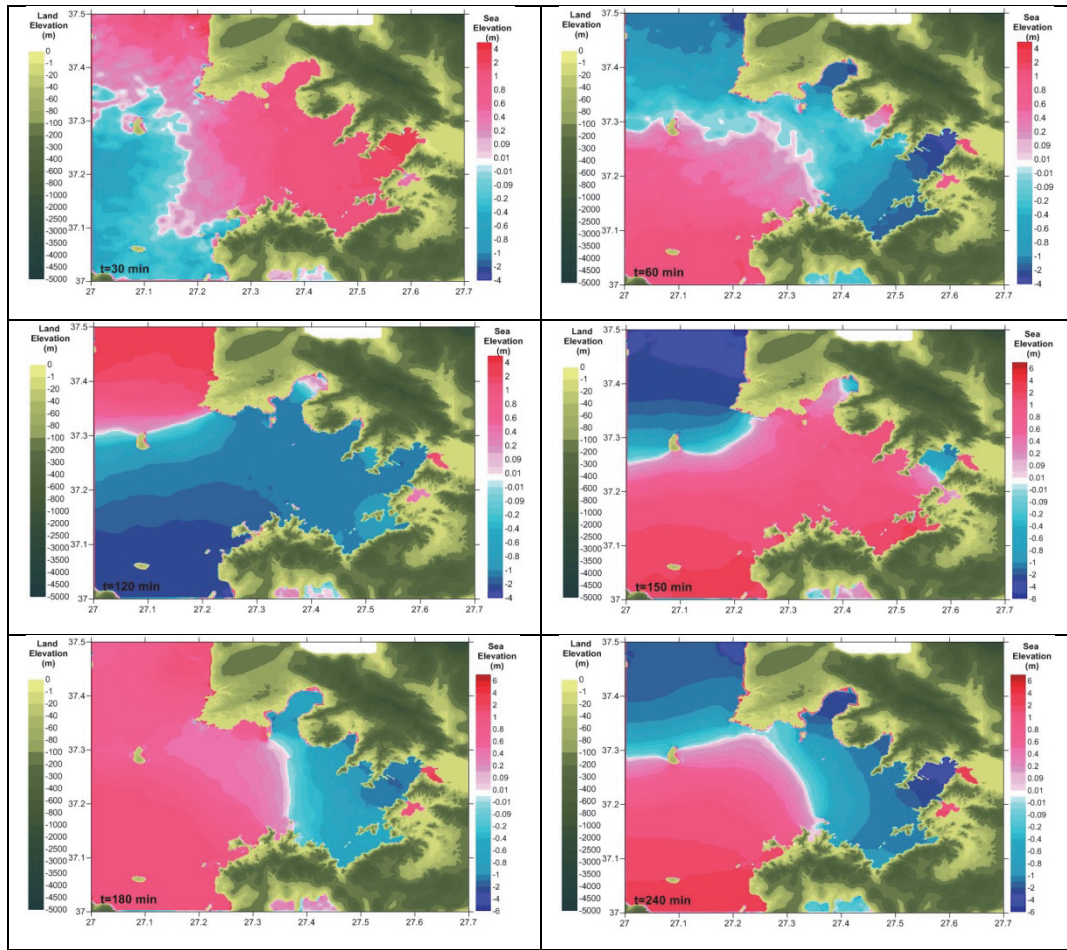


**Figure 4.7:** Sea states at different time steps ( $t=30, 60, 120, 150, 180$  and  $240$  min) in Domain D according to seismic source (s18-z22)

### **Tsunami parameters according to seismic source (s18-z22)**

The computed distribution of tsunami parameters due to seismic tsunami source s18-z22 in Domain B and Domain D are shown in Figure 4.8.

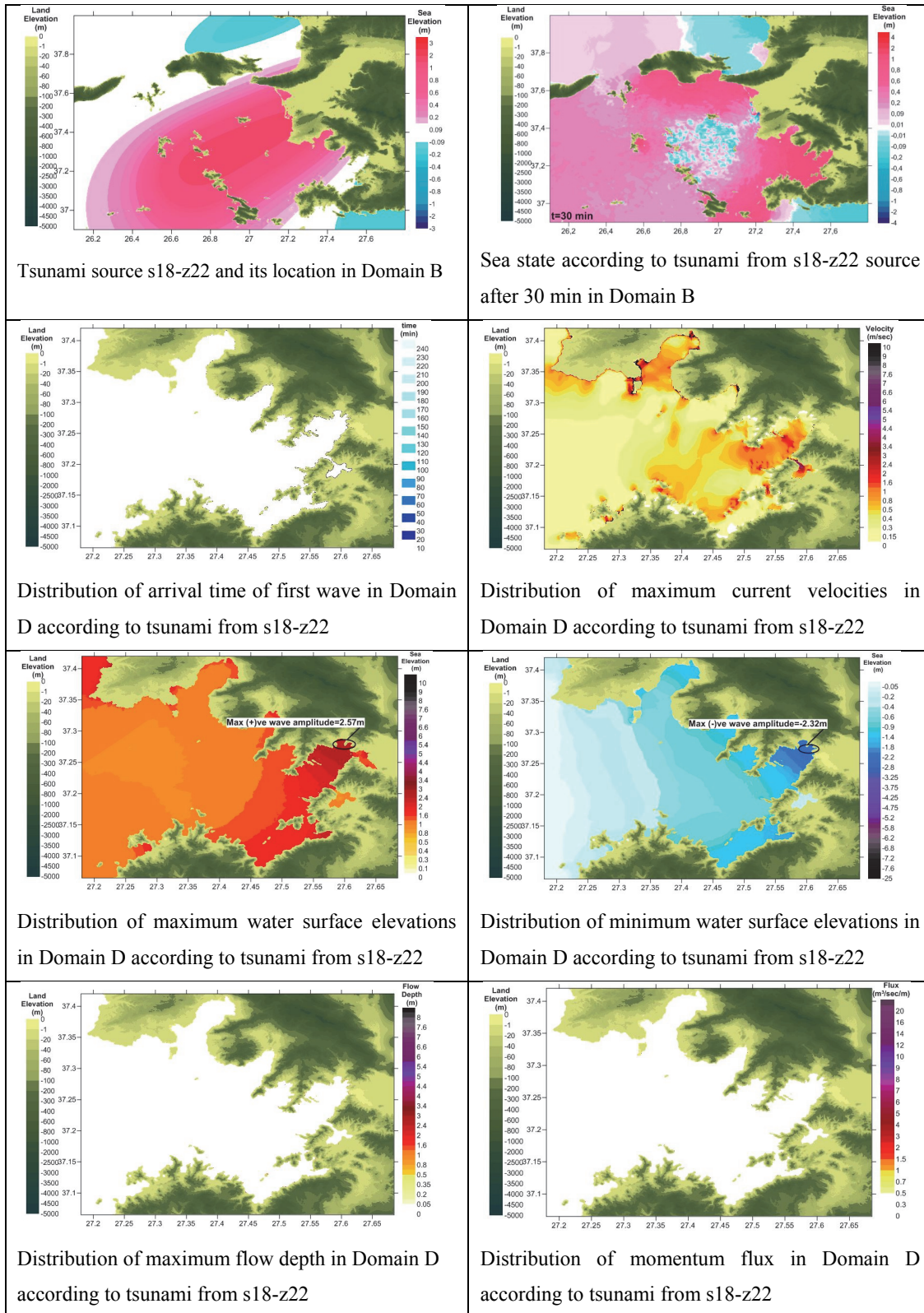


**Figure 4.8:** Tsunami parameters due to tsunami source s18-z22 according to simulation duration of 240 min

First wave arrives the coast in Domain D shortly after tsunami source (s18-z22) is generated. Maximum positive wave amplitude is computed as 2.57m, and maximum negative wave amplitude is computed as -2.32m around Güllük region (see Figure 4.8).

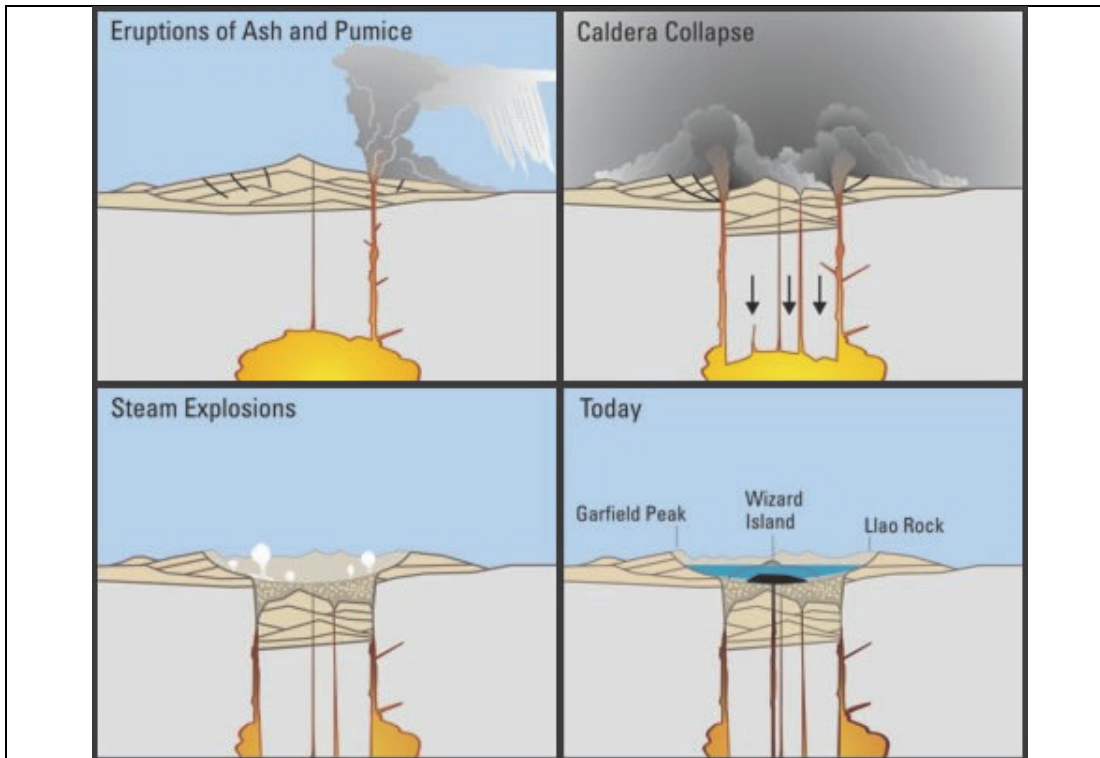
Possible effects of seismic source (s18-z22) should be determined to avoid hazards along Güllük coasts. Wave characteristics due to tsunami from s18-z22 are given in between Figures 4.18 and 4.21 for selected numerical gauge locations.

#### **4.3.3 Estimation of probable non-seismic tsunami sources for Güllük bay**

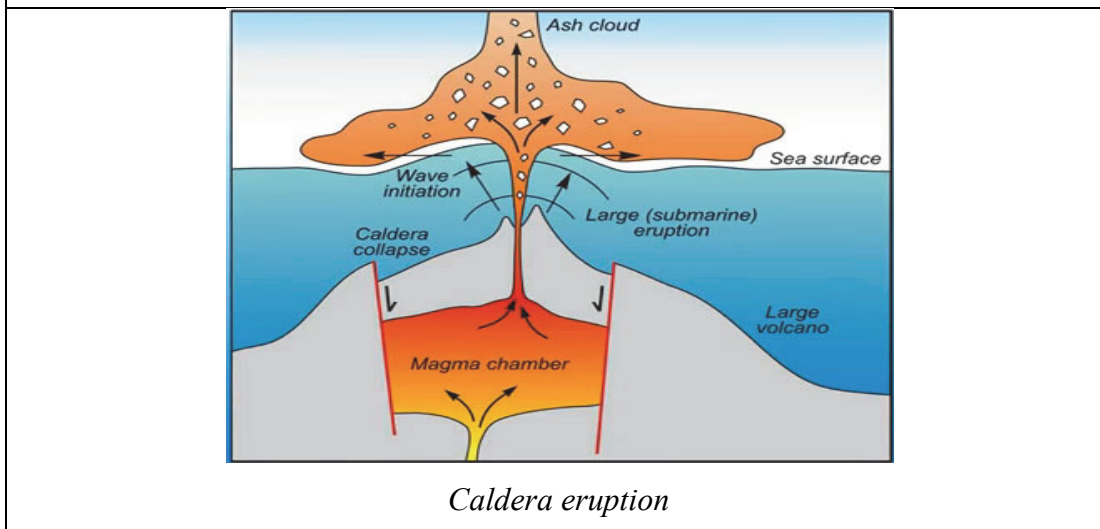
A tsunami is generated when there is ground uplift and/or subsidence. As a result of this movement, water is pushed up above normal sea level. There has several tsunami generation mechanisms such as earthquakes, submarine landslides, tectonic movements, volcanic dynamisms under the sea.

Volcanoes can produce tsunamis through different mechanisms. Some of these mechanisms are volcanic earthquakes, undersea eruptions, landslides, caldera collapse. The most destructive volcanic based tsunami was recorded as the eruption of Krakatoa in 1883. Wave heights were exceeded 40m and killed 36000 people.

Caldera collapse of volcanos has been seen in Aegean Sea and Eastern Mediterranean in the past. A caldera is usually formed by collapse at the volcano crater at the end of volcanic eruption. Figure 4.9 represents generation mechanism of caldera collapse/eruption. In the simulations of the volcano induced tsunami, the caldera collapse of Santorini and Columbus volcanos are selected as input of simulations. Santorini and Columbus are located along the volcanic arc in southern Aegean Sea (see Figure 4.10).



*Caldera collapse*



*Caldera eruption*

**Figure 4.9:** Generation of a caldera eruption/collapse due to volcanic eruption

(above picture: <http://geology.com/articles/caldera/>, below picture:

<http://www.shtfplan.com/headline-news/frightening-methane-explosion-steam-volcano-may-cause-massive-tsunami>)

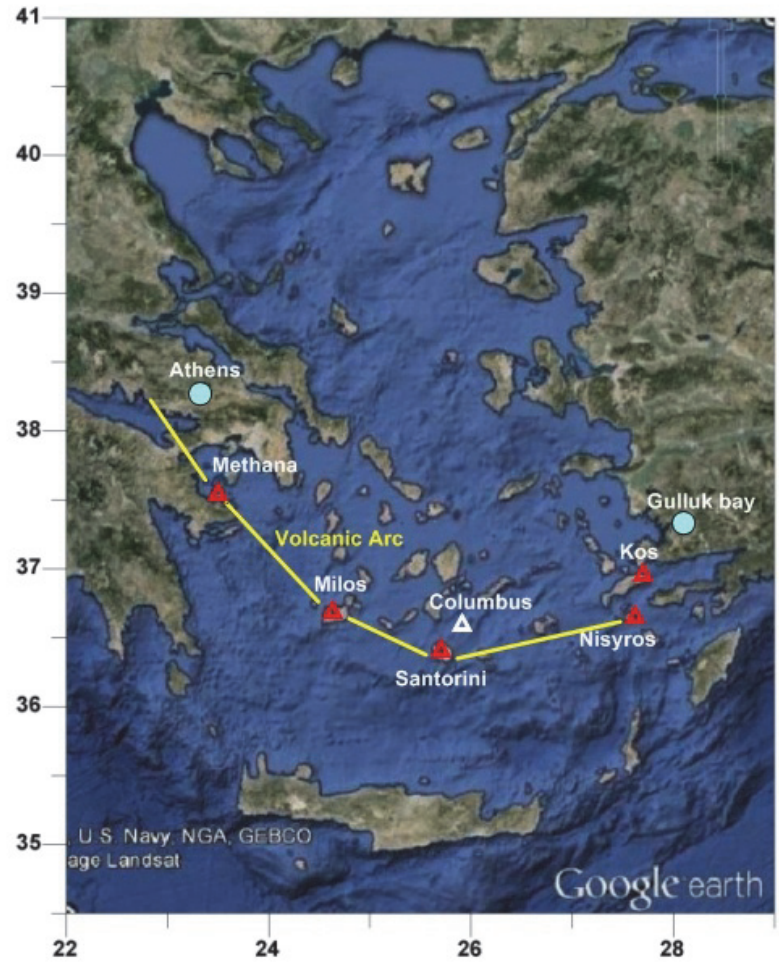


**Figure 4.10:** Location of volcanic arc on Google Earth satellite images

Tsunami generation parameters of those scenarios are defined according to historical data. In this section, caldera collapse of Santorini and Columbus are selected as non-seismic tsunami sources for numerical modeling. Simulations are completed to visualize possible effects of non-seismic source scenarios in Gullük region.

The rupture parameters and the visualization of initial wave are given for selected non-seismic tsunami sources in between Tables 4.10 and 4.12.

**Table 4.10:** The Estimated Rupture Parameters and Initial Sea State of Non-seismic Source Scenario-1 (Caldera Collapse of Santorini)

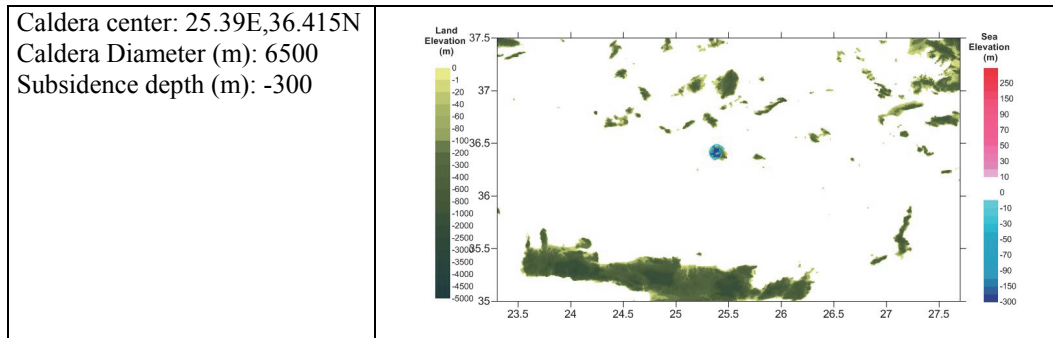


**Table 4.11:** The Estimated Rupture Parameters and Initial Sea State of Non-seismic Source Scenario-2 (Caldera Collapse of Columbus)

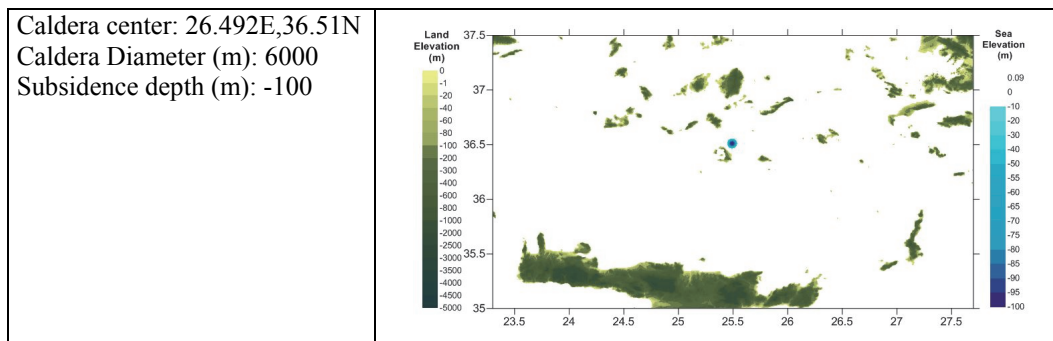
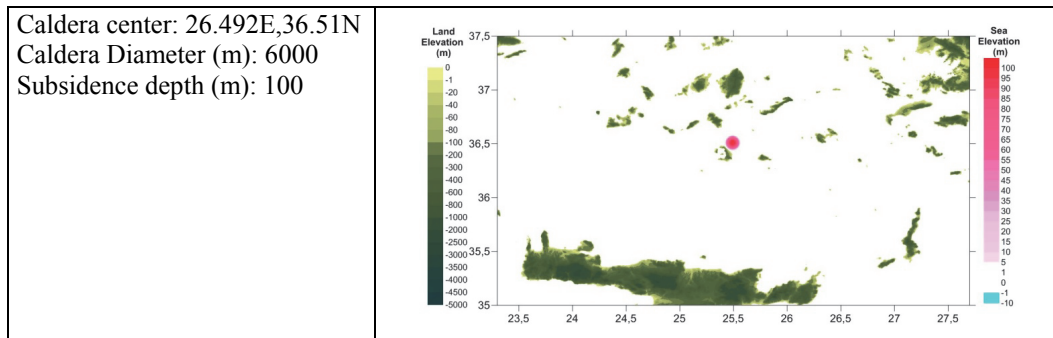


**Table 4.12:** The Estimated Rupture Parameters and Initial Sea State of Non-seismic Source Scenario-3 (Caldera Eruption of Columbus)





#### 4.3.4 Simulations of probable non-seismic tsunami sources case

Three different non-seismic tsunami scenarios are determined and simulated. These scenarios are named as non-seismic source scenario 1, 2 and 3. Caldera collapse of Santorini are i) non-seismic source-1 (caldera collapse of Santorini), ii) non-seismic source-2 (caldera collapse of Columbus), iii) non-seismic source-3 (caldera eruption of Columbus), (see Tables 4.10, 4.11 and 4.12).

Simulation duration is selected as 5 hours. This duration is sufficient to see the maximum effects of potential tsunamis in Güllük bay coming from the selected locations. The grid size of nested domains B, C, D are 270m, 90m and 30m respectively. The selected nested domains have already been presented in Figure 4.5, and boundary coordinates of these domains are given in Table 4.2.

Tsunami parameters (the distribution of maximum and minimum water surface elevations, the distribution of arrival time of first wave, the maximum current velocity, the maximum flow depth and momentum flux on land) and the output data at selected numerical gauge points are presented for the simulated source. Sea states at different time steps are visualized to identify wave's generation, propagation and reach the coast for selected tsunami scenario. Location of the numerical gauge points are given in Figure 4.17, coordinates and depths of the numerical gauge points are given in Table 4.13.

#### **Propagation of tsunami due to non-seismic source scenario-1 (300m caldera collapse of Santorini)**

Wave propagation of the tsunami due to caldera collapse of Santorini is simulated for simulation duration 300 min. The computed sea states at different time steps ( $t=60, 90, 120, 150, 180$  and  $240$  min) in Domain D are represented in Figure 4.11.

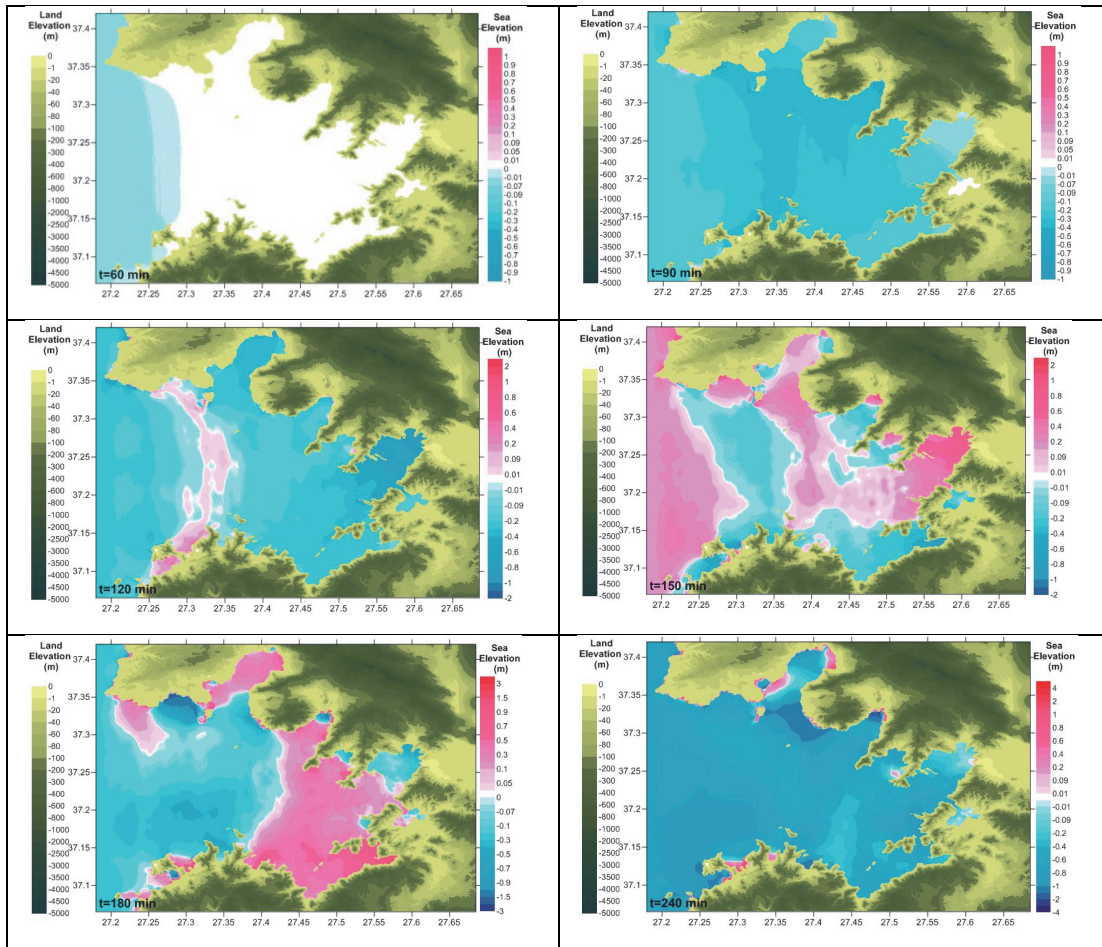


**Figure 4.11:** Sea states at different time steps (t=60, 90, 120, 150, 180 and 240 min) in Domain D according to caldera collapse of Santorini

### **Tsunami parameters due to the simulation of non-seismic source scenario-1**

The computed distribution of tsunami parameters due to non-seismic tsunami source-1 (caldera collapse of Santorini) in Domain B and Domain D are shown in Figure 4.12.

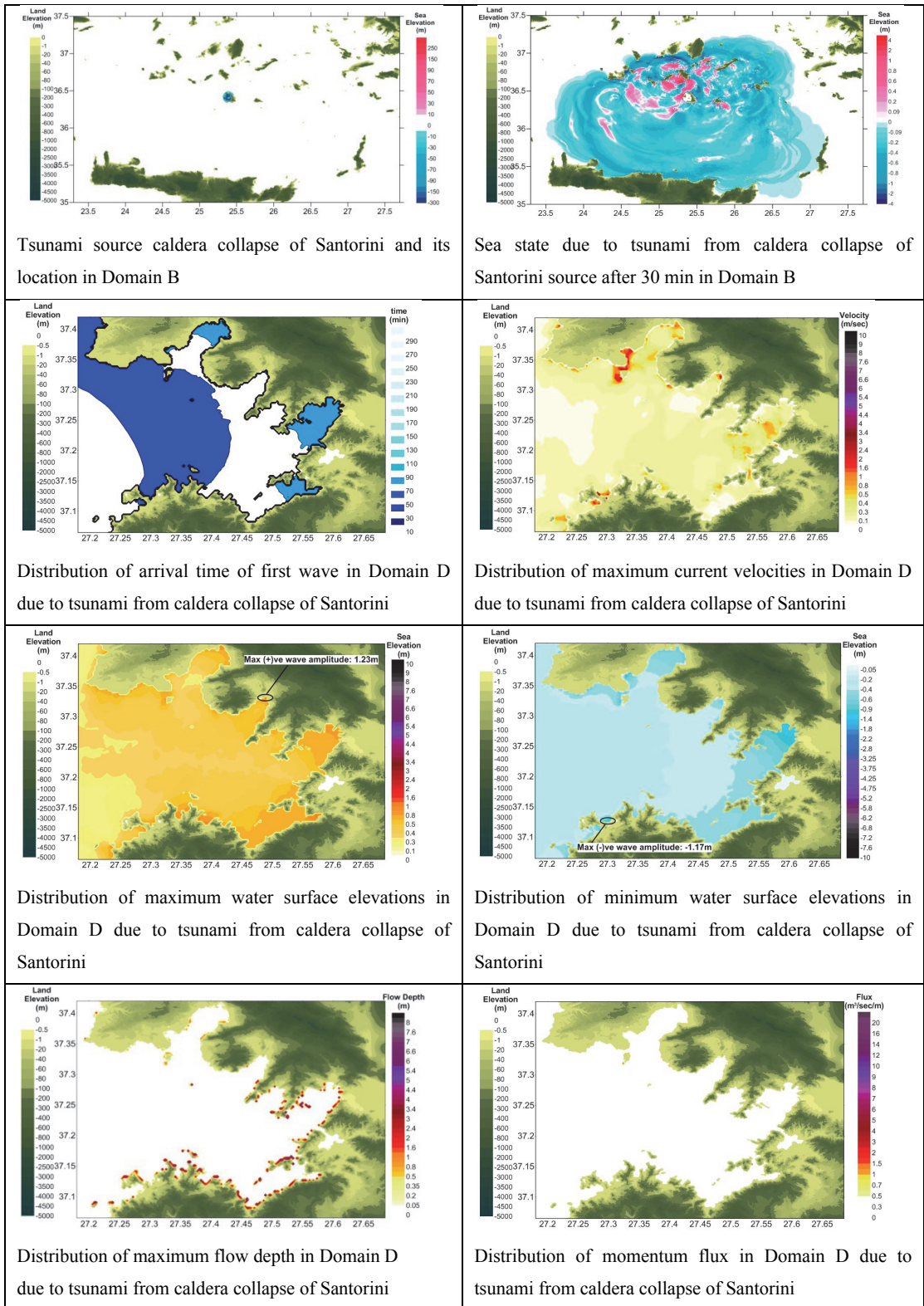


**Figure 4.12:** Tsunami parameters due to 300m caldera collapse of Santorini according to simulation duration 300 min

First wave arrives the coast in Domain D nearly 90 min after then when tsunami source (caldera collapse of Santorini) is generated. Maximum positive wave amplitude is measured as 1.23m at Gürçamlar village which is located in northeast of Güllük region, and maximum negative wave amplitude is measured as -1.17m around Yalıkavak region (see Figure 4.12).

Caldera collapse of Santorini does not seem to cause large damages in Güllük bay when compared to seismic source. Although caldera collapse of Santorini is an effective non-seismic source around Santorini and nearby islands in southern Aegean Sea, the energy of the initial wave is dissipated until the tsunami reaches Güllük coasts. The time histories of water level fluctuations at selected numerical gauge points due to tsunami source from caldera collapse of Santorini are given in between Figures 4.18 and 4.21.

## Propagation of tsunami due to non-seismic source scenario-2 (100m caldera collapse of Columbus)

Wave propagation of the tsunami due to caldera collapse of Columbus is simulated for simulation duration 300 min. The computed sea states at different time steps ( $t=60, 90, 120, 150, 180$  and  $240$  min) in Domain D are represented in Figure 4.13.

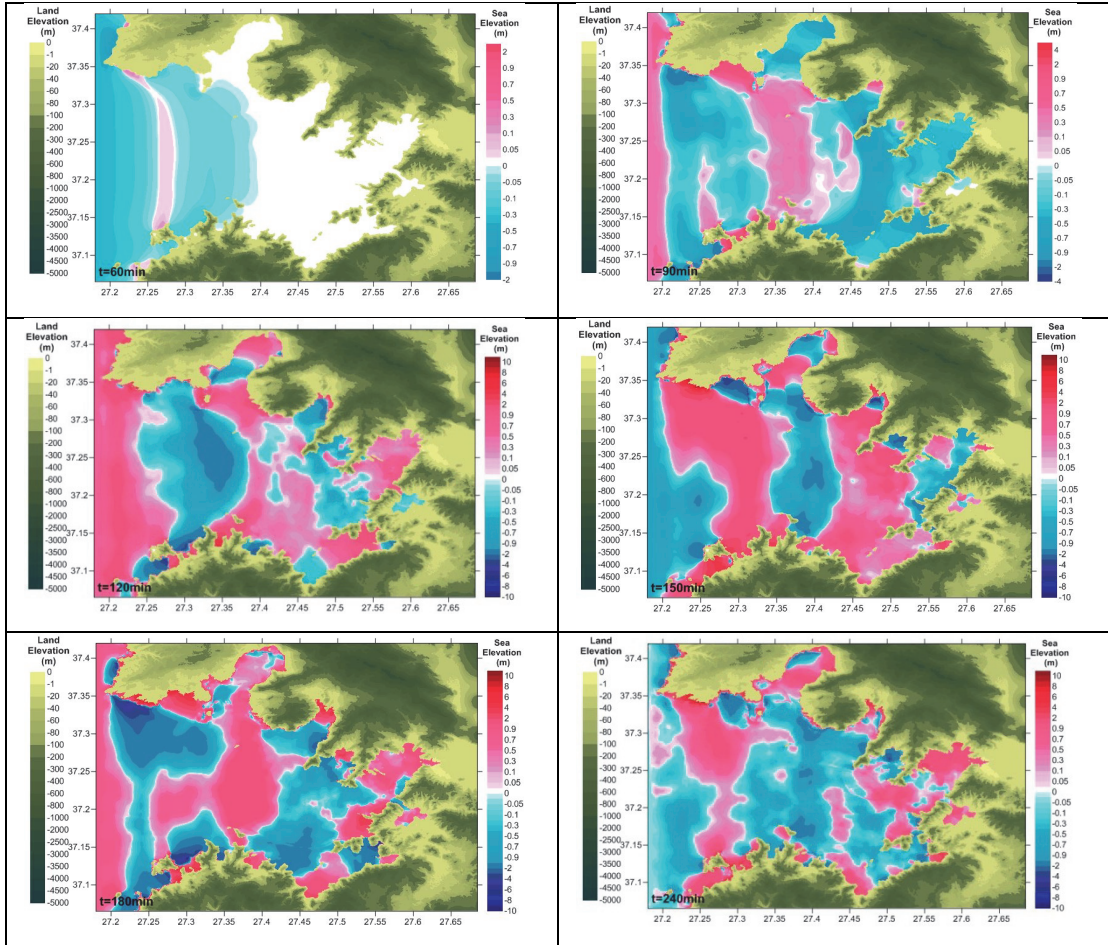


**Figure 4.13:** Sea states at different time steps ( $t=60, 90, 120, 150, 180$  and  $240$  min) in Domain D according to caldera collapse of Columbus

## Tsunami parameters due to the simulation of non-seismic source scenario-2

The computed distribution of tsunami parameters due to non-seismic tsunami source-2 (caldera collapse of Columbus) in Domain B and Domain D are shown in Figure 4.14.

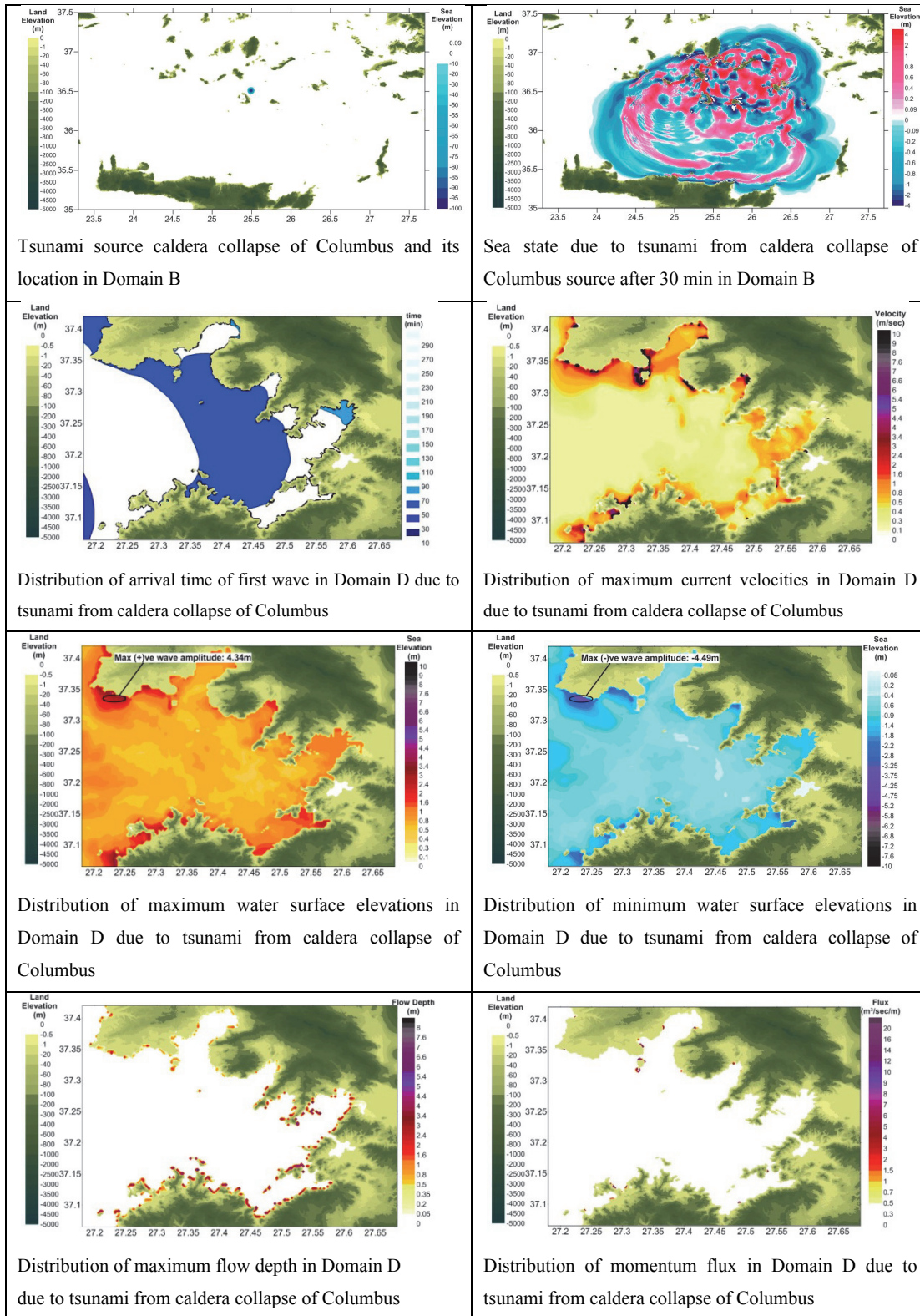


**Figure 4.14:** Tsunami parameters due to 100m caldera collapse of Columbus according to simulation duration 300 min

First wave reaches the coast nearly 80 min later after then tsunami source (caldera collapse of Columbus) is generated. Maximum positive wave amplitude is measured as 4.34m around Didim region, and maximum negative wave amplitude is measured as -4.49m around Didim region (see Figure 4.14).

Caldera collapse of Columbus is more effective non-seismic source that may cause damages in Güllük bay comparing to caldera collapse of Santorini. Wave characteristics due to tsunami from caldera collapse of Columbus are given in between Figures 4.18 and 4.22 for selected numerical gauge locations.

**Propagation of tsunami due to non-seismic source scenario-3 (100m caldera eruption of Columbus)**

Wave propagation of the tsunami due to caldera collapse of Columbus is simulated for simulation duration 300 min. The computed sea states at different time steps ( $t=60, 90, 120, 150, 180$  and  $240$  min) in Domain D are represented in Figure 4.15.

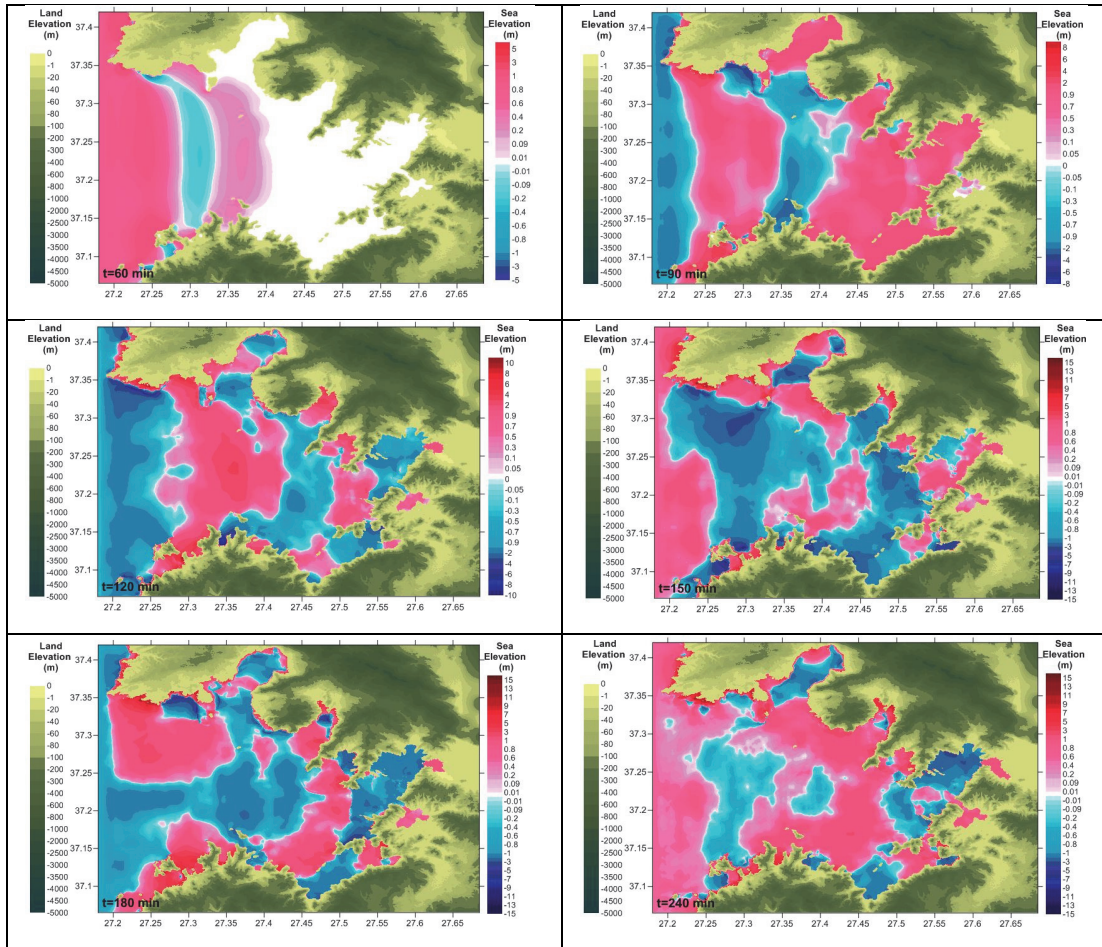


**Figure 4.15:** Sea states at different time steps ( $t=60, 90, 120, 150, 180$  and  $240$  min) in Domain D according to caldera eruption of Columbus

**Tsunami parameters due to the simulation of non-seismic source scenario-3**

The computed distribution of tsunami parameters due to non-seismic tsunami source-3 (caldera eruption of Columbus) in Domain B and Domain D are shown in Figure 4.16.



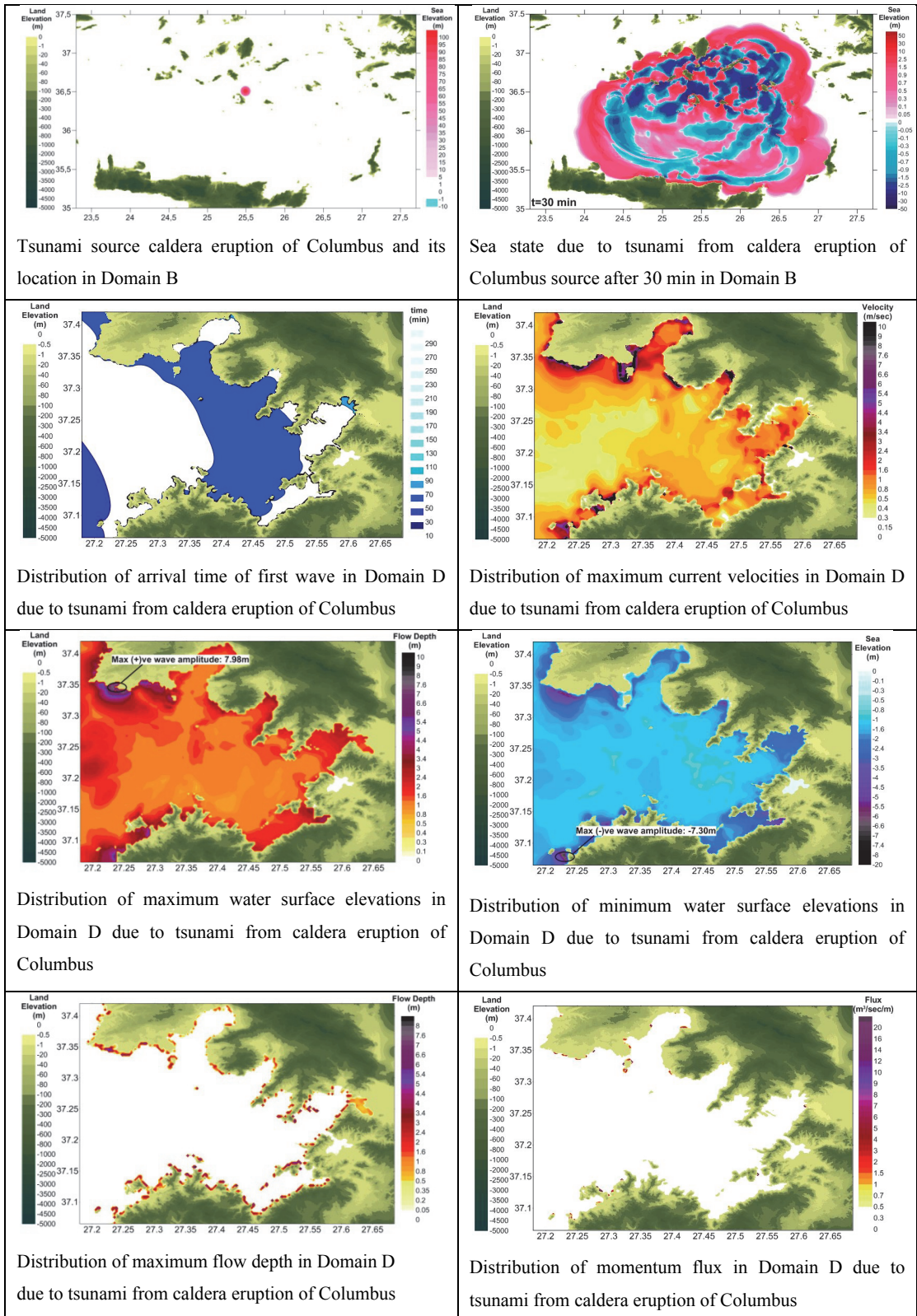


**Figure 4.16:** Tsunami parameters due to 100m caldera eruption of Columbus according to simulation duration 300 min

First wave arrives the coast in Domain D nearly 80 min after then tsunami source (caldera eruption of Columbus) is generated. Maximum positive wave amplitude is measured as 7.98m around Didim region, and maximum negative wave amplitude is measured as -7.38m around Yalıkavak region (see Figure 4.16).

Caldera eruption of Columbus is the most effective non-seismic source that may cause damages in Güllük bay. Caldera eruption of Columbus is more powerful source than caldera collapse of Columbus, although location and initial parameters (diameter and level of collapse/eruption) of those sources are the same for Güllük bay. Wave characteristics due to tsunami from caldera eruption of Columbus are given in between Figures 4.18 and 4.21 for selected numerical gauge locations.

#### **Wave characteristics due to seismic and non-seismic tsunami scenarios for selected numerical gauge locations**

Selected seismic and non-seismic tsunami scenarios are simulated to analyze probable effects of those sources in Güllük bay. "Didim-Tekağaç", "Yalıkavak", "Güllük", and "Fish Farms" are selected numerical gauge points that provide to see probable effects of tsunami from selected sources at critical regions in Güllük bay. Location of the numerical gauge points are shown in Figure 4.17, X-Y coordinates and depths of those points are given in Table 4.13. Water elevation, current velocity, momentum and discharge fluxes are given in between Figures 4.18 and 4.21 for selected numerical gauge points.

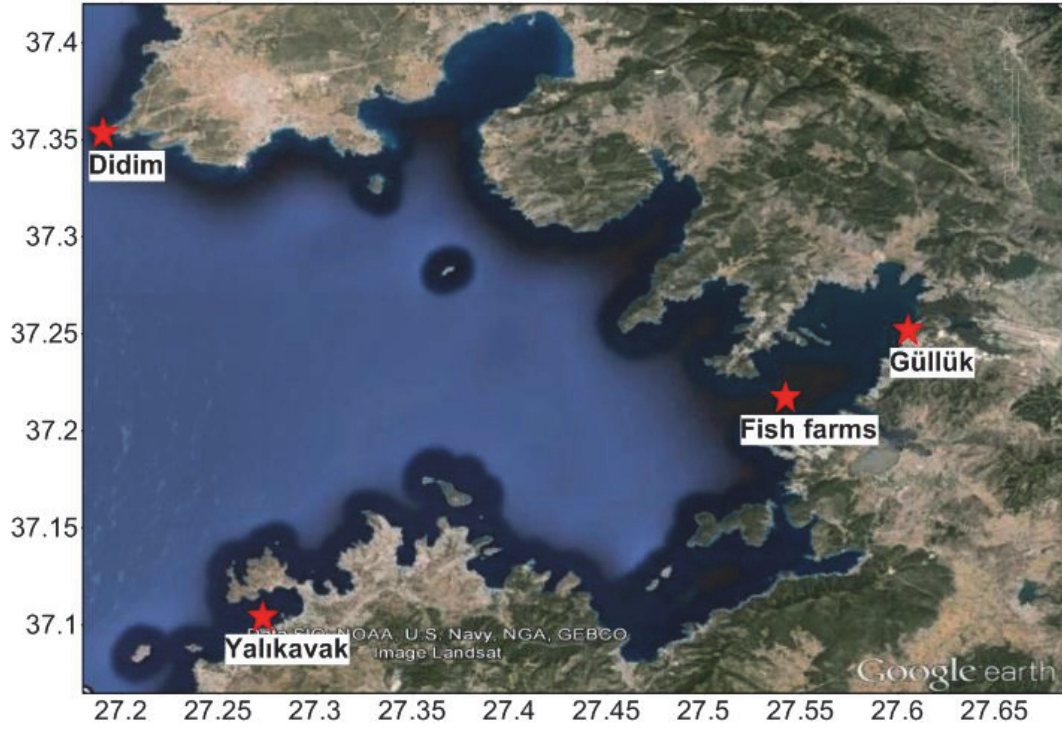


**Figure 4.17:** Locations of selected numerical gauge points in Domain D

**Table 4.13:** X-Y coordinates and depths of selected numerical gauge points

Numerical Gauge Points	X coordinate	Y coordinate	Depth of point (m)
Didim Tekağaç	27.190	37.353	13.0
Fish farms	27.542	37.217	39.6
Güllük	27.605	37.252	16.8
Yalıkavak	27.273	37.104	22.3

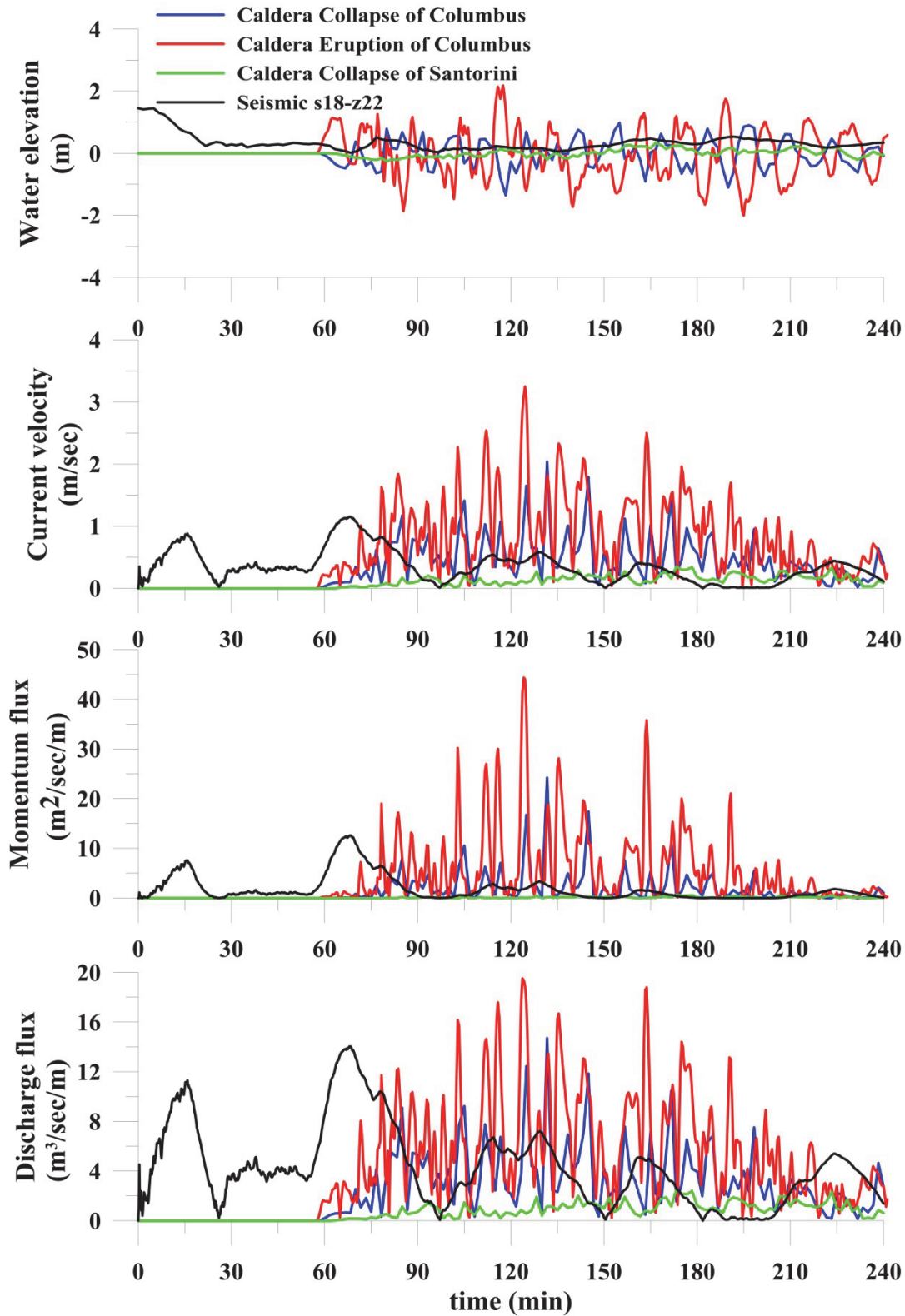


**Figure 4.18:** Wave characteristics for gauge point "Didim-Tekağaç"  
(water depth at the point is 13.0m)

Traces of historical tsunamis are found in Didim Tekağaç from excavation works around the region; therefore, probable tsunami effects should be examined for marinas, coastal communities and residential areas around the region (Papadopoulos et al., 2012).

The time histories of water level fluctuations and computed near shore tsunami parameters at numerical gauge point near Didim Tekağaç is given in Figure 4.18. Tsunami from caldera eruption of Columbus has the largest wave amplitude as around 2.2m, current velocity is around 3.3 m/sec, momentum flux is around 44  $\text{m}^3/\text{sec}^2/\text{m}$ , and discharge flux is around 20  $\text{m}^3/\text{sec}/\text{m}$  at a point of 13.0m deep located near Didim Tekağaç (see Figure 4.18). Computed near shore tsunami parameters according to selected tsunami scenarios for "Didim-Tekağaç" numerical gauge point are summarized in Table 4.14.

**Table 4.14:** Computed near shore tsunami parameters for "Didim-Tekağaç" (water depth at the point is 13.0m) numerical gauge point according to selected tsunami scenarios

Selected Tsunami Scenario	Arrival time of first wave (min)	Arrival time of max wave (min)	Max (+)ve amp. (m)	Max (-)ve amp. (m)	Max current velocity (m/sec)	Max momentum flux ( $\text{m}^3/\text{s}^2/\text{m}$ )	Max discharge flux ( $\text{m}^3/\text{s}/\text{m}$ )
seismic s18-z22	0	1	1.61	0.00	1.16	12.67	14.06
caldera collapse of Santorini	62	168	0.42	-0.32	0.40	0.83	2.79
caldera collapse of Columbus	58	80	1.12	-1.37	2.26	27.41	15.39
caldera eruption of Columbus	57	117	2.19	-2.06	3.25	44.44	19.58

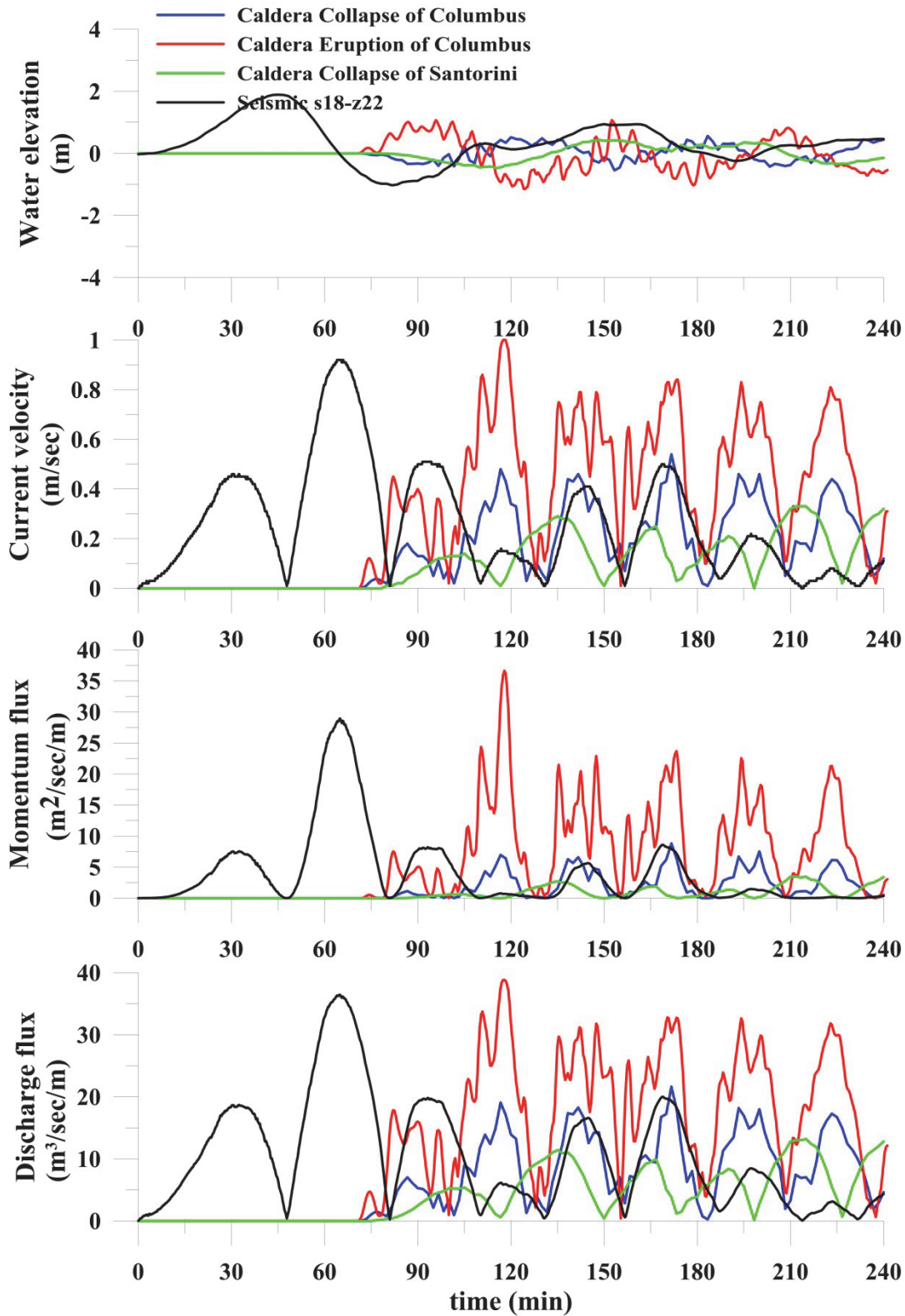


**Figure 4.19:** Wave characteristics for gauge point "Fish Farms"  
 (water depth at the point is 39.6m)

Probable wave effects should be examined around fish farms' region due to their vulnerability not only for long wave actions but also small wave oscillations. Fish farms are located around Güllük region, and gauge point "Fish Farms" represents wave characteristics around fish farms' region. Tsunami from s18-z22 has the largest wave amplitude as around 1.9m at a point of 39.6m deep located near fish farms (see Figure 4.19). Current velocity reaches maximum magnitude around 1 m/sec, momentum flux is around 37 m<sup>3</sup>/sec<sup>2</sup>/m, and discharge flux is around 39 m<sup>3</sup>/sec/m due to tsunami from caldera eruption of Columbus. Computed near shore tsunami parameters according to selected tsunami scenarios for "Fish farms" numerical gauge point are summarized in Table 4.15.

Although maximum wave amplitude, current velocity, momentum and discharge fluxes are important wave characteristics for all selected numerical gauge points, magnitude of current velocity places a particular importance for fish farms. Fish farms can move in both vertical and horizontal directions due to Sea states and magnitude of current velocities respectively. Vertical movements can cause breaking of steel ropes that stabilizing fish farm's system at a selected location; on the other hand, horizontal movements also can cause breaking of steel ropes as a result of dragging force due to high current velocities. Strengthening of fish farms should be done according to selected wave characteristics to avoid probable damages.

**Table 4.15:** Computed near shore tsunami parameters for "Fish farms" (water depth at the point is 39.6m) numerical gauge point according to selected tsunami scenarios

Selected Tsunami Scenario	Arrival time of first wave (min)	Arrival time of max wave (min)	Max (+)ve amp. (m)	Max (-)ve amp. (m)	Max current velocity (m/sec)	Max momentum flux (m <sup>3</sup> /s <sup>2</sup> /m)	Max discharge flux (m <sup>3</sup> /s/m)
seismic s18-z22	0	46	1.90	-1.03	0.92	28.98	36.47
caldera collapse of Santorini	76	148	0.45	-0.47	0.33	3.66	13.22
caldera collapse of Columbus	72	183	0.56	-0.55	0.54	8.91	21.69
caldera eruption of Columbus	70	153	1.07	-1.16	1.00	36.66	38.83

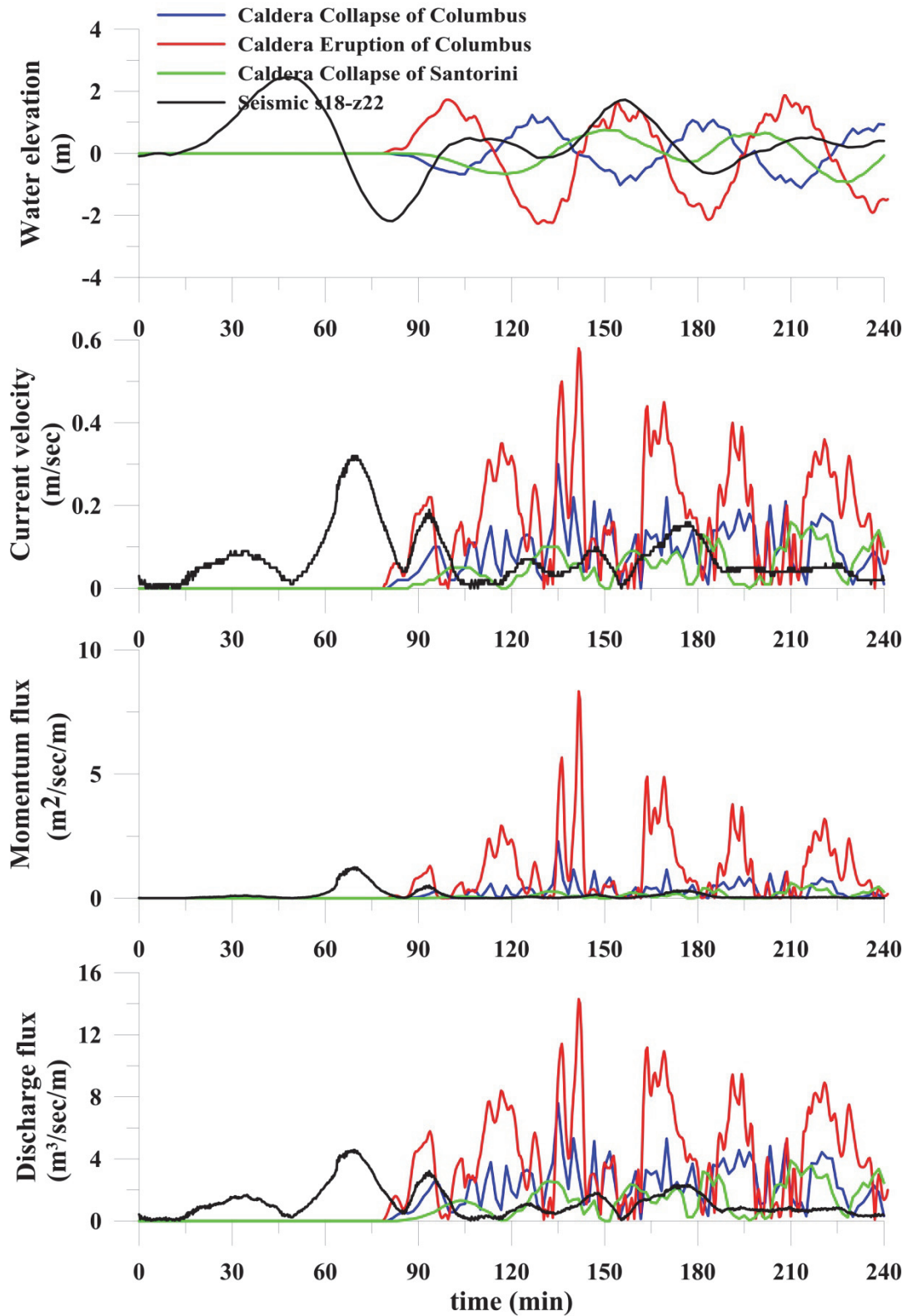


**Figure 4.20:** Wave characteristics for gauge point "Güllük"  
 (water depth at the point is 16.8m)



Muğla Milas Bodrum Airport is located in northern part of Güllük region. Airport was constructed on the low land area (see Figure 4.2). When tsunami waves enter Güllük bay, they will directly inundate the low land area between the airport and the shoreline.

The time histories of water level fluctuations and computed near shore tsunami parameters at numerical gauge point near Güllük village is given in Figure 4.20. Tsunami from s18-z22 has the largest wave amplitude as around 2.5m at a point of 16.8m deep located near airport (see Figure 4.20). Current velocity reaches maximum magnitude around 1.4 m/sec, momentum flux is around 8 m<sup>3</sup>/sec<sup>2</sup>/m, and discharge flux is around 14 m<sup>3</sup>/sec/m due to tsunami from caldera eruption of Columbus. Computed near shore tsunami parameters according to selected tsunami scenarios for "Fish farms" numerical gauge point are summarized in Table 4.16.

**Table 4.16:** Computed near shore tsunami parameters for "Güllük"  
(water depth at the point is 16.8m) numerical gauge point according to selected tsunami scenarios

Selected Tsunami Scenario	Arrival time of first wave (min)	Arrival time of max wave (min)	Max (+)ve amp. (m)	Max (-)ve amp. (m)	Max current velocity (m/sec)	Max momentum flux (m <sup>3</sup> /s <sup>2</sup> /m)	Max discharge flux (m <sup>3</sup> /s/m)
seismic s18-z22	0	48	2.47	-2.19	0.32	1.27	4.60
caldera collapse of Santorini	84	150	0.76	-0.94	0.21	0.64	3.98
caldera collapse of Columbus	80	127	1.24	-1.12	1.03	2.39	7.76
caldera eruption of Columbus	78	265	2.31	-2.26	1.36	8.42	14.38

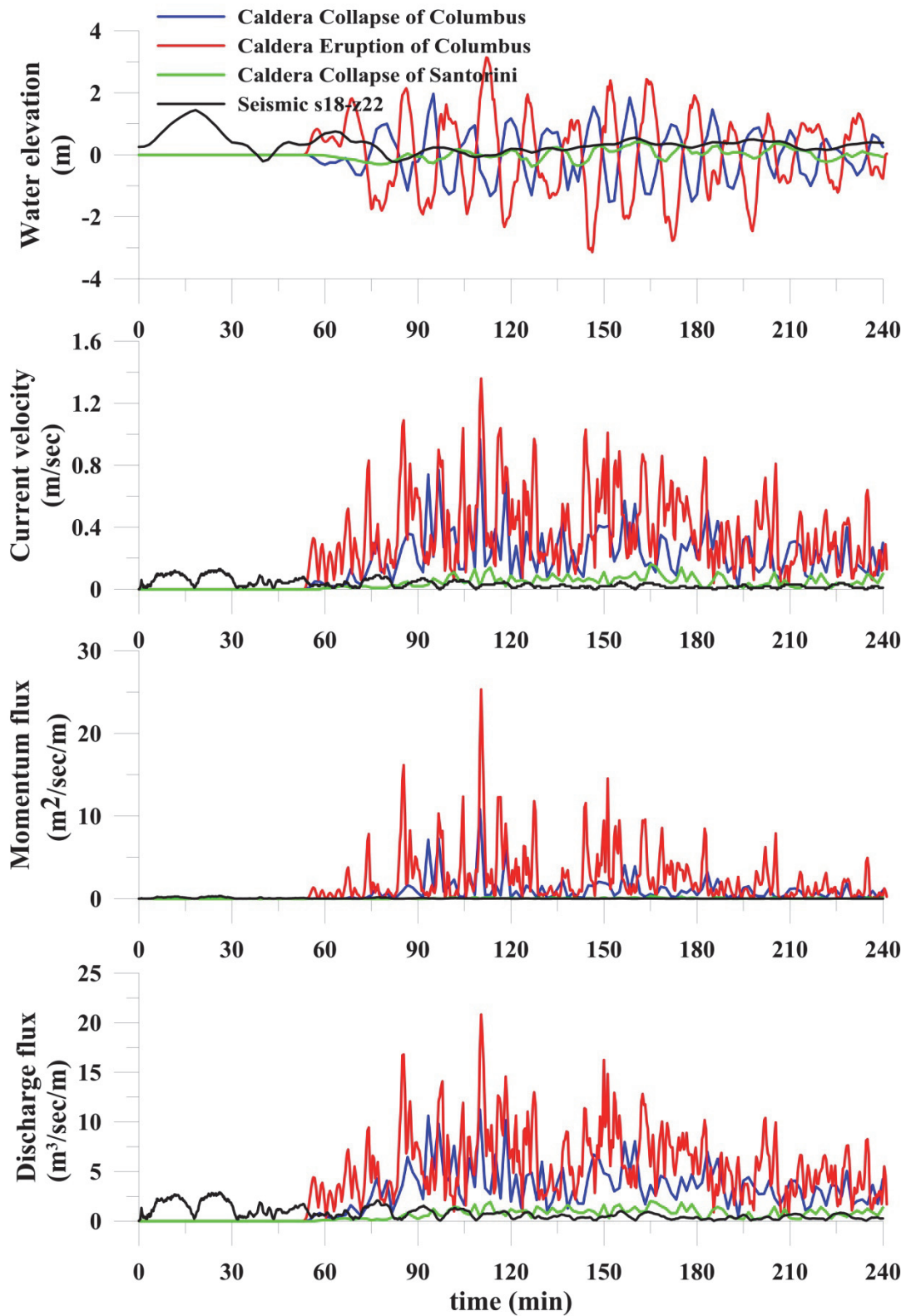


**Figure 4.21:** Wave characteristics for gauge point "Yalıkavak"  
(water depth at the point is 22.3m)

Yalıkavak is located at south-west of Güllük bay, and this region is open to wave effects that will come from southern Aegean Sea. In this respect, Yalıkavak marina, nearby touristic coastal utilities and residential areas become critical nodes in tsunami hazard analysis. Probable tsunami effects and inundation should also be examined in this region.

The time histories of water level fluctuations and computed near shore tsunami parameters at numerical gauge point near Yalıkavak is given in Figure 4.21. Tsunami from caldera eruption of Columbus has the largest wave amplitude around 3.2m, current velocity is around 1.4 m/sec, momentum flux is around 25 m<sup>3</sup>/sec<sup>2</sup>/m, and discharge flux is around 21 m<sup>3</sup>/sec/m at a point of 22.3m deep located near Yalıkavak (see Figure 4.21). Computed near shore tsunami parameters according to selected tsunami scenarios for "Fish farms" numerical gauge point are summarized in Table 4.17.

**Table 4.17:** Computed near shore tsunami parameters for "Yalıkavak" (water depth at the point is 22.3m) numerical gauge point according to selected tsunami scenarios

Selected Tsunami Scenario	Arrival time of first wave (min)	Arrival time of max wave (min)	Max (+)ve amp. (m)	Max (-)ve amp. (m)	Max current velocity (m/sec)	Max momentum flux (m <sup>3</sup> /s <sup>2</sup> /m)	Max discharge flux (m <sup>3</sup> /s/m)
seismic s18-z22	0	18	1.45	-0.24	0.13	0.34	2.89
caldera collapse of Santorini	57	162	0.44	-0.43	0.21	0.57	2.65
caldera collapse of Columbus	54	95	2.00	-1.84	1.03	12.50	12.33
caldera eruption of Columbus	53	112	3.17	-3.14	1.36	25.39	20.83

#### 4.4 Estimation of seismic tsunami sources according to 100, 500 and 1000 years return periods for Güllük bay (probabilistic approach)

Considering the earthquake magnitudes and the associated hazards, two main seismic belts attract considerable attention. One is the Pacific Seismic Belt surrounding the Pacific Ocean which is especially effective in Japan; and the other is the Himalayas–Mediterranean Seismic Belt that extends from Gibraltar to Indonesian Islands covering Turkey. A large portion of Turkey is in earthquake zone, since there are many small plates between the large plates in the region. Turkey is under the effect of three main plates known as Eurasian, Arabian and African Plates (Figure 4.22).

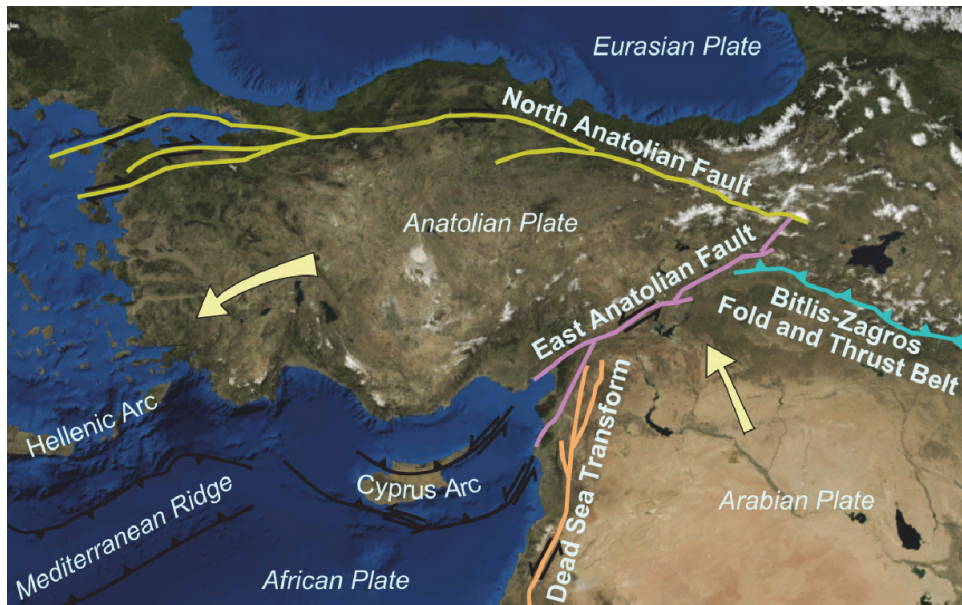


**Figure 4.22:** Location of plates and seismic dynamisms in Turkey  
([http://en.wikipedia.org/wiki/List\\_of\\_earthquakes\\_in\\_Turkey](http://en.wikipedia.org/wiki/List_of_earthquakes_in_Turkey))

African Plate dives beneath the Eurasian Plate (or Anadolu Plate, a part of it) in the Mediterranean Sea called as the Hellenic-Cyprus Arc. The Arabian Plate moves to the north compressing the Anatolian Plate. Bitlis-Zagros Suture Zone is formed as a result of this compression. The compression going on makes the Anatolian Plate move to west along the north and south fault lines. The north border of Anatolian

Plate is the North Anatolian Fault that 17 August 1999 Gölcük Earthquake has occurred. The East Anatolian Fault and the Hellenic-Cyprus Arc constitute the south border.

Turkey is located a seismically active area. Seismic hazard is mostly seen along the plate boundaries, but there has a remarkable earthquake risk almost whole part of the country. Boğaziçi University Kandilli Observatory and Earthquake Research Institute make daily seismic measurements and observations everywhere in the country by using electromagnetic seismographs and satellites. According to seismic measurements and historical data seismic activity in Turkey and surrounding area between 1900-2013 years are represented in Figure 4.23. <http://www.koeri.boun.edu.tr> web site includes instant and historical information about seismic activities in Turkey and surrounding area.

In this thesis, seismic activities for study region (35E, 23.3N and 37.5E, 35N) are taken from earthquake catalogue of Boğaziçi University Kandilli Observatory and Earthquake Research Institute's (KOERI) web site (<http://www.koeri.boun.edu.tr>) between years 1950-2014. Figure 4.24 represents the seismic activity in study region.

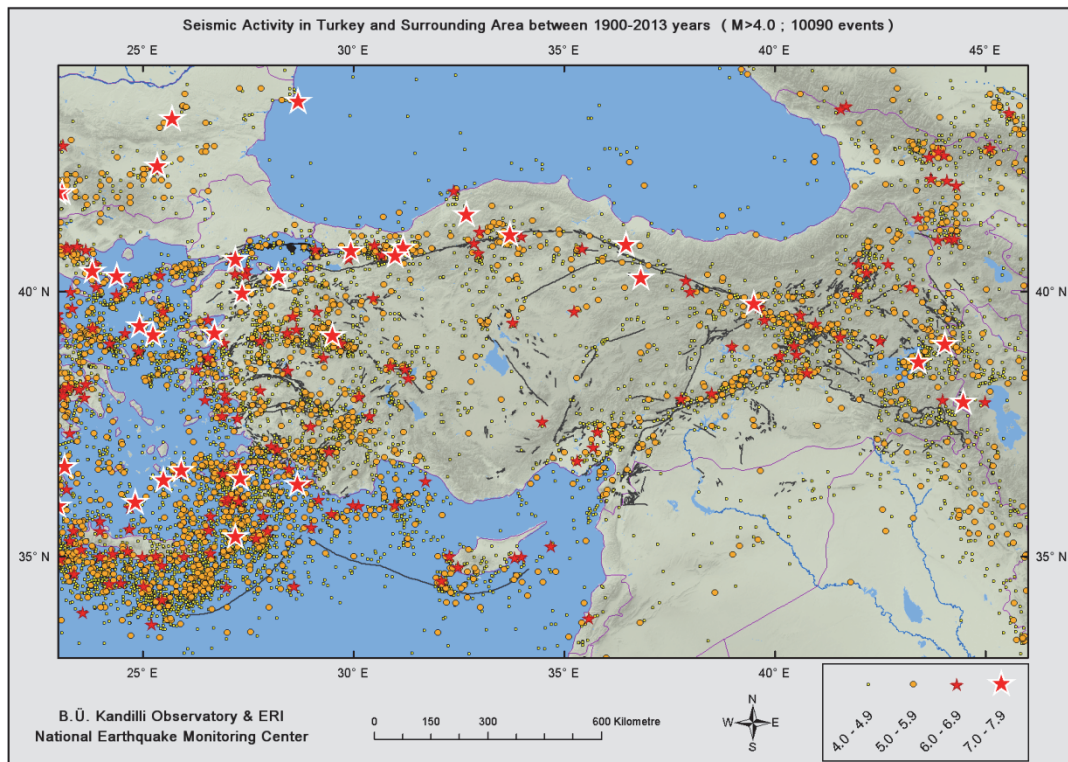


**Figure 4.23:** Seismic activity in Turkey and surrounding area between 1900-2013 years (<http://www.koeri.boun.edu.tr>)

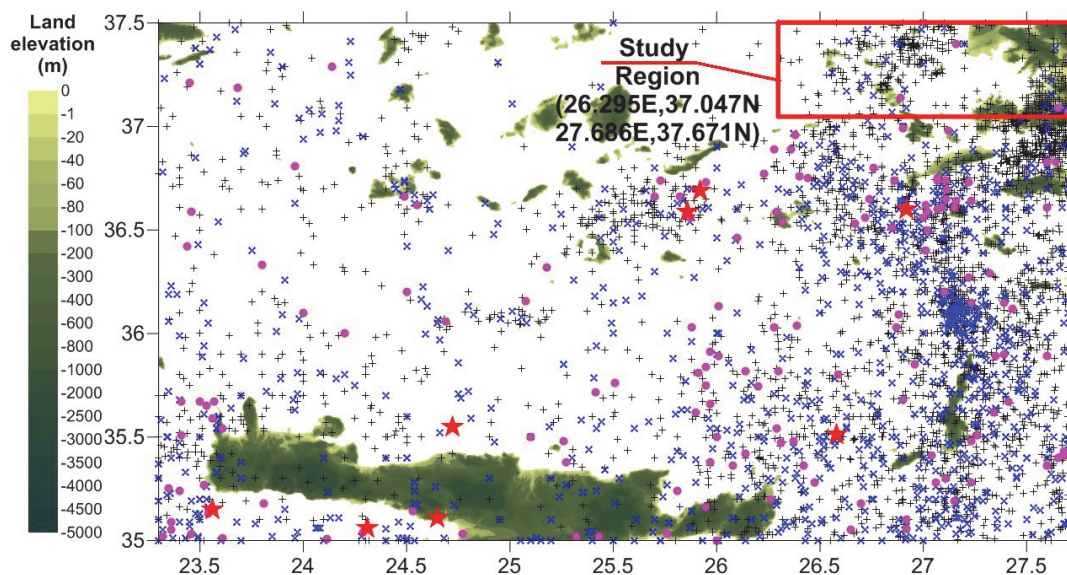


**Figure 4.24:** Epicenters of the earthquakes with the magnitudes  $M > 3$  and in southern part of Aegean Sea between 1950-2014 years (+ symbols show  $3 < M < 3.99$ , x symbols show  $4 < M < 4.99$ , • symbols show  $5 < M < 5.99$ , red star symbols show  $M > 7$ )

Kalafat et al. (2009) includes the source parameters of strong earthquakes catalogue for Turkey and surrounding area. This catalogue is used to define estimated rupture parameters of seismic source that can be effective for probabilistic hazard analysis of Güllük bay. Source parameters of historical earthquakes according to the source parameters of strong earthquakes catalogue (Kalafat et al., 2009) cannot be used in probabilistic approach due to missing data in some years between 1938-2008 years. Data continuity is preferred during extreme value statistics to obtain more accurate results. Source parameters of recent earthquakes between 1938-2008 years in the study region are given in Appendix - A (Kalafat et al., 2009).

Historical earthquakes give an idea about frequency, magnitude and epicenter of probable earthquakes around a specified region. Historical data gives an opportunity of estimating rupture parameters of a seismic source. Evaluation of probabilities and frequencies of seismic activities will give probable earthquakes with their rupture parameters. In this section, probabilistic tsunami hazard analysis is done by using extreme value statistics with historical seismic data in study region.

#### **4.4.1 Extreme value statistics**

Analysis of extremes is a need to design safer structures in civil engineering. Flood discharges for floodwalls, hurricane winds for suspension bridges, storm surge heights for coastal structures are examples of requirement of extreme values in civil engineering. In this study, extreme value analysis is done to find probable maximum earthquake magnitudes within a period of years for Güllük region.

First step of extreme value statistics is selection of the highest earthquake magnitudes in each year in the selected region. Seismic data of earthquakes (KOERI's data between years 1950-2014) is filtered and the earthquakes whose magnitudes are greater than 4 are selected. Maximum earthquake magnitudes of

each year are selected as a representative value of that year in extreme value statistics. These sets of data are called as *sample* during statistical analysis.

Fitting of samples can be done with many theoretical distribution functions in extreme value analysis. It is a good method that applying different functions to the sample, and selecting most probable distribution which is the best-fit one. Distribution functions that are using in extreme value analysis are given below.  $F(x)$  denotes cumulative distribution,  $f(x)$  represents probability density function, and  $x$  represents extreme variate (for this study it denotes earthquake magnitude ( $M_w$ )).

- Fisher-Tippett type-I (FT-I) or Gumbel distribution

$$F(x) = \exp \left[ -\exp \left( -\frac{x-B}{A} \right) \right] : -\infty < x < \infty$$

- Fisher-Tippett type-II (FT-II) or Frechét distribution

$$F(x) = \exp \left[ -\left( 1 + \frac{x-B}{kA} \right)^{-k} \right] : B - kA \leq x < \infty$$

- Weibull distribution

$$F(x) = 1 - \exp \left[ -\left( -\frac{x-B}{A} \right)^k \right] : -B \leq x < \infty$$

- Lognormal distribution

$$f(x) = \frac{1}{\sqrt{2\pi}Ax} \exp \left[ -\left( \frac{(\ln x - B)^2}{2A^2} \right)^k \right] : 0 < x < \infty$$

where  $A$ : scale parameter (linear scale of  $x$ )



$B$ : location parameter (fixes the location of the axis of  $x$ )

$k$ : shape parameter (functional shape of distribution)

Modes, means and standard deviations of those distributions are given in Table 4.18.

**Table 4.18:** Characteristics of distribution functions for extreme value analysis

Distribution	Mode	Mean	Standard Deviation
<b>FT-II</b>	$B + kA \left[ \left( \frac{k}{1+k} \right)^{1/k} - 1 \right]$	$B + kA \left[ \Gamma \left( 1 - \frac{1}{k} \right)^{1/k} - 1 \right]$	$kA \left[ \Gamma \left( 1 - \frac{2}{k} \right) - \Gamma^2 \left( 1 - \frac{1}{k} \right) \right]^{1/2}$
<b>FT-I</b>	<b>B</b>	<b>B+A<math>\gamma</math></b>	$\frac{\pi}{\sqrt{6}} A$
<b>Weibull</b>	$B + A \left( 1 - \frac{1}{k} \right)^{1/k}$	$B + A \Gamma \left( 1 + \frac{1}{k} \right)$	$A \left[ \Gamma \left( 1 + \frac{2}{k} \right) - \Gamma^2 \left( 1 + \frac{1}{k} \right) \right]^{1/k}$
<b>Lognormal</b>	$\exp(B - A^2)$	$\exp \left( B + \frac{A^2}{2} \right)$	$\exp \left( B + \frac{A^2}{2} \right) (\exp A^2 - 1)^{1/2}$

*\* $\Gamma(\cdot)$  is gamma function,  $\gamma$  is Euler constant (0.5772)*

A sample of data is needed to arrange with plotting position formulas. An unbiased plotting position formula varies based on applied distribution function. The plotting position formula is given in following expression:

$$F_{(m)} = 1 - \frac{m - \alpha}{N + \beta}, m = 1, 2, \dots, N$$

where  $N$ : number of sample data

$\alpha, \beta$ : constants

$\alpha, \beta$  constants of unbiased plotting position formula are given in Table 4.19 for different distribution functions (Goda, 2000).

**Table 4.19:** Constants  $\alpha$ ,  $\beta$  of unbiased plotting position formula

<b>Distribution</b>	<b><math>\alpha</math></b>	<b><math>\beta</math></b>
FT-II	$0.44+0.52/k$	$0.12-0.11/k$
FT-I	0.44	0.12
Weibull	$0.20+0.27/k^{1/2}$	$0.20+0.23/k^{1/2}$
Normal	0.375	0.25
Lognormal	0.375	0.25

Gumbel distribution is selected as theoretical distribution function for extreme value analysis due to giving best-fitted results with available earthquake magnitude data. Results of extreme value statistics are given in Figure 4.25 with different return periods (2, 5, 10, 20, 50, 100, 200, 500, 1000, 2000, 5000, 10000 years).

Earthquake magnitudes ( $M_w$ ) with return periods of 100, 500 and 1000 years are selected from extreme value analysis results to be used in probabilistic tsunami hazard analysis in Güllük bay.  $M_w$  is selected as 7.4, 8.2 and 8.5 for return periods of 100, 500 and 1000 years respectively.

Seismic activities that occurred in Güllük bay between years 1950-2014 are used in extreme value analysis. Results of extreme value statistics represent the maximum earthquake magnitudes for different return periods in Güllük bay. In the estimation of rupture parameters for numerical modeling, those maximum earthquakes are assumed to occur in selected fault which is same with deterministic approach (seismic source s18-z22).

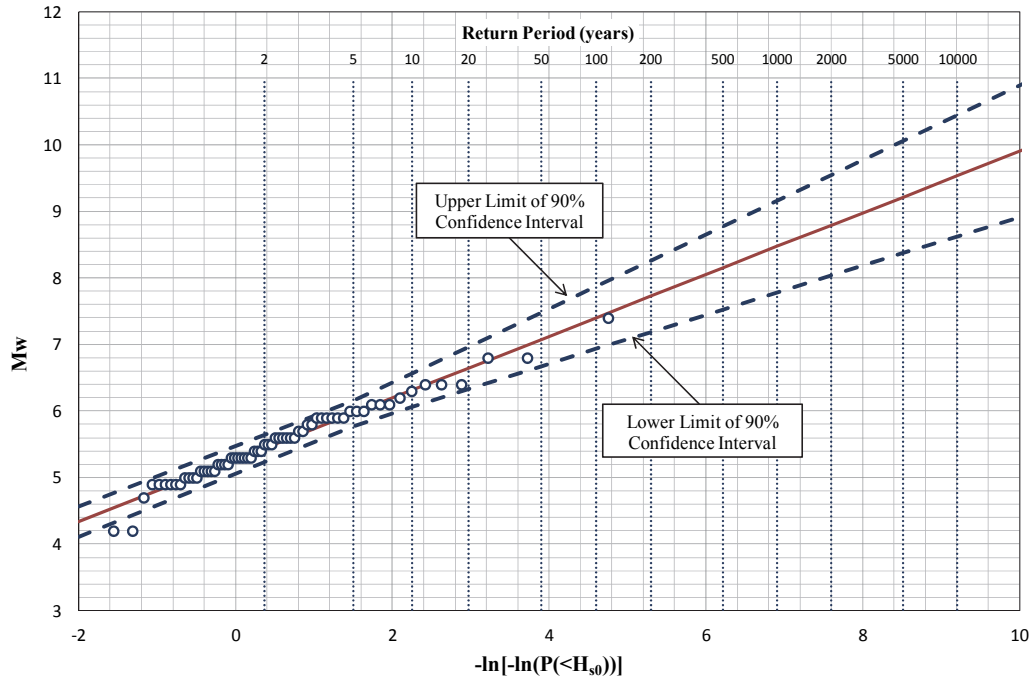


**Figure 4.25:** Results of extreme value statistics for probable earthquake magnitudes ( $M_w$ ) in the study region with different return periods

#### 4.4.2 Poisson Distribution

In seismology, the Gutenberg–Richter law expresses the relationship between the magnitude and total number of earthquakes in any selected region. Available earthquake data are filtered to represent study region with boundary coordinates 26.295E,37.047N and 27.686E,37.671N (see Figure 4.24). Relationship between earthquake magnitude and total number of earthquakes is expressed as:

$$\log N = a - bM$$

where

$N$ : number of events having a magnitude  $>M$

$a, b$ : constants

Frequency analysis is performed for available earthquake data with 0.2 magnitude intervals (see Table 4.20). According to results, relationship between magnitude and frequency is represented in Figure 4.25.

**Table 4.20:** Magnitude-frequency analysis according to Gutenberg–Richter law

M	N	N/P	Log(N/P)
4.0	42	0.6462	-0.1897
4.2	31	0.4769	-0.3216
4.4	22	0.3385	-0.4705
4.6	17	0.2615	-0.5825
4.8	9	0.1385	-0.8587
5.0	3	0.0462	-1.3358
5.2	3	0.0462	-1.3358
5.4	2	0.0308	-1.5119
5.6	1	0.0154	-1.8129
5.8	1	0.0154	-1.8129
6.0	1	0.0154	-1.8129
6.2	1	0.0154	-1.8129
6.6	1	0.0154	-1.8129
6.6	1	0.0154	-1.8129
6.8	1	0.0154	-1.8129

\*Catalog Period (P): 65

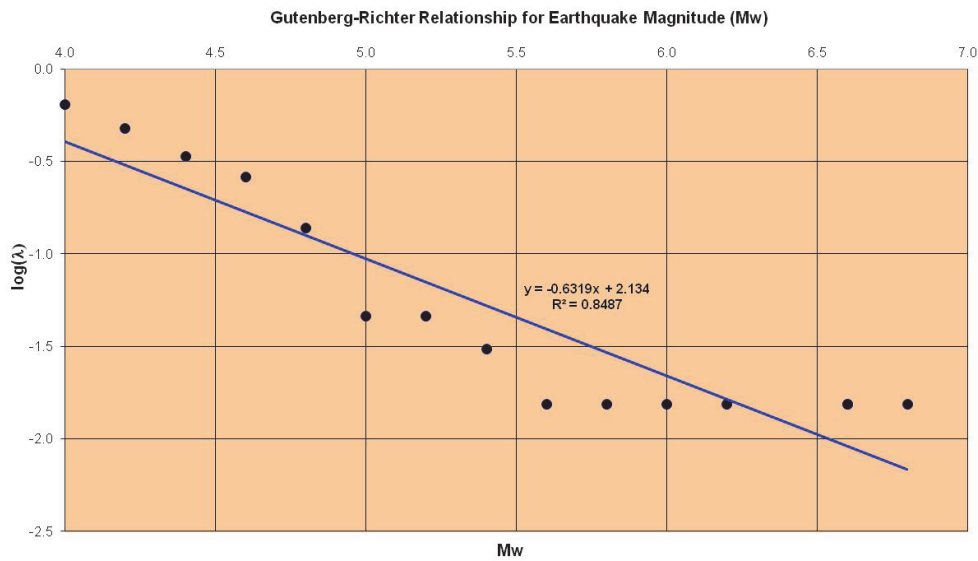


**Figure 4.26:** Gutenberg-Richter relationship for earthquake magnitude (Mw)

Poisson distribution is widely used in probabilistic analysis of seismic events. Occurrence probability of a specified earthquake magnitude in a specified return period is described with following expressions in Poisson distribution. Probable

earthquake magnitudes with 100, 500 and 1000 years return periods for Güllük bay are computed by using Poisson distribution (see Table 4.21).

$$\lambda=10^{a-bM}$$

$$\lambda=1/Rp$$

where

$\lambda$ : occurrence probability of an event in a specified period ( $0 \leq \lambda \leq 1$ )

$Rp$ : return period

$a, b$ : regression coefficients that obtained from Gutenberg–Richter relationship

$M$ : earthquake magnitude

**Table 4.21:** Probable earthquake magnitudes with 100, 500 and 1000 years return periods according to Poisson distribution

<b>Rp (yr)</b>	<b><math>\lambda</math></b>	<b>Mw</b>
100	0.01	6.5
500	0.002	7.6
1000	0.001	8.0

Extreme Value Statistics and Poisson Distribution are performed to estimate probable earthquake magnitudes with 100, 500 and 1000 years return periods. Largest magnitude for each year is selected in Extreme Value Statistics from KOERI's data; however, there has no seismic activity greater than 3 in each year between years 1950-2014 in study region. Therefore, wider boundary coordinates are selected to perform Extreme Value Statistics. Boundaries which represent study region and wider domain for Extreme Value Statistics are shown in Figure 4.24. Boundary which represents study region is used in Poisson distribution. Different boundary coordinates are used in Extreme Value Statistics and Poisson distribution, therefore comparison of these approaches is impracticable for this study.

In this study, Extreme Value Statistics are preferred to obtain larger effects of co-seismic tsunamis for Güllük bay with 100, 500 and 1000 years return periods. Poisson distribution is widely used approach for seismic events, therefore it is performed in this study to guide future seismic hazard assessments. Comparison of

Poisson distribution and Extreme Value Statistics can be done for a specified region with same boundary coordinates in further assessments.

#### **4.4.3 Determination of rupture parameters for seismic source (s18-z22) according to 100, 500 and 1000 years return periods**

Probable earthquake magnitudes in Güllük region are obtained from extreme value statistics according to return periods of 100, 500 and 1000 years. Rupture parameters should be known to analyze probable seismic based tsunami hazards in study region. Epicenter of earthquake, length and width of fault, focal depth, displacement, strike, dip and rake angles should be obtained to define initial wave from probable seismic source.

Different approaches have been used to obtain length (L), width (W) and displacement (u) of the fault from earthquake magnitude ( $M_w$ ). Empirical relationships between  $M_w$  and L-W-u are given below for different approaches.

Seismic Moment ( $M_o$ ) is a quantity that links between earthquake magnitude and rupture parameters. Seismic Moment is calculated from following equation:

$$M_o = \mu u_{ave} A$$

*where  $\mu$ : shear modulus (usually  $3 \times 10^{11}$  dyne/cm<sup>2</sup> for crustal faults as recommended in Hanks and Kanamori (1979)),  
 $u_{ave}$ : is the average displacement across fault surface,  
 $A$ : area of ruptured fault surface.*

Hanks and Kanamori (1979) relates  $M_o$  and  $M_w$  with following empirical equation:

$$M_w = 2/3 \log M_o - 10.7$$

Wells and Coppersmith (1994) developed empirical relationships by compiling the source parameters such as seismic moment ( $M_o$ ), moment magnitude ( $M_w$ ), length (L) and width of fault (W) and surface displacement (u) for the 244 earthquakes worldwide. Log-linear regressions were well correlated between  $M_w$ , L, W, A and u in the light of database. Following equation of is used in this study to determine  $M_w$  from rupture area (Wells and Coppersmith, 1994).

$$M_w = 1.02 \log(A) + 3.93$$

Konstantinou et al. (2005) defines a new empirical relationship between earthquake magnitude and area of ruptured fault surface, and this relationship is given below. Table 4.22 presents another relationships between rupture length, width, area and earthquake magnitude according to Konstantinou et al. (2005).

$$M_w = 1.23 * \log(A) + 3.17$$

**Table 4.22:** Empirical relationships between  $M_w$  and log (L, W, A)

	Relationship	Region	Validity
Subsurface Rupture Length	$\log L = -2.44 + 0.59 M_w$	Global	4.8-8.1
Subsurface Rupture Width	$\log W = -1.01 + 0.32 M_w$	Global	4.8-8.1
Surface Rupture Length	$\log l = -3.22 + 0.69 M_w$	Global	5.2-8.1
Rupture Area	$\log A = -3.49 + 0.91 M_w$	Global	4.8-7.9

Hanks and Bakun (2002) computes  $M_w$  values for the large earthquake scaling, rupture area of more than 1000km<sup>2</sup> and earthquake magnitude of greater than 7. The seismic moment  $M_o$  for rectangular and strike –slip faults is defined as:

$$M_o = \mu u L W$$

where  $\mu$ : shear modulus ( $3 * 10^{11}$  dyne/cm<sup>2</sup>)

Hanks and Bakun (2002) proposes the following relation for  $A > 537 \text{ km}^2$ :

$$M_w = (4/3) \log (A) + (3.07 \pm 0.04)$$

Probable earthquake magnitudes according to 100, 500 and 1000 years return periods are obtained from extreme value analysis. Rupture parameters (dimensions of the fault plane and slip displacement) are defined by using different approaches that explained above. Computed rupture parameters ( $M_0$ , L, W, A, u) are given in Table 4.23.

**Table 4.23:** Computed rupture parameters (L, W, u) from  $M_w$  with different empirical relationships

Rp (years)	Mw	"Mo" and "u" from Hanks and Kanamori		"A" from Wells&Coppersmith (1994)			"L&W" from Konstantinou et al. (2005)		"A" from Konstantinou et al. (2005)			"A" from Hanks and Bakun (2002)		
		M <sub>0</sub>	u (m)	A (km <sup>2</sup> )	L (m)	W (m)	L (km)	W (km)	A (km <sup>2</sup> )	L (m)	W (m)	A (km <sup>2</sup> )	L (m)	W (m)
100	7.4	1.41E+27	3.49	2 523	120	21	84	23	1 754	120	15	1 995	120	17
500	8.2	2.24E+28	9.69	15 356	120	128	250	41	9 376	120	78	7 943	120	66
1000	8.5	6.31E+28	12.37	30 227	120	252	376	51	17 579	120	146	13 335	120	111

Dimensions and surface displacement of fault (L,W and u) are computed from different empirical equations that explained in previous part. Dimensions of fault are selected in the light of rupture parameters of historical earthquakes (Yalciner et al., 2008).

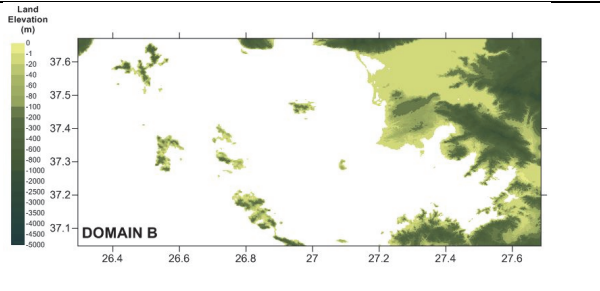
Epicenter of earthquake is selected as same with deterministic s18-z22 source. Strike angle and focal depth of fault is also selected as same with deterministic s18-z22 source according to similarity between s18-z22 source rupture parameters and average values of Kalafat et al. (2009) data in the study region.

Dip and rake angles are selected as 45° that same with deterministic s18-z22 source. However, the seismic data (Kalafat et al., 2009) shows different depending



angles of some earthquakes whose epicenter is near Güllük bay. Therefore the effect of rake angle on the amplitude of tsunami source is tested by using two different values of rake angles as  $45^\circ$  and  $-45^\circ$ . Testing simulations are done with two different rake angles for deterministic s18-z22 tsunami source. Map of sources are presented together with its rupture parameters (see Figures 4.27 and 4.28). Simulation duration is selected as 4 hours. Single Domain B with 30m grid size is used as bathymetric/topographic data. Domain B is presented with its boundary coordinates in Table 4.24.

**Table 4.24:** Domain B with its boundary coordinates for probabilistic approach

<i>Boundary Coordinates of Domain B</i>		
Left Longitude ( $^\circ$ )	26.295E	
Right Longitude ( $^\circ$ )	27.686E	
Bottom Latitude ( $^\circ$ )	37.047N	
Top Latitude ( $^\circ$ )	37.671N	
Resolution (m)	30	

Comparison of simulation results for rake angle is  $45^\circ$  and  $-45^\circ$  are given in Figure 4.26 and Figure 4.27 respectively. As it can be seen from simulation results, distribution of tsunami parameters are closer to each other, therefore the rake angle is selected as  $45^\circ$  (same with deterministic approach) in the simulations for the return periods 100, 500 and 1000 years in probabilistic tsunami hazard analysis.

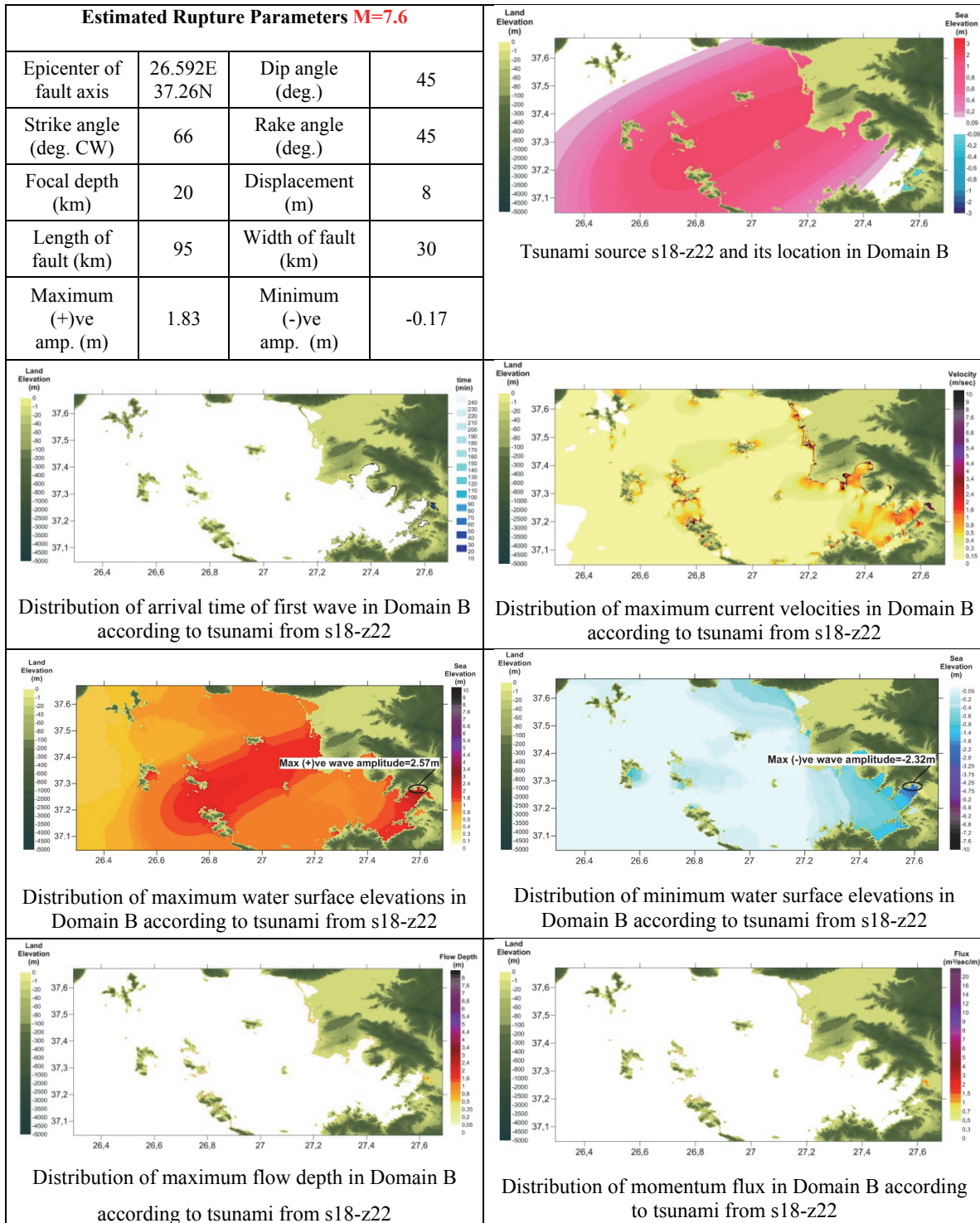


**Figure 4.27:** Tsunami parameters due to tsunami source s18-z22 with  $45^\circ$  rake angle according to simulation duration of 240 min

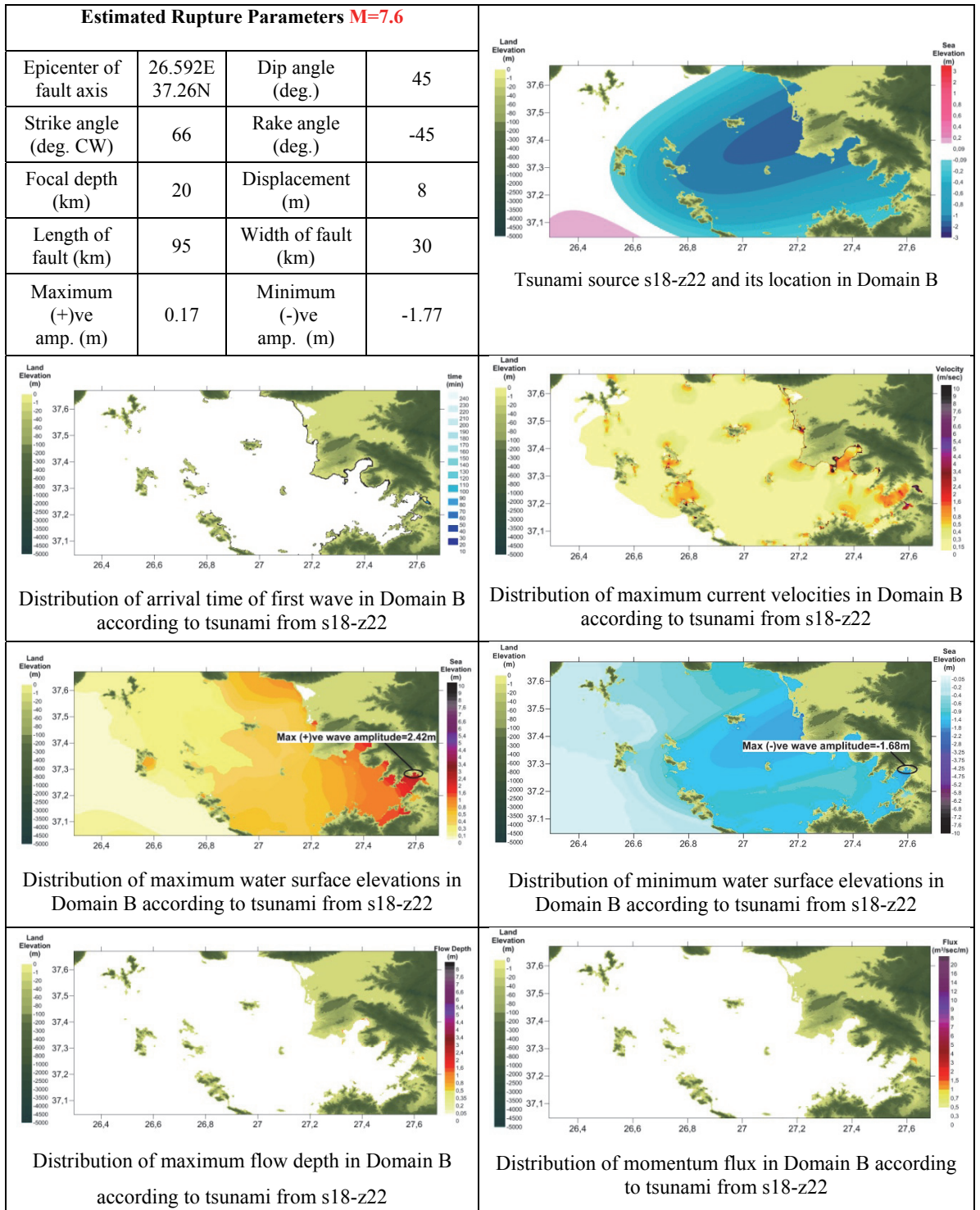


**Figure 4.28:** Tsunami parameters due to tsunami source s18-z22 with  $-45^\circ$  rake angle according to simulation duration of 240 min

In the light of previous discussions, the estimated rupture parameters for seismic source (s18-z22) according to 100, 500 and 1000 years return periods are defined and summarized in Table 4.25. The rupture parameters and the visualization of initial wave are given for each selected tsunami source between Tables 4.26 and 4.28.

**Table 4.25:** The estimated rupture parameters for seismic source (s18-z22) according to 100, 500 and 1000 years return periods

Rp (years)	Mw	Epicenter	u (m)	L (m)	W (m)	Focal depth (m)	Strike angle	Dip angle	Rake angle	Max (+)ve wave amplitude (m)	Max (-)ve wave amplitude (m)
100	7.4	26.592E, 37.26N	3.5	90	15	20	66	45	45	0.51	-0.07
500	8.2	26.592E, 37.26N	9.7	220	35	20	66	45	45	2.43	-0.08
1000	8.5	26.592E, 37.26N	12.4	340	50	20	66	45	45	3.65	-0.12

**Table 4.26:** The estimated rupture parameters and initial sea state of seismic tsunami source (s18-z22) according to 100 years return period

Estimated Rupture Parameters <b>M=7.4</b>			
Epicenter of fault axis	26.592E 37.26N	Dip angle (deg.)	45
Strike angle (deg. CW)	66	Rake angle (deg.)	45
Focal depth (km)	20	Displacement (m)	3.5
Length of fault (km)	90	Width of fault (km)	15
Maximum (+)ve amp. (m)	0.51	Minimum (-)ve amp. (m)	-0.07

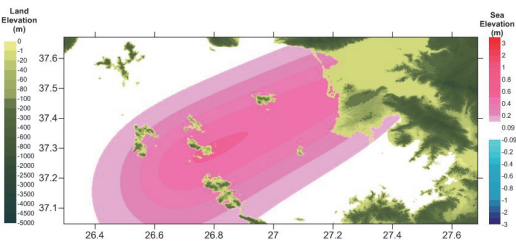


**Table 4.27:** The estimated rupture parameters and initial sea state of seismic tsunami source (s18-z22) according to 500 years return period

Estimated Rupture Parameters <b>M=8.2</b>			
Epicenter of fault axis	26.592E 37.26N	Dip angle (deg.)	45
Strike angle (deg. CW)	66	Rake angle (deg.)	45
Focal depth (km)	20	Displacement (m)	9.7
Length of fault (km)	220	Width of fault (km)	35
Maximum (+)ve amp. (m)	2.43	Minimum (-)ve amp. (m)	-0.08

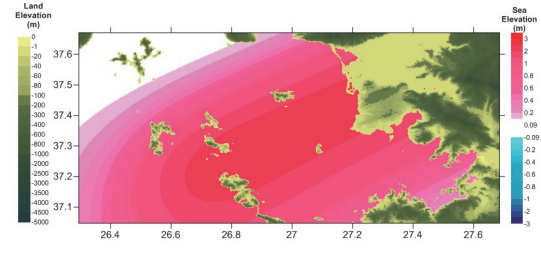
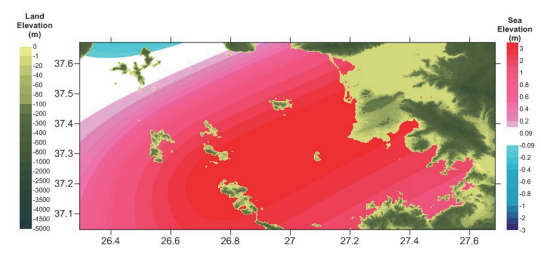


**Table 4.28:** The estimated rupture parameters and initial sea state of seismic tsunami source (s18-z22) according to 1000 years return period

Estimated Rupture Parameters <b>M=8.5</b>			
Epicenter of fault axis	26.592E 37.26N	Dip angle (deg.)	45
Strike angle (deg. CW)	66	Rake angle (deg.)	45
Focal depth (km)	20	Displacement (m)	12.4
Length of fault (km)	340	Width of fault (km)	50
Maximum (+)ve amp. (m)	3.65	Minimum (-)ve amp. (m)	-0.12



#### 4.4.4 Simulations of probable seismic tsunami sources according to 100, 500 and 1000 years return periods

240 min tsunami simulation gives time histories of water surface fluctuations, wave amplitudes at every grid point, inundation and runup on the shore for single Domain B. Wave characteristics such as water elevation, current velocity, flux, Froude number are plotted for selected numerical gauge points, and Surfer<sup>®</sup> version 12 is used to take snapshots of any time for nested domains.

In this section, tsunami simulations are done for seismic source (s18-z22) according to 100, 500 and 1000 years return periods for probabilistic tsunami hazard analysis. Sources are presented in a frame with its fault parameters and the plot of initial wave occurred due to the rupture (see Tables 4.26, 4.27 and 4.28). Simulation duration is selected as 4 hours. This time is sufficient to see the maximum effects of potential tsunamis in Güllük bay. Single Domain B with 30m grid size is used as bathymetric/topographic data (see Table 4.17).

Tsunami parameters (the distribution of maximum and minimum water surface elevations, the distribution of arrival time of first wave, the maximum current velocity, the maximum flow depth and momentum flux on land) and the output data at selected numerical gauge points are presented for the simulated sources. Sea level changes at different time steps are visualized to identify wave's generation, propagation and reach the coast for selected tsunami scenario. Location of the numerical gauge points are given in Figure 4.17, coordinates and depths of the numerical gauge points are given in Table 4.13.

#### **Propagation of tsunami according to seismic source (s18-z22) with 100 years return period**

Wave propagation of the tsunami due to seismic source (s18-z22) according to 100 years return period is simulated for the simulation duration 240 min. The computed sea states at different time steps ( $t=30, 60, 120, 150, 180$  and 240 min) in Domain B are represented in Figure 4.29.

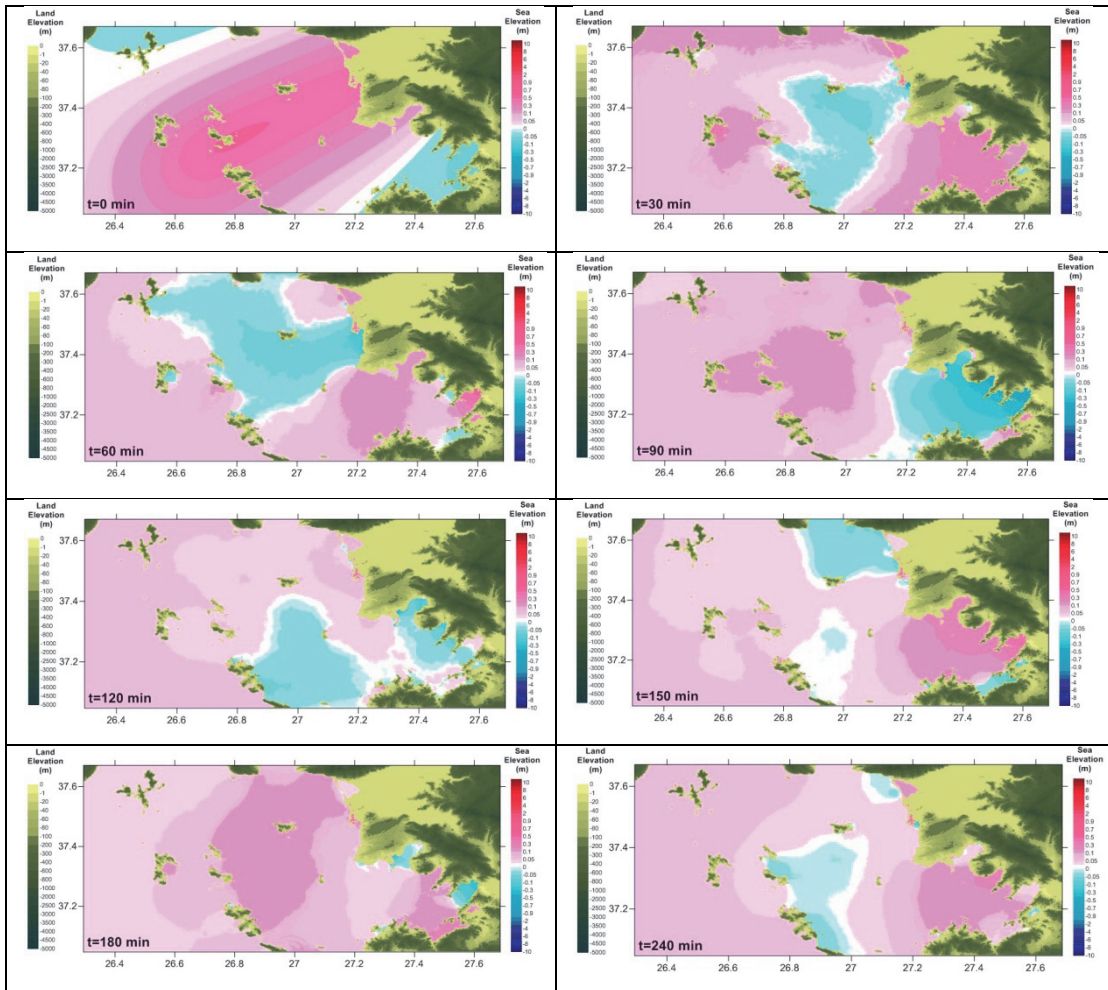


**Figure 4.29:** Sea states at different time steps ( $t=30, 60, 120, 150, 180$  and  $240$  min) in Domain B according to s18-z22 with 100 years return period

**Tsunami parameters according to seismic source (s18-z22) with 100 years return period**

The computed distribution of tsunami parameters due to seismic tsunami source s18-z22 according to 100 years return period in Domain B is shown in Figure 4.30.

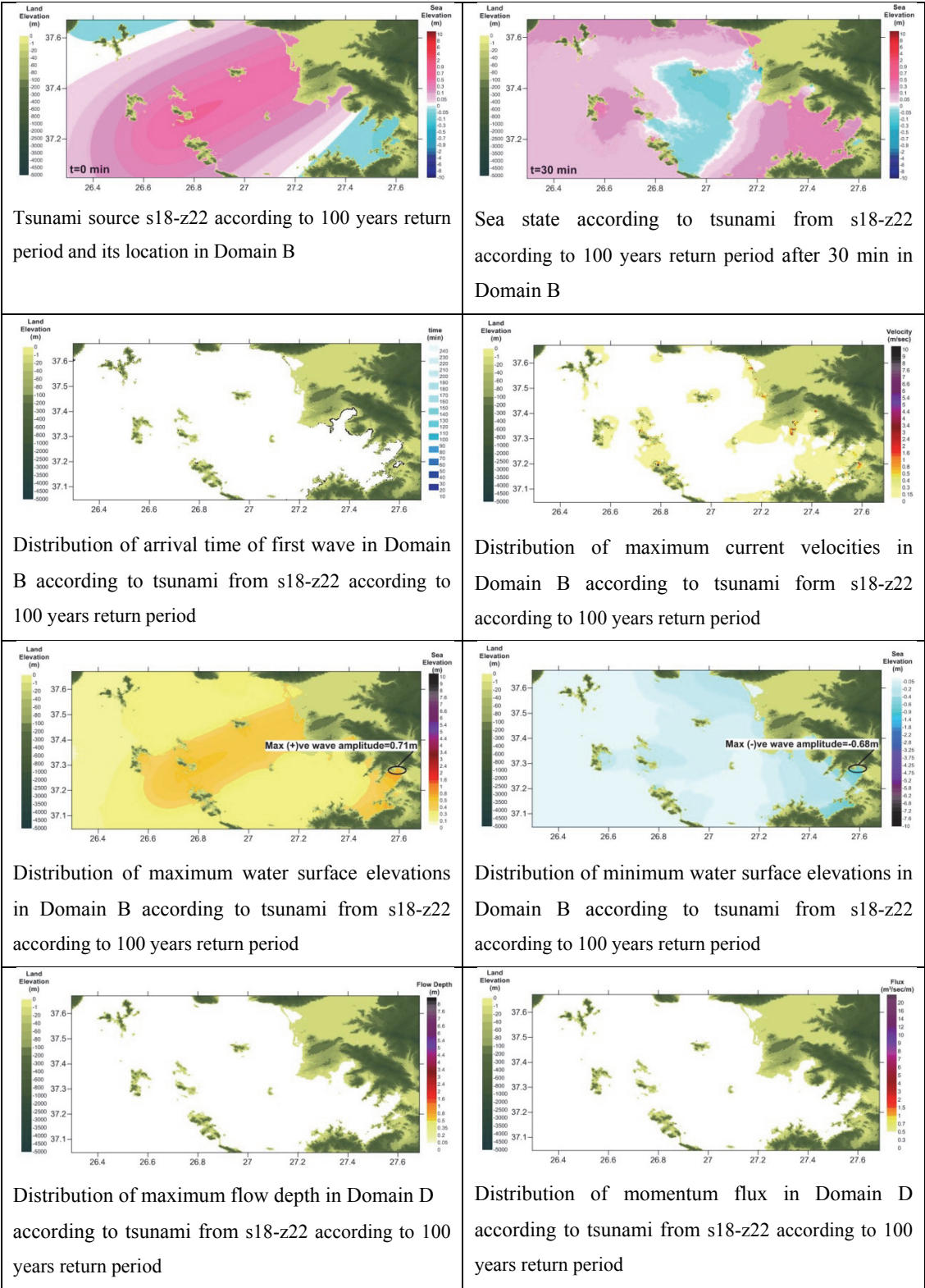


**Figure 4.30:** Tsunami parameters due to tsunami source s18-z22 according to 100 years return period for simulation duration of 240 min



First wave arrives the coast shortly after tsunami source (s18-z22 according to 100 years return period) is generated. Maximum positive wave amplitude is computed as 0.71m, and maximum negative wave amplitude is computed as -0.68m around Güllük region (see Figure 4.30).

**Propagation of tsunami according to seismic source (s18-z22) with 500 years return period**

Wave propagation of the tsunami due to seismic source (s18-z22) according to 500 years return period is simulated for the simulation duration 240 min. The computed sea states at different time steps ( $t=30, 60, 120, 150, 180$  and 240 min) in Domain B are represented in Figure 4.31.

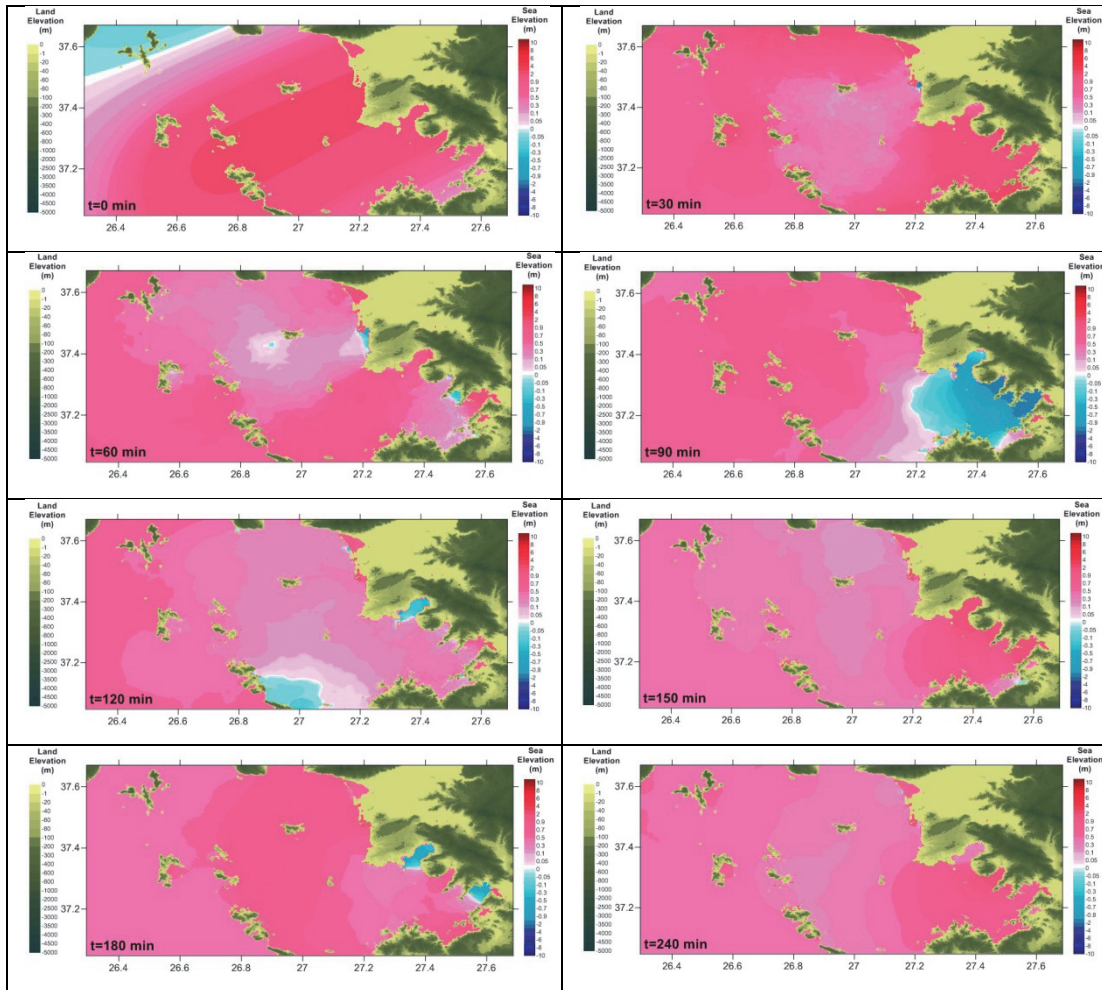


**Figure 4.31:** Sea states at different time steps ( $t=30, 60, 120, 150, 180$  and  $240$  min) in Domain B according to s18-z22 with 500 years return period

**Tsunami parameters according to seismic source (s18-z22) with 500 years return period**

The computed distribution of tsunami parameters due to seismic tsunami source s18-z22 according to 500 years return period in Domain B is shown in Figure 4.32.

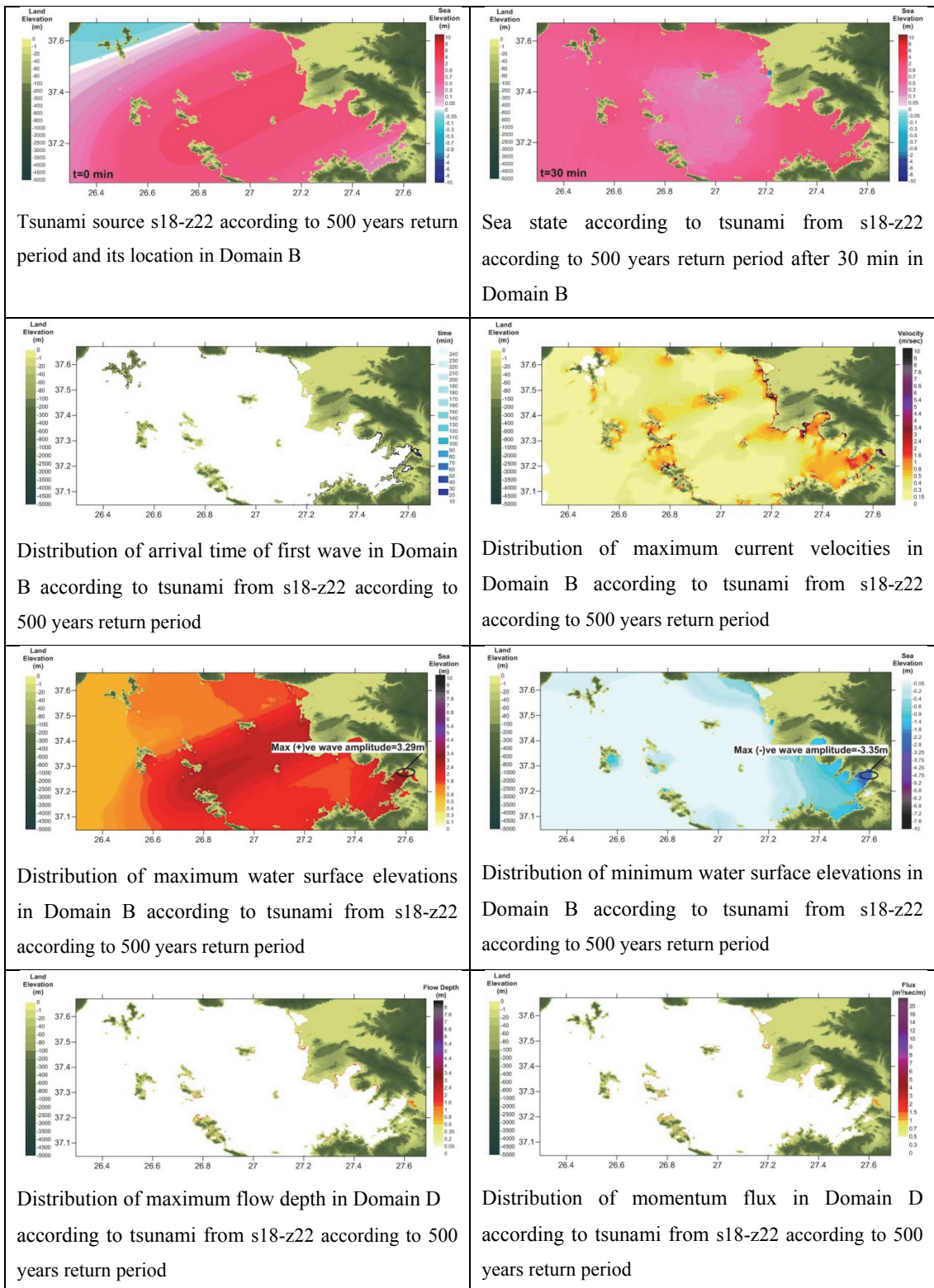


**Figure 4.32:** Tsunami parameters due to tsunami source s18-z22 according to 500 years return period for simulation duration of 240 min

First wave arrives the coast shortly after tsunami source (s18-z22 according to 500 years return period) is generated. Maximum positive wave amplitude is computed as 3.29m, and maximum negative wave amplitude is computed as -3.35m around Güllük region (see Figure 4.32).

**Propagation of tsunami according to seismic source (s18-z22) with 1000 years return period**

Wave propagation of the tsunami due to seismic source (s18-z22) according to 1000 years return period is simulated for the simulation duration 240 min. The computed sea states at different time steps ( $t=30, 60, 120, 150, 180$  and 240 min) in Domain B are represented in Figure 4.33.

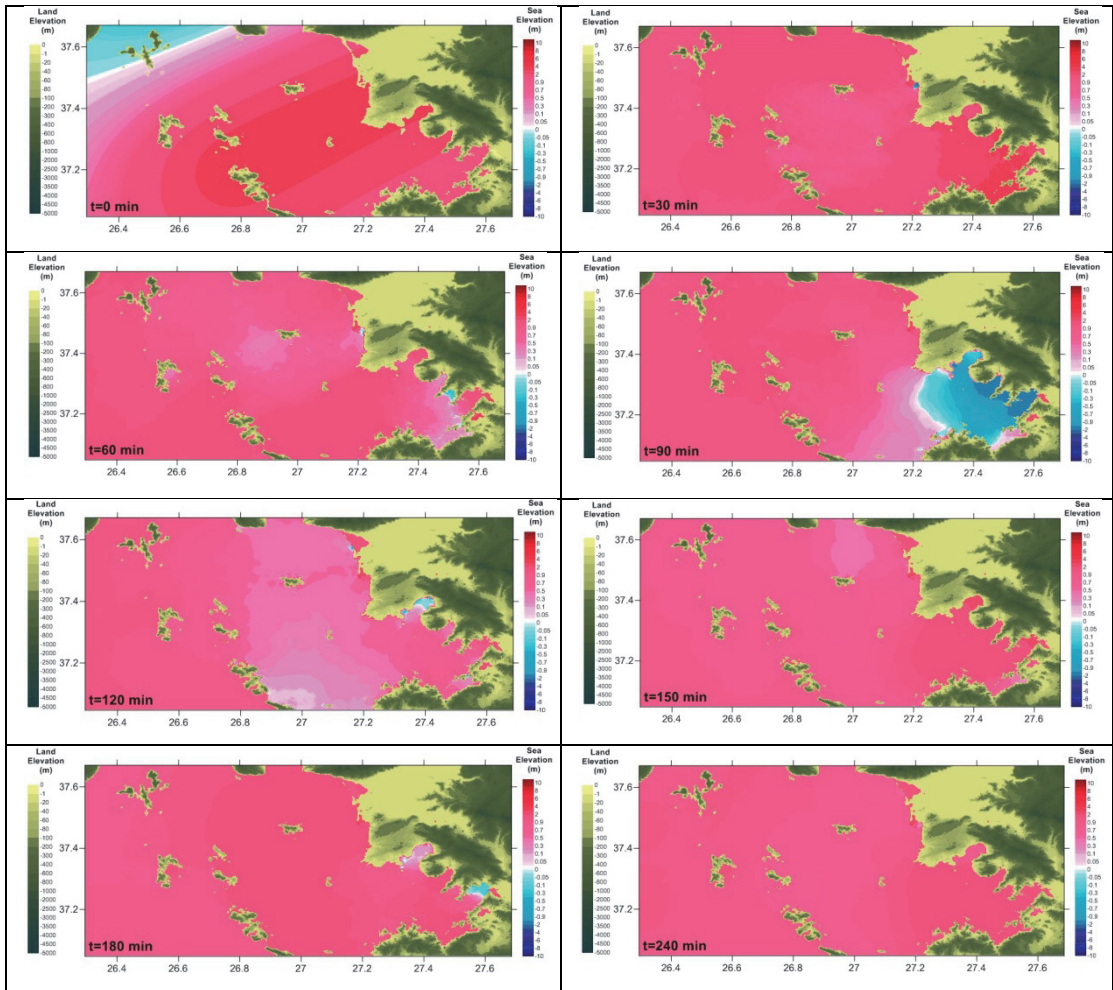


**Figure 4.33:** Sea states at different time steps ( $t=30, 60, 120, 150, 180$  and  $240$  min) in Domain B according to s18-z22 with 1000 years return period

**Tsunami parameters according to seismic source (s18-z22) with 1000 years return period**

The computed distribution of tsunami parameters due to seismic tsunami source s18-z22 according to 1000 years return period in Domain B is shown in Figure 4.34.

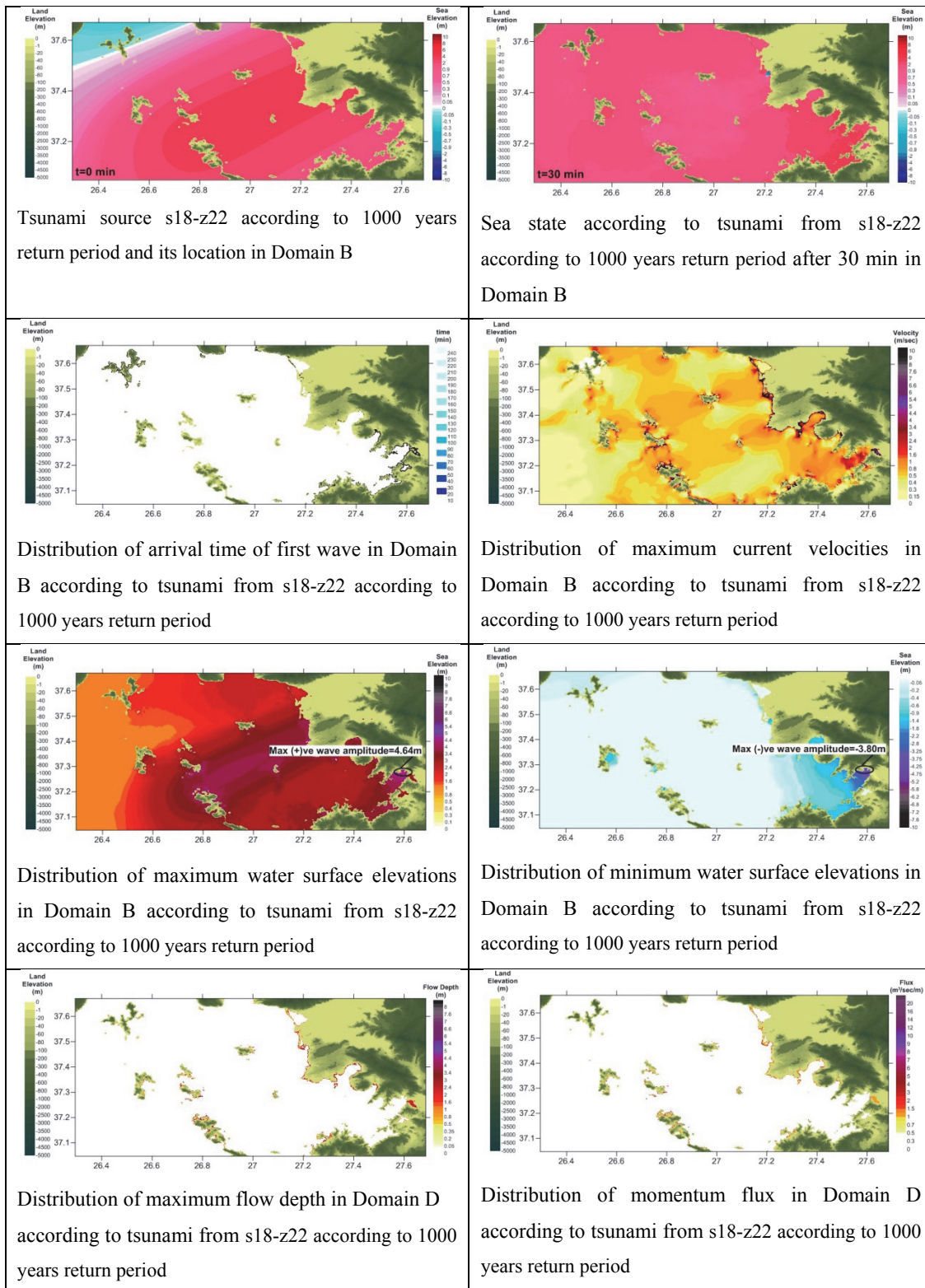


**Figure 4.34:** Tsunami parameters due to tsunami source s18-z22 according to 1000 years return period for simulation duration of 240 min

First wave arrives the coast shortly after tsunami source (s18-z22 according to 1000 years return period) is generated. Maximum positive wave amplitude is computed as 4.64m, and maximum negative wave amplitude is computed as -3.80m around Güllük region (see Figure 4.34).

**Wave characteristics of tsunami from deterministic seismic source (s18-z22) and probabilistic seismic sources (s18-z22) according to 100, 500 and 1000 years return periods for selected numerical gauge locations**

Tsunami scenarios for deterministic seismic source (s18-z22) and probabilistic seismic sources (s18-z22) according to 100, 500 and 1000 years return periods are simulated to analyze probable effects of those sources in Güllük bay. Water elevation, current velocity, momentum and discharge fluxes are given in between Figures 4.35 and 4.38 for selected numerical gauge points (see Figure 4.17).

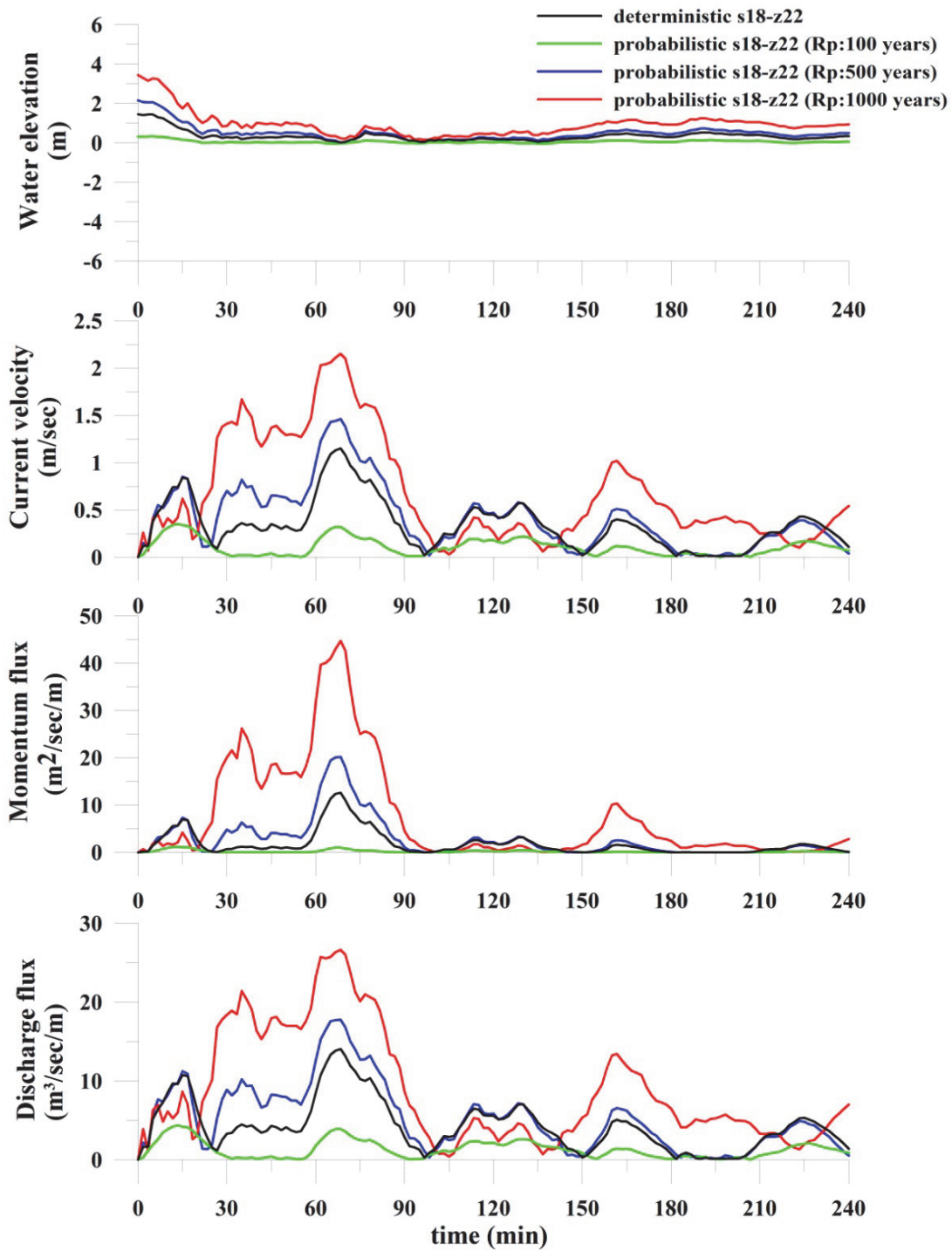


**Figure 4.35:** Wave characteristics for gauge point "Didim-Tekağaç"  
(water depth at the point is 13.0m)



The time histories of water level fluctuations and computed near shore tsunami parameters at numerical gauge point near Didim Tekağaç is given in Figure 4.34. Maximum wave amplitude is around 3.7m, current velocity is around 2.2 m/sec, momentum flux is around 46 m<sup>3</sup>/sec<sup>2</sup>/m, and discharge flux is around 27 m<sup>3</sup>/sec/m at a point of 13.0m deep located near Didim Tekağaç (see Figure 4.34). Computed near shore tsunami parameters according to selected tsunami scenarios for "Fish farms" numerical gauge point are summarized in Table 4.29.

**Table 4.29:** Computed near shore tsunami parameters for "Didim Tekağaç" (water depth at the point is 13.0m) numerical gauge point according to selected tsunami scenarios

Selected Tsunami Scenario	Arrival time of first wave (min)	Arrival time of max wave (min)	Max (+)ve amp. (m)	Max (-)ve amp. (m)	Max current velocity (m/sec)	Max momentum flux (m <sup>3</sup> /s <sup>2</sup> /m)	Max discharge flux (m <sup>3</sup> /s/m)
seismic s18-z22 (deterministic)	0	1	1.61	0.00	1.16	12.67	14.06
seismic s18-z22 (Rp 100 years)	0	6	0.35	-0.05	0.36	1.23	4.43
seismic s18-z22 (Rp 500 years)	0	1	2.36	0.00	1.46	20.19	17.79
seismic s18-z22 (Rp 1000 years)	0	1	3.70	0.00	2.18	45.69	27.02

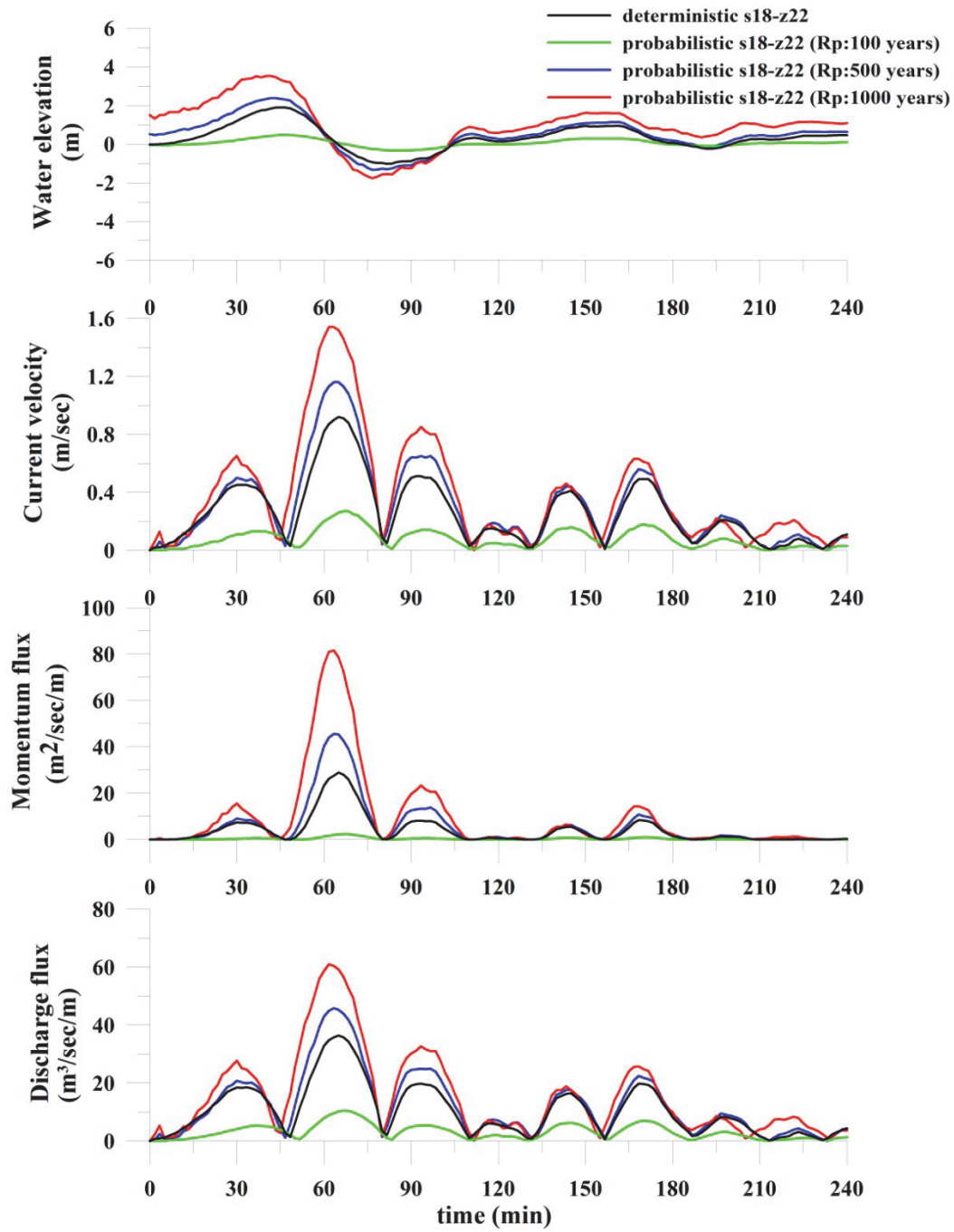


**Figure 4.36:** Wave characteristics for gauge point "Fish Farms"  
(water depth at the point is 39.6m)

The time histories of water level fluctuations and computed near shore tsunami parameters at numerical gauge point near fish farms is given in Figure 4.35. Maximum wave amplitude is around 3.6m, current velocity is around 1.6 m/sec, momentum flux is around 82 m<sup>3</sup>/sec<sup>2</sup>/m, and discharge flux is around 61 m<sup>3</sup>/sec/m at a point of 39.6m deep located near fish farms (see Figure 4.36). Computed near shore tsunami parameters according to selected tsunami scenarios for "Fish Farms" numerical gauge point are summarized in Table 4.30.

**Table 4.30:** Computed near shore tsunami parameters for "Fish Farms" (water depth at the point is 39.6m) numerical gauge point according to selected tsunami scenarios

Selected Tsunami Scenario	Arrival time of first wave (min)	Arrival time of max wave (min)	Max (+)ve amp. (m)	Max (-)ve amp. (m)	Max current velocity (m/sec)	Max momentum flux (m <sup>3</sup> /s <sup>2</sup> /m)	Max discharge flux (m <sup>3</sup> /s/m)
seismic s18-z22 (deterministic)	0	46	1.90	-1.03	0.92	28.98	36.47
seismic s18-z22 (Rp 100 years)	0	45	0.47	-0.33	0.27	2.41	10.56
seismic s18-z22 (Rp 500 years)	0	42	2.39	-1.36	1.17	46.71	46.03
seismic s18-z22 (Rp 1000 years)	0	43	3.57	-1.79	1.55	82.31	61.24

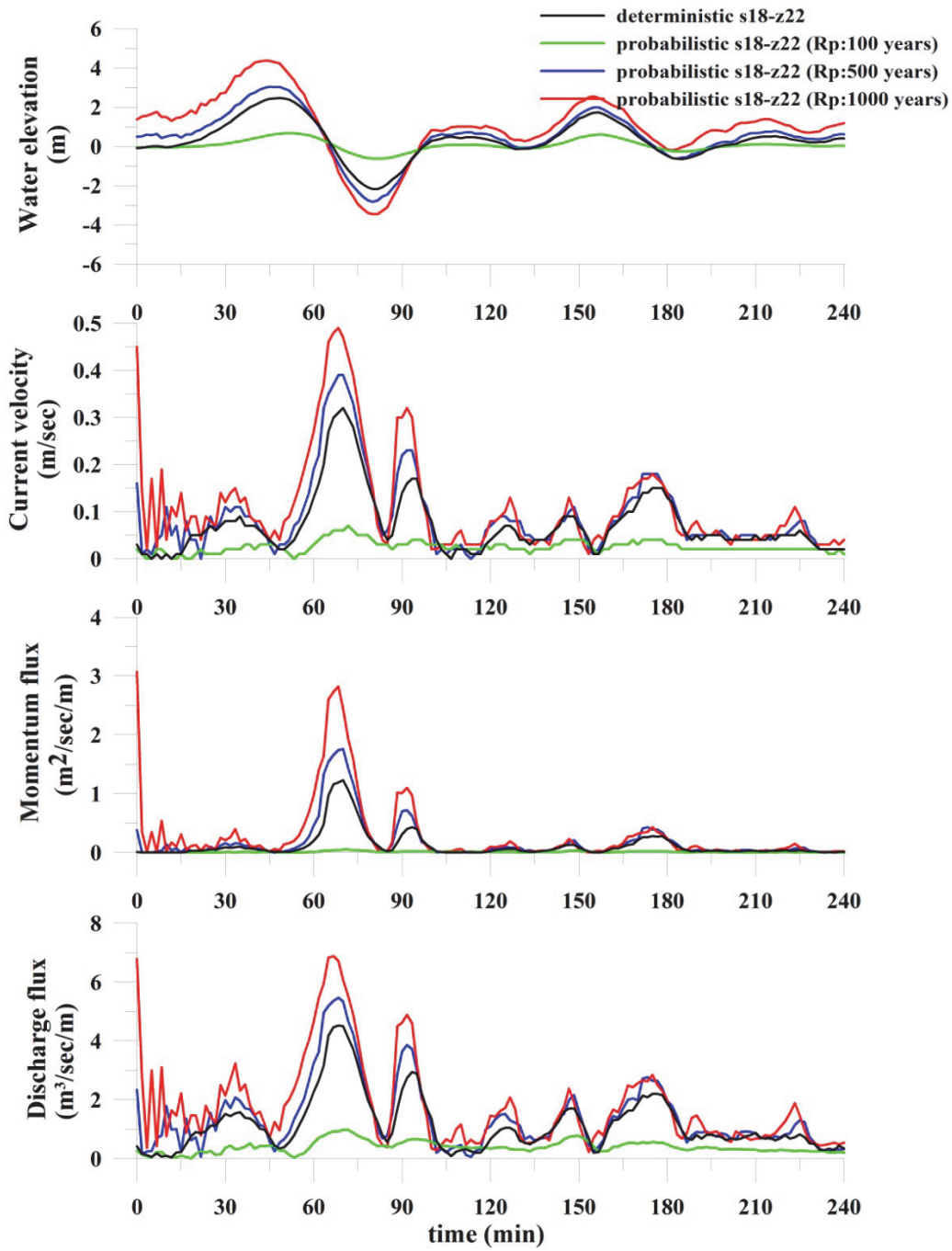


**Figure 4.37:** Wave characteristics for gauge point "Güllük"  
 (water depth at the point is 16.8m)

The time histories of water level fluctuations and computed near shore tsunami parameters at numerical gauge point near fish farms is given in Figure 4.36. Maximum wave amplitude is around 4.5m, current velocity is around 0.5 m/sec, momentum flux is around  $2.9 \text{ m}^3/\text{sec}^2/\text{m}$ , and discharge flux is around  $6.9 \text{ m}^3/\text{sec}/\text{m}$  at a point of 16.8m deep located near Güllük region (see Figure 4.37). Computed near shore tsunami parameters according to selected tsunami scenarios for "Güllük" numerical gauge point are summarized in Table 4.31.

**Table 4.31:** Computed near shore tsunami parameters for "Güllük"  
(water depth at the point is 16.8m) numerical gauge point according to selected  
tsunami scenarios

Selected Tsunami Scenario	Arrival time of first wave (min)	Arrival time of max wave (min)	Max (+)ve amp. (m)	Max (-)ve amp. (m)	Max current velocity (m/sec)	Max momentum flux ( $\text{m}^3/\text{s}^2/\text{m}$ )	Max discharge flux ( $\text{m}^3/\text{s}/\text{m}$ )
seismic s18-z22 (deterministic)	0	18	1.45	-0.24	0.13	0.34	2.89
seismic s18-z22 (Rp 100 years)	0	52	0.69	-0.64	0.07	0.05	1.03
seismic s18-z22 (Rp 500 years)	0	46	3.10	-2.85	0.40	1.91	5.77
seismic s18-z22 (Rp 1000 years)	0	44	4.51	-3.50	0.47	2.90	6.90

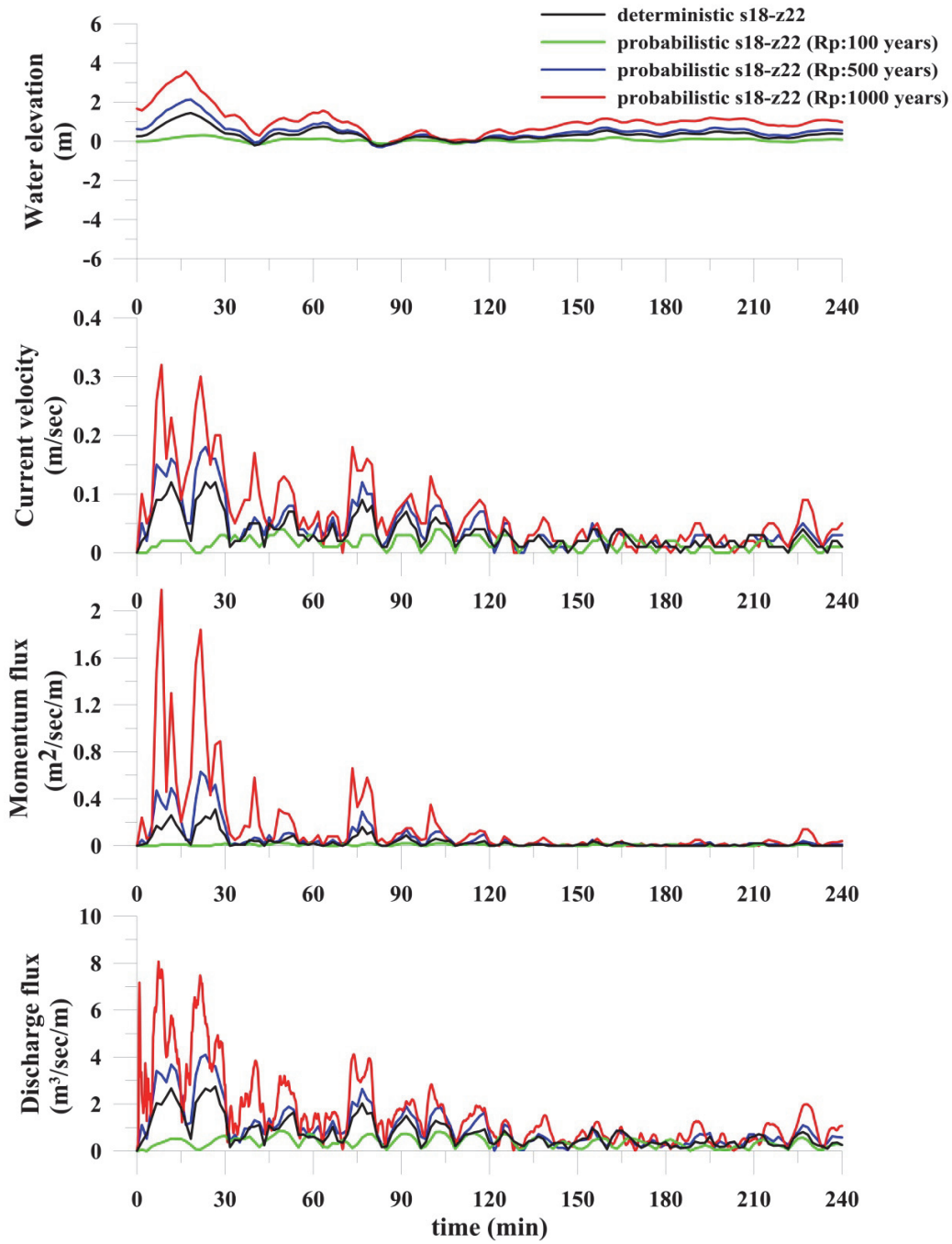


**Figure 4.38:** Wave characteristics for gauge point "Yalıkavak"  
(water depth at the point is 22.3m)

The time histories of water level fluctuations and computed near shore tsunami parameters at numerical gauge point near fish farms is given in Figure 4.38. Maximum wave amplitude is around 3.6m, current velocity is around 0.3 m/sec, momentum flux is around 2.3 m<sup>3</sup>/sec<sup>2</sup>/m, and discharge flux is around 8.1 m<sup>3</sup>/sec/m at a point of 22.3m deep located near Yalıkavak region (see Figure 4.38). Computed near shore tsunami parameters according to selected tsunami scenarios for "Yalıkavak" numerical gauge point are summarized in Table 4.32.

**Table 4.32:** Computed near shore tsunami parameters for "Yalıkavak" (water depth at the point is 22.3m) numerical gauge point according to selected tsunami scenarios

Selected Tsunami Scenario	Arrival time of first wave (min)	Arrival time of max wave (min)	Max (+)ve amp. (m)	Max (-)ve amp. (m)	Max current velocity (m/sec)	Max momentum flux (m <sup>3</sup> /s <sup>2</sup> /m)	Max discharge flux (m <sup>3</sup> /s/m)
seismic s18-z22 (deterministic)	0	18	1.45	-0.24	0.13	0.34	2.89
seismic s18-z22 (Rp 100 years)	0	22	0.32	-0.17	0.04	0.03	0.90
seismic s18-z22 (Rp 500 years)	0	18	2.16	-0.31	0.18	0.70	4.25
seismic s18-z22 (Rp 1000 years)	0	17	3.57	-0.23	0.33	2.30	8.12





## CHAPTER 5

### DISCUSSION OF RESULTS AND CONCLUSIONS

Deterministic and probabilistic tsunami hazard analysis are performed for Güllük bay. Accurate bathymetry/topography data and rupture parameters of tsunami source are the required inputs for convenient numerical modeling in order to perform tsunami hazard analysis.

Bathymetry/topography data are obtained from GEBCO<sup>®</sup> with 900m resolution in the sea, and from ASTER satellite data with 30m resolution at land. In order to improve the quality of the data in the shallow zone and data of shoreline the additional digitization using navigational charts are performed. Gridded data sets are developed from the available bathymetry/topography data and also digitized data for both nested and single domain simulations with different grid sizes.

In deterministic approach, probable worst case seismic tsunami sources (s18-z22) with their estimated rupture parameters and non-seismic tsunami sources (caldera motion of Santorini and Columbus volcanos) with their dimensional parameters are determined and simulated.

In probabilistic approach, the data based on seismic monitoring between 1950-2014 years is used and the earthquake magnitudes which may occur in 100, 500, 1000 years return periods are computed statistically by extreme value analysis. The rupture parameters are determined by the help of measured rupture parameters from past earthquakes in the region.

The tsunami numerical tool NAMI DANCE is used as the computational tool in numerical modeling. Simulations are performed for each selected tsunami scenario according to 240min simulation duration (for seismic cases) and 300min simulation duration (for non-seismic cases). Simulation durations are determined according to distance between tsunami source and the study region to properly compute and visualize generation, propagation and coastal amplification of tsunami. In deterministic approach, nested domain gridded data are used (Domain B with 270m grid size, Domain C with 90m grid size, Domain D with 30m grid size). Single domain gridded data are used (Domain B with 30m grid size) in probabilistic approach. Nested and single domain simulation results are very close to each other, though the results can be compared with confidently.

Some of the main critical regions under tsunami attack in the Güllük bay are selected as numerical gauge points. Among those "Didim Tekağaç" is selected as one of the numerical gauge location because of the findings of the traces of historical tsunamis (Santorini eruption approximately in 1600 BC) from the excavations (Papadopoulos et al., 2012) in the region. Another vulnerable locations in the region are "Fish Farms". Those are selected due to their vulnerability not only against storm waves but also long waves. Another numerical gauge point is selected at Gulluk village called "Güllük" where the–Milas Bodrum Airport is located on the low land area at the end of Gulluk Bay. The commercial port near Güllük village is another critical structure in Gulluk Bay. "Yalıkavak" is selected as another numerical gauge point to monitor the probable coastal amplifications around Yalıkavak marina, nearby touristic coastal utilities and residential areas. The time histories of water level fluctuations and computed near shore tsunami parameters for those numerical gauge points are obtained to provide data for the tsunami hazard analysis for Güllük bay.

The summary of determining parameters to feedback to main conclusions are given in Table 5.1 - 5.2 and discussed in the following.

**Table 5.1:** Summary table of tsunami hazard analysis with maximum positive wave amplitudes for numerical gauge points according to selected tsunami sources

Tsunami Scenarios		Didim Tekağaç	Fish Farms	Güllük	Yalıkavak
		<i>(max (+)ve wave amplitudes (m))</i>			
seismic sources	s18-z22 (deterministic)	1.61	1.45	1.45	1.90
	s18-z22 (Rp 100 years)	0.35	0.32	0.69	0.47
	s18-z22 (Rp 500 years)	2.36	2.16	3.10	2.39
	s18-z22 (Rp 1000 years)	3.70	3.57	4.51	3.57
non-seismic sources	caldera collapse of	0.42	0.44	0.76	0.45
	caldera collapse of	1.12	2.00	1.24	0.56
	caldera eruption of	2.19	3.17	2.31	1.07

**Table 5.2:** Summary table of tsunami hazard analysis with maximum current velocities for numerical gauge points according to selected tsunami sources

Tsunami Scenarios		Didim Tekağaç	Fish Farms	Güllük	Yalıkavak
		<i>(max (+)ve wave amplitudes (m))</i>			
seismic sources	s18-z22 (deterministic)	1.16	0.92	0.13	0.13
	s18-z22 (Rp 100 years)	0.36	0.27	0.07	0.04
	s18-z22 (Rp 500 years)	1.46	1.17	0.40	0.18
	s18-z22 (Rp 1000 years)	2.18	1.55	0.47	0.33
non-seismic sources	caldera collapse of	0.40	0.33	0.21	0.21
	caldera collapse of	2.26	0.54	1.03	1.03
	caldera eruption of	3.25	1.00	1.36	1.36

Among the scenarios in deterministic analysis, the tsunami due to caldera eruption of Columbus is found to cause higher tsunami parameters in Güllük bay comparing to other sources. Probable effects of this source should be considered as one of the important tsunami source for deterministic tsunami hazard analysis, however the activity of Columbus and Santorini volcanos are uncertain at this moment. Maximum wave amplitudes are computed as 2.19m for “Didim Tekağaç”, 3.17m for “Fish Farms”, 2.31m for “Güllük” and 1.07m for “Yalıkavak”. Higher water elevations will cause higher level of effects and resulting damages along Güllük coasts. In addition, maximum current velocities are computed as 3.25 m/sec for “Didim Tekağaç”, 1 m/sec for “Fish Farms”, 1.36 m/sec for “Güllük” and 1.36 m/sec for “Yalıkavak”. Current velocity near fish farms is 1 m/sec. This is a critical value that when current velocity exceeds 1 m/sec, it will cause damages on the supporting structures of fish farms (Otsuka et al., 2009).

Among the scenarios in probabilistic analysis, the tsunami due to seismic source (s18-z22) according to 1000 years return period is found to cause higher tsunami parameters in Güllük bay comparing to other sources. In addition to this source, probable effects of seismic source (s18-z22) according to 500 years return period should be considered as important tsunami sources for probabilistic tsunami hazard analysis. Maximum wave amplitudes are computed as 3.7m for “Didim Tekağaç”, 3.57m for “Fish Farms”, 4.51m for “Güllük” and 3.57m for “Yalıkavak”. In addition, maximum current velocities are computed as 2.18 m/sec for “Didim Tekağaç”, 1.55 m/sec for “Fish Farms”, 0.47 m/sec for “Güllük” and 0.33 m/sec for “Yalıkavak”. Current velocity near fish farms is greater than 1 m/sec (1.17 m/sec according to 500 years return period simulation, 1.55 m/sec according to 1000 years return period simulation).

Probabilistic analysis gives important and reliable results comparing to deterministic seismic source (s18-z22) results. Extreme value analysis gives earthquake magnitudes on the same plane with deterministic approach. Rupture parameters (dimensions of the fault, surface displacement) are estimated by the help of available and valid empirical equations (see Section 4.3.5.2). In the light of probabilistic analysis results, deterministic seismic source (s18-z22) has the probability to occur less than 500 years return period.

It does not seem that devastating tsunami effects and resulting damages may not be foreseeable in the near future in Güllük bay according to the resolution of the data used hazard analysis here. However, marinas, commercial port, aquaculture plants (fish farms), airport, nearby touristic coastal utilities and residential areas located in Güllük bay are still critical locations even a small size tsunami enters Güllük bay. These critical regions will be extended under the tsunami effect with 500 and 1000 years return periods. Inundation zones are formed along Güllük coasts especially in low elevated coastal areas (see Figure 4.31 and 4.33).

In this thesis, tsunami hazard analysis is performed according to bathymetry/topography data with 900m grid size in the sea and 30m grid size in the land from available satellite measurements. For further assessments and more detailed analysis, the bathymetric/topographic data should be in highest resolution based on field measurements. Therefore highest resolution inundation maps can also be produced.



## REFERENCES

Altinok, Y., (2009), "*Historical Tsunamis in Eastern Mediterranean*", Internal Report of Work Package 1 of TRANSFER Project.

Ambraseys, N.N., (1962), "*Catalogue of Tsunamis in the Eastern Mediterranean from Antiquity to Present Times*", *Annali di Geofisica*, Vol. 32, pp. 113-130.

Balas C. E., Ergin A., (2000), "*Rubble mound breakwaters under tsunami effect*", *Submarine Landslides and Tsunamis*, pp. 293-302, Kluwer Academic Publishers, printed in Netherlands.

Cita M.B., Rimoldi B., (1997), "*Geological and Geophysical Evidence for a Holocene Tsunami Deposit in the Eastern Mediterranean Deep-Sea Record*", *J. Geodynamics*, Vol.24. No:1-7 pp. 293-304.

Cornell, C.A., (1968), "*Engineering seismic risk analysis*", *Bull. Seismol. Soc. Am.*, 58, 1583-1606.

Çevre Hukuk, <http://www.cevrehukuk.com>, last accessed on December 2014.

Druitt, T.H.; Francaviglia, V., (1992), "*Caldera formation on Santorini and the physiography of the islands in the late Bronze Age*", *Bulletin of Volcanology*, 54, 484-493.

Flouri, E.T., Mitsoudis, D.A., Chrysoulakis, N., Kamarianakis, Y., Okal, E.A. and Synolakis, C.E., (2011), "*Tsunami hazard in the southeast Aegean Sea*", *Coastal Engineering* (60), pp. 136-148, February 2012.

Friedrich, W.L., Seidenkrantz, M. S., Nielsen, O.B., (2000) "*Santorini before the Minoan eruption: a reconstruction of the ring island based on geological and archaeological evidence*", In *The Archaeology of Geological Catastrophes*, The Geological Society.

Galanopoulos, A.G., (1960), "*Tsunamis Observed on the Coasts of Greece from Antiquity to Present Time*", *Annali di Geofisica*, Vol. 13, pp. 369-386.

Geist, E. L. and Parsons, T., (2006), "*Probabilistic analysis of tsunami hazards*", *Nat. Hazards*, 37, 277-314.

Geist, E. L., Parsons, T., ten Brink, U. S. and Lee, H. J., (2009), "*Tsunami probability*", in *The Sea*, Volume 15, edited by A. R. Robinson and E. N. Bernard, Harvard University Press, Boston, MA, 93-135.

Geist, E.L., Lynett, P.J., (2014), "*Source processes for the probabilistic assessment of tsunami hazards*", *Oceanography* 27(2), 86-93.

Geology, <http://geology.com/articles/caldera>, last accessed on December 2014.

Goda, Y., (2010), "*Random Seas and Design of Maritime Structures*", 3<sup>rd</sup> Edition, World Scientific Publishing, ISBN-13: 978-981-4282-40-6, 708 pp.

Gonzalez F.I., Geist E.L., Jaffe B., Kanoğlu U., Mofjeld H., Synolakis C.E., Titov V.V., Arcas D., Bellomo D., Carlton D., Horning T., Johnson J., Newman J., Parsons T., Peters R., Peterson C., Priest. G., Venturato A., Weber J., Wong F., Yalciner A.C., "*Probabilistic tsunami hazard assessment at Seaside, Oregon, for near- and far-field seismic sources*", *Journal of Geophysical Research*, vol.114, 2009.



Goto, C. and Ogawa, Y., (1991), *"Numerical Method of Tsunami Simulation With the Leap-Frog Scheme"*, Translated for the TIME Project by Prof. Shuto, N., Disaster Control Res. Cent., Faculty of Engg., Tohoku Univ. Sendai, Japan.

Guidoboni, E., Comastri, A., and Traina, G., (1994), *"Catalogue of Ancient Earthquakes in the Mediterranean Area up to the 10th Century"*, Istituto Nazionale di Geofisica, Rome.

Imamura F., (1989), *"Tsunami Numerical Simulation with the staggered leap-frog scheme (Numerical code of TUNAMI-N1)"*, School of Civil Engineering, Asian Inst. Tech. and Disaster Control Research Center, Tohoku University.

Imamura, F., Imteaz, M.A., (1995). *"Long waves in two layer, governing equations and numerical model"*, J. Sci. Tsunami Hazards 13, 3-24.

Imamura F., (2011), *"Tohoku University Source Model version 1.0 of Great East Japan Tsunami"*, due on June 06, 2011.

Kajiura, K., (1963), *"The leading wave of a tsunami"*, Bull. Res. Inst., University of Tokyo, 41, pp. 525- 571.

Kalafat, D., Kekovali, K., Gunes, Y., Yilmazer, M., Kara, M., Deniz, P. and Berberoglu, M., (2009), *"A catalogue of source parameters of moderate and strong earthquakes for Turkey and its surrounding area (1938-2008)"*, KOERI, January 2009.

KOERI, *"Earthquake Database of Bosphorus University, Kandilli Observatory and Earthquake Research Institute"*, 2014, <http://www.koeri.boun.edu.tr>, last accessed on December 2014.

Konstantinou, K. I., Papadopoulos, G.A. and Fokaefs, A. and K. Orphanogiannakib, (2005), *"Empirical relationships between aftershock area dimensions and magnitude for earthquakes in the Mediterranean Sea region"* Tectonophysics (403), pp.95-115.

Liu F., Yeh H., Synolakis C., (2008), *"Advanced Numerical Models for Simulating Tsunami Waves and Runup"*, World Scientific Publishing Co. Pte. Ltd., Singapore.

Løvholt, F., Glimsdal, S., Harbitz, C.B., Zamora, N., Nadim, F., Peduzzi, P., Dao, H. and Smebye H., (2012), *"Tsunami hazard and exposure on the global scale"*, Earth-Science Reviews, Vol 110, Issues 1–4, pp.58-73, January 2012.

METU-OERC, (2008b), *"Bathymetry and Topography Data Processing, Tsunami Modeling and Visualization for Western Coast of Greece"*, SEHELLARC Interim Report for the Second Annual Meeting in Pylos, June, 2008.

Nadim, F., Lovholt, F., Setiadi, N.J., Birkmann, J., Harbitz, C.B., Bach C., Fernando, N. and Kaiser, G. (2014), *"Tsunami risk reduction - are we better prepared today than in 2004?"*, International Journal of Disaster Risk Reduction, v. 10, part A, pp.: 127-142, December 2014.

NAMI DANCE (2011), *"Manual of Numerical Code NAMI DANCE"*, <http://namidance.ce.metu.edu.tr>, last accessed on December 2014.

Onat, Y, (2011), *"Database Development for Tsunami Warning System in Mediterranean Basin by Tsunami Modeling"*, M.Sc. Thesis, METU Department of Civil Engineering, Coastal and Ocean Engineering Division, Ankara Turkey, July 2011, 166 pages.

Otsuka K., Satoh K., Fujima K., (2010), *"The Behavior of Tsunami-Induced Driftage and Its Problem in Fishing Areas"*, PACON 2010.

Ozbay, I., (2000), *"Two Layer Model for Tsunami Generation"*, M.Sc. Thesis. Middle East Technical University, Civil Engineering Department, Ocean Engineering Research Center.

Ozer C., (2012), *"Tsunami Hydrodynamic in Inundation Zone"*, PhD Thesis, METU Department of Civil Engineering, Coastal and Ocean Engineering Division, March 2012, 177 pages (in press)

Papadopoulos G. A. and Chalkis, B. J., (1984), *"Tsunamis observed in Greece and the surrounding area from antiquity to the present times"*, Marine Geol. 56 (1984), pp.309–317.

Papadopoulos G. A., *"Seismic faulting and nonseismic tsunami generation in Greece"*, In: Proc. IUGG/IOC International Tsunami Symposium, 23–27 August, Wakayama Japan (1993), pp.115–123.

Papadopoulos G.A., *"Tsunamis in the East Mediterranean, A Catalogue for the Area of Greece and Adjacent Seas"*, in: Proc. Joint IOC-IUGG International Workshop Tsunami Risk Assessment Beyond 2000: Theory, Practice & Plans, Moscow, pp.34-43, (2000).

Papadopoulos G.A., (2003), *"Tsunami Hazard in the Eastern Mediterranean: Strong Earthquakes and Tsunamis in the Corinth Gulf, Central Greece"*, Natural Hazards (29), pp.437-464.

Papadopoulos G.A. and Fokaefs A., (2005), *"Strong Tsunamis in the Mediterranean Sea; A re-evaluation"*, ISET Journal of Earthquake Technology, Paper No. 463, Vol. 42, No. 4, pp. 159-170, (2005).

Papadopoulos G. A., Daskalaki E., Fokaefs A., and Giraleas N., *"Tsunami hazards in the Eastern Mediterranean: strong earthquakes and tsunamis in the East Hellenic Arc and Trench system"*, Nat. Hazards Earth Syst. Sci., 7, 57–64, (2007).

Papadopoulos G. A., Minoura K., Imamura F., Kuran U., Yalciner A. C., Fokaefs A., Takahashi T., (2012), "*Geological evidence of tsunamis and earthquakes at the Eastern Hellenic Arc: correlation with historical seismicity in the eastern Mediterranean Sea*", Research in Geophysics, vol.2 e:12,90-99.

Shaw B., Ambraseys N. N., England P. C., Floyd M. A., Gorman G. J., Higham T. F. G., Jackson J. A., Nocquet J.-M., Pain C. C., Piggott M. D., (2008), "*Eastern Mediterranean tectonics and tsunami hazard inferred from the AD 365 earthquake*", Nature Geoscience (1), pp.268 - 276, 2008.

SHTF Plan, <http://www.shtfplan.com/>, last accessed on December 2014.

Shuto, N., Goto, C., Imamura, F. (1990), "*Numerical simulation as a means of warning for near field tsunamis*", Coastal Engineering in Japan. 33, No:2 173-193.

Sørensen, M. B., Spada, M., Babeyko, A., Wiemer, S. and Grünthal, G. (2011), "*Probabilistic tsunami hazard in the Mediterranean Sea*" (Accepted for publication in Journal of Geophysical Research – Solid Earth).

Synolakis, C. E, Liu, P. L. F., Yeh, H., (1994), "*Workshop on Long Wave Runup Models*", Organized by NSF in Catalina Island LA, USA, June 1994.

Synolakis, C. E, Liu, P. L. F., Yeh, H., (2004), "*Workshop on Long Wave Runup Models*", Organized by NSF in Catalina Island LA, USA, June 2004.

Synolakis C.E., Bernard E.N., Titov V., Kânoğlu U., González F., Standards, Criteria, and Procedures For NOAA, 2007, "*Evaluation of Tsunami Numerical Models*", NOAA Technical Memorandum OAR PMEL-135, (2007).

Taymaz T., Yolsal, S., Yalciner, A. C., (2007), "*Understanding Tsunamis, Potential Source Regions and Tsunami- Prone Mechanisms in the Eastern Mediterranean, from the Geodynamics of the Aegean and Anatolia*", (Eds. Taymaz.

T, Yılmaz Y., Dilek Y.), Geological Society, London, Special Publications, 291, pp: 201-230, 2007.

Tinti S., Gavagni I., Piatanesi A., *"A finite-element numerical approach for modeling tsunamis"*, Annali di Geofisica, Vol XXXVII, N.5, 1994.

Titov V.V., Gonzalez F.I., Bernard E.N., Eble M.C., Mofjeld H.O., Newman J.C. and Venturato A.J., *"Real-time Tsunami Forecasting: Challenges and Solutions"*, Natural Hazards 35:41-58, 2005.

TRANSFER, (2009), Deliverables of EU Funded TRANSFER (Tsunami Risk And Strategies For European Region), <http://www.transferproject.eu>, last accessed on December 2014.

UNESCO/IOC Tsunami and Civil Protection Workshop: *"Tsunami hazard in the North-eastern Atlantic, the Mediterranean and connected seas (NEAM region) – A challenge for Science and Civil protection"*, 15-16 June, JRC-Ispra, Italy.

USGS , (2011), <http://www.usgs.gov>, last accessed on December 2014.

Wells & Coppersmith, (1994), *"New Empirical Relationships among Magnitude, Rupture Length, Rupture Width, Rupture Area, and Surface Displacement"*, Bulletin of the Seismological Society of America, Vol. 84, No. 4, pp. 974-1002, August 1994.

Wikipedia, <http://en.wikipedia.org>, last accessed on December 2014.

Yalciner, A.C., Kuran, U., Akyarlı, A. and Imamura, F., (1995), *"An Investigation on the Generation and Propagation of Tsunamis in the Aegean Sea by Mathematical Modeling"*, *"Tsunami: Progress in Prediction, Disaster Prevention and Warning"*, chapter in the book series of Advances in Nat. and Tech. Hazards Res. by Kluwer Academic Publishers, Ed. Yashuito Tsuchiya and Nobuo Shuto, pp 55-71.

Yalciner, A.C., Synolakis, C.E., Alpar, B., Borrero, J., Altinok, Y., Imamura, F., Tinti, S., Ersoy, S., Kuran, U., Pamukcu, S., Kanoglu, U., (2001), "*Field surveys and modeling of the 1999 Izmit Tsunami*", proceedings of the International Tsunami Symposium 2001, August 7-10 2001, Seattle, WA, pp. 557-564.

Yalciner, A.C., Alpar, B., Altinok, Y., Ozbay,I., Imamura, F., (2002a), "*Tsunamis in the Sea of Marmara: Historical Documents for the Past, Models for Future*", Marine Geology, 2002, 190, pp:445-463.

Yalciner, A.C., Pelinovsky, E.N., Talipova, T.G., Kurkin, A.A., Kozelkov, A.C., Zatsev, A.I., (2002b), "*Tsunamis in the Black Sea: comparison of the historical, instrumental and numerical data*", J. Geophys.Research, 2004, vol. 109, No. C12, C12023 10.1029/2003JC002113.

Yalciner, A.C., Imamura, F., Synolakis, E.C., (2002c), "*Simulation of Tsunami Related to Caldera Collapse and a Case Study of Thera Volcano in Aegean Sea*", Abstract Published and paper presented in EGS XXVII General Assembly, Nice, France, April 2002 Session NH8.

Yalciner, A.C., Pelinovsky, E., Synolakis C., Okal, E., (2003), "*NATO SCIENCE SERIES, Submarine Landslides and Tsunamis*", publisher: Kluwer Academic Publishers, Netherlands, (Editors; Yalciner, A.C., Pelinovsky, E., Synolakis, C., Okal, E.), 329 Pages, ISBN: 1-4020-1348-5 (HB), ISBN: 1-4020-1349-3 (PB).

Yalciner, A., Pelinovsky, E., Talipova, T., Kurkin, A., Kozelkov, A. and Zaitsev, A. (2004), "*Tsunamis in the Black Sea: Comparison of the Historical, Instrumental, and Numerical Data*", J. Geophys. Res., AGU, V 109, C12023, doi:10.1029/2003JC002113.

Yalciner, A.C., Pelinovsky, E. (2005), "*A Short Cut Numerical Method for Determination of Resonance Periods of Free Oscillations in Irregular Shaped Basins*", Submitted to Ocean Engineering Journal.

Yalciner, A.C., Karakus, H., Ozer, C., Ozyurt, G., (2005), "*Short Courses on Understanding the Generation, Propagation, Near and Far-Field Impacts of TSUNAMIS and Planning Strategies to Prepare for Future Events*" Course Notes prepared by METU Civil Eng. Dept. Ocean Eng. Res. Center Ankara, Turkey, for the Short Courses in the University of Technology Malaysia (UTM) held in Kuala Lumpur on July 11-12, 2005, and in Technology Development Division, Astronautic Technology (M) Sdn. Bhd (ATSB) Malaysia held in Kuala Lumpur on April 24-May 06, 2006, and in UNESCO Training Course I on Tsunami Numerical Modeling held in Kuala Lumpur on May 08-19 2006 and in Belgium Oostende on June 06-16, 2006 and in Pakistan Karachi December 2009.

Yalciner, A. C., Pelinovsky, E., Zaitsev, A., Kurkin, A., Ozer, C., and Karakus, H., (2007a), "*Modeling and visualization of tsunamis: Mediterranean examples, from, Tsunami and Nonlinear Waves*", (Ed: Anjan Kundu), Springer, 2007, 2731-2839.

Yalciner, A. C., Synolakis, C. E , Gonzales, M., Kanoglu, U., (2007b), "*Joint Workshop on Improvements of Tsunami Models, Inundation Map and Test Sites of EU TRANSFER Project*", June 11-14, Fethiye, Turkey.

Yalciner A. C., Dilmen I. D., Insel I. (2008), "*An Investigation on the Tsunami Risk Map of Turkey*", Report of the Project ODTÜ, 06-03-03-2-02-05, for Ministry of Transport Turkey.

Yalciner A. C., Suppasri A., Mas E., Kalligeris N., Necmioglu O., Imamura F., Ozer C., Zaytsev A., Ozel M. N., Synolakis C., (2011), "*Field Survey on the Coastal Impacts of March 11, 2011 Great East Japan Tsunami*", submitted to Journal of Pure and Applied Geophysics, (in review).

Yiğitbaşoğlu, H., (2003), "*Santorini volkanı ve minoan püskürmesinin Türkiye'deki izleri*", Coğrafi Bilimler Dergisi, 1 (1) 69-74.

Yolsal, S., Taymaz, T. and Yalciner, A.C., (2007), *"Understanding tsunamis, potential source regions and tsunami-prone mechanisms in the Eastern Mediterranean"*, Geological Society, London, Special Publications, v. 291, pp.201-230.

Youngs, R. R. and Coppersmith, K. J., (1985), *"Implications of fault slip rates and earthquake recurrence models to probabilistic seismic hazard estimates"*, Bull. Seism. Soc. Am., 75, 939-964.

Zaytsev, A., Karakus, H., Yalciner, A.C., Chernov, A., Pelinovsky, E., Kurkin, A., Ozer, C., Insel, I., Ozyurt, G., Dilmen, D.I., (2008), *"Tsunamis in Eastern Mediterranean, Histories, Possibilities and Realities"*, COPEDEC VII, DUBAI, UAE.



## APPENDIX A

### RUPTURE PARAMETERS OF HISTORICAL EARTHQUAKES IN PROJECT REGION

**Table A.1:** Rupture parameters of historical earthquakes in project region  
(Kalafat et al., 2009)

Date	Latitude (°)	Longitude (°)	depth (km)	Mw	Strike angle	Dip angle	Rake angle	Region
16.07.1955	37.65	27.26	40	6.5	292	55	-49	Söke-Balat-Western Turkey
09.07.1956	36.69	25.92	10	7	154	83	-29	Amargos-Southern Aegean Sea
18.07.1964	36.13	26.01	99	5.3	355	14	108	Dodecanese Islands-Aegean Sea
07.02.1968	36.65	26.74	153	5.3	238	24	101	Dodecanese Islands-Aegean Sea
06.04.1969	38.47	26.41	16	5.9	116	60	-90	Karaburun-Western Turkey
05.02.1974	36.74	26.86	156	5	337	52	96	Dodecanese Islands-Aegean Sea
17.08.1976	36.74	27.07	160	5.3	341	46	-179	İstanköy (Kos) Island-Aegean Sea
18.08.1977	35.27	24.08	45	5.7	318	81	-78	Greece
27.10.1977	37.87	27.88	16	5	176	56	-46	Aydın-Germencik-Western Turkey
28.11.1977	35.18	27.94	85	5.4	356	73	133	Mediterranean Sea
16.12.1977	38.41	27.19	24	5.6	127	59	-178	İzmir-Western Turkey
01.03.1978	35.97	27.15	94	5	323	19	65	Dodecanese Islands-Aegean Sea
28.11.1978	36.04	26.39	114	5.3	210	26	60	Dodecanese Islands-Aegean Sea
14.06.1979	37.58	26.4	15	5.8	253	59	-120	Dodecanese Islands-Aegean Sea
16.06.1979	38.46	26.77	15	5.4	255	58	-124	Dursunbey-Western Turkey
23.07.1979	35.29	26.75	15	5.6	186	68	-119	Mediterranean Sea
22.08.1979	35.75	27.89	94	5.3	273	75	-78	Mediterranean Sea
16.05.1980	35.89	27.35	57	5.3	259	53	-179	Dodecanese Islands-Aegean Sea
04.03.1981	37.93	23.25	10	6.3	39	55	-114	Greece
05.03.1981	37.77	23.01	15	5.5	58	54	-115	Greece
07.03.1981	37.62	23.34	15	5.4	262	50	-95	Greece
29.12.1981	38.38	25.06	15	5.4	235	81	152	Greece
27.09.1983	36.97	27.7	170	5.4	54	78	46	Milas-SW Turkey
28.02.1984	36.18	25.64	158	4.8	305	67	52	Dodecanese Islands-Aegean Sea
23.04.1984	37.83	26.87	27	4.9	228	36	34	Sisam (Samos)-Kuşadası-Aegean Sea
21.06.1984	35.74	23.8	34	6.2	298	85	-86	Greece
23.12.1985	36.81	26.62	25	5	242	37	110	Dodecanese Islands-Aegean Sea
21.02.1986	36.38	26.52	146	4.9	296	70	60	Dodecanese Islands-Aegean Sea
12.04.1987	35.4	23.27	15	5.1	342	90	0	Mediterranean Sea
30.12.1987	36.88	27.72	30	4.9	53	79	-116	Gulf of Gökova-SW Turkey
21.12.1988	35.35	27.43	42	5	51	88	-96	Mediterranean Sea
27.04.1989	36.71	27.75	15	5.5	276	54	-87	Datça-SW Turkey
28.04.1989	36.95	27.79	15	5.6	285	50	-80	Muğla-SW Turkey
01.11.1989	36.47	26.99	141	4.1	339	12	-166	Dodecanese Islands-Aegean Sea
22.04.1990	36.53	26.88	149	4.7	238	41	52	Dodecanese Islands
18.07.1991	36.08	27.19	106	4.8	309	19	77	Dodecanese Islands
20.03.1992	36.85	24.16	15	5.2	113	45	-90	Greece
30.04.1992	35.04	26.2	33	5.8	12	53	-78	Mediterranean Sea

**Table A.1 (continued)**

Date	Latitude (°)	Longitude (°)	depth (km)	Mw	Strike angle	Dip angle	Rake angle	Region
06.11.1992	37.84	26.98	25	6.1	238	85	-167	Kuşadası -Western Turkey
06.11.1992	38.16	27	17	5.8	42	75	8	İzmir-Aegean Sea
23.05.1994	35.02	24.89	81	6.1	76	70	151	Mediterranean Sea
02.04.1996	37.83	26.94	15	5.4	127	59	-62	Sisam (Samos) Island-Aegean Sea
12.04.1996	36.47	27.14	15	5.2	50	85	46	Dodecanese Islands-Aegean Sea
20.07.1996	36.07	26.92	15	6.2	30	53	-81	Mediterranean Sea
22.07.1996	36.11	26.91	15	5.1	29	55	-99	Mediterranean Sea
07.09.1999	37.87	23.64	15	6	284	52	-98	Greece
13.06.2000	35.16	26.74	15	5.4	47	80	-46	Mediterranean Sea
01.05.2001	35.33	27.17	33	5.2	12	66	-83	Mediterranean Sea
10.06.2001	38.32	25.66	34	5.6	244	79	-164	Aegean Sea
22.01.2002	35.53	26.59	90	6.2	271	89	-58	Mediterranean Sea
21.05.2002	36.34	24.41	100	5.9	350	89	9	Mediterranean Sea
06.06.2002	35.56	26.26	110	5.2	263	77	-112	Mediterranean Sea
10.04.2003	38.05	26.86	15	5.7	250	76	-160	Seferihisar-İzmir-Western Turkey
17.04.2003	37.92	26.75	15	5.2	256	78	-138	Sisam (Samos) Island-Aegean Sea
13.09.2003	35.93	27	160	5.3	360	84	129	Mediterranean Sea
07.02.2004	35.82	26.89	16	5.1	19	64	-95	Mediterranean Sea
25.05.2004	35.86	27.27	17	4.8	146	68	-122	Mediterranean Sea
03.08.2004	37.08	27.6	20	4.7	312.5	86.3	-15.5	Gökova-Muğla-SW Turkey
03.08.2004	36.77	27.93	12	5.2	263	52	-84	Gulf of Gökova-Mediterranean Sea
04.08.2004	36.8	27.88	12	5.6	262	50	-85	Gulf of Gökova-Mediterranean Sea
04.08.2004	36.82	27.97	12	5.2	278	52	-73	Gulf of Gökova-Mediterranean Sea
04.08.2004	36.81	27.91	12	5.3	260	49	-87	Gulf of Gökova-Mediterranean Sea
21.09.2004	35.13	27.71	27	4.9	42	90	11	Mediterranean Sea
26.09.2004	38.02	24.05	18	4.6	77	88	-143	Greece
07.10.2004	36.27	26.72	130	5.5	75	81	50	Mediterranean Sea
07.10.2004	36.56	26.9	78	5.7	82.3	81.9	140.5	Mediterranean Sea
10.01.2005	36.84	27.87	15	5.5	255	51	-114	Gulf of Gökova-SW Turkey
10.01.2005	37.01	27.8	14	5.5	293.3	84.5	-81.5	Gulf of Gökova-SW Turkey
11.01.2005	36.84	27.84	12	5.1	255	60	-103	Gulf of Gökova-SW Turkey
11.01.2005	37.02	27.75	4	4.5	289.9	74.4	-60	Gulf of Gökova-SW Turkey
29.01.2005	38.17	26.66	10	4.6	55.4	87.7	101.6	Seferihisar-İzmir_W. Turkey
23.06.2005	37.82	26.7	30	4.3	308	80	17	Dodecanese Islands, Aegean Sea
03.07.2005	35.21	27.05	21	4.8	166	69	-145	Mediterranean Sea
01.08.2005	36.29	26.74	15	4.8	36	90	63	Mediterranean Sea
11.10.2005	35.53	27.42	21	4.9	319	66	-148	Mediterranean Sea
17.10.2005	38.21	26.59	15	5.5	145	78	-30	Karaburun-İzmir-Western Turkey
17.10.2005	38.15	26.66	12	5.8	141	87	-14	Karaburun-İzmir-Western Turkey
17.10.2005	38.17	26.52	10	5.6	14	87	-175	Karaburun-İzmir-Western Turkey
17.10.2005	38.16	26.59	18	5.2	146	78	-50	Karaburun-İzmir-Western Turkey
17.10.2005	37.95	25.8	22	4.9	260.3	83.5	-153.9	Aegean Sea
19.10.2005	38.15	26.67	10	4.5	326.7	84.9	41	Seferihisar-İzmir-Western Turkey
20.10.2005	38.15	26.71	13	5.9	138	80	-17	Seferihisar-İzmir-Western Turkey
20.10.2005	38.16	26.58	6	5.7	264.6	81.1	60.9	Seferihisar-İzmir-Western Turkey
31.10.2005	38.13	26.57	10	4.7	326.1	81.7	18.4	Seferihisar-İzmir-Western Turkey
09.12.2005	35.29	27.24	26	4.8	328	74	-125	Mediterranean Sea
20.12.2005	38.17	26.58	7	5.6	47	82	150	Near of the coast of Western Turkey
08.01.2006	35.93	23.29	64	6.8	66	55	119	Mediterranean Sea
08.01.2006	36.2	23.09	6	6.8	169	79	44	Mediterranean Sea
22.02.2006	35.12	26.94	34	4.7	62	79	157	Crete, Greece
04.04.2006	36.98	27.75	8	3.8	191	77	-75	Dodecanese Islands, Aegean Sea
09.04.2006	35.34	27.29	26	5.3	356	58	-72	Dodecanese Islands, Aegean Sea
09.04.2006	35.04	27.18	34	5.2	219	55	-131	Dodecanese Islands, Aegean Sea
13.04.2006	38.2	26.49	8	4.2	332	60	138	Near of the coast of Western Turkey
19.04.2006	36.66	26.94	38	4.7	5	70	49	Dodecanese Islands, Aegean Sea
05.05.2006	38.46	23.36	8	4	135	54	-75	Greece

**Table A.1 (continued)**

Date	Latitude (°)	Longitude (°)	depth (km)	Mw	Strike angle	Dip angle	Rake angle	Region
12.06.2006	38.18	26.68	6	3.9	135	68	-138	Near of the coast of Western Turkey
13.07.2006	35.15	26.6	32	4.5	229	84	170	Crete, Greece
22.08.2006	35.17	27.11	12	5.1	267	89	99	Mediterranean Sea
22.08.2006	35.12	26.94	32	5	232	73	-84	Crete, Greece
24.10.2006	35.06	27.2	34	5	185	86	10	Dodecanese Islands, Aegean Sea
09.05.2007	35.03	27.27	26	3.8	12.8	84.4	149.4	Mediterranean Sea
21.05.2007	35.14	27.62	18	5	1	39	-146	Mediterranean Sea
31.08.2007	36.59	26.32	16	5.2	71	25	-83	Dodecanese Islands-Aegean Sea
31.08.2007	36.97	26.25	24	5.1	33.8	87.3	158.2	Dodecanese Islands-Aegean Sea
23.09.2007	35.24	26.92	18	5.4	234	41	-23	Mediterranean Sea
11.11.2007	38.3	26.47	10	4.2	221.4	85.8	-146.1	Urta-Western Turkey
31.12.2007	38.34	25.81	24	3.9	38.2	83	171.5	Khios Island-Aegean Sea
01.02.2008	36.55	27.2	22	4	187	84	-118	Dodecanese Islands-Aegean Sea
07.02.2008	35.41	27.36	24	3.9	41	77	164	Mediterranean Sea
01.03.2008	37.85	26.75	14	4.1	120	87	-23	Aegean Sea
05.03.2008	36.07	27.23	20	4.5	173	77	76	Mediterranean Sea
07.03.2008	37.3	23.83	50	4.6	308	74	-55	Greece
28.03.2008	35.01	25.38	39	5.5	64	63	115	Crete, Greece
11.04.2008	37.62	26.76	18	4.4	211	62	-100	Aegean Sea
03.05.2008	36.16	27.5	18	4.4	197	77	-138	Dodecanese Islands, Aegean Sea
18.06.2008	35.36	26.99	28	4.7	307	61	90	Mediterranean Sea
15.07.2008	35.7	27.68	35	6.4	356	47	-173	Dodecanese Islands, Aegean Sea
15.07.2008	35.95	27.86	46	6.3	355.4	86.7	-27.2	Rodhos Island-Aegean Sea
19.08.2008	35.57	27.69	18	4	42.9	82.5	-166.6	Mediterranean Sea
27.08.2008	36.27	27.7	26	4	2	79.7	162	Mediterranean Sea
11.10.2008	35.6	27.81	42	4.5	5.2	82.4	-45	Mediterranean Sea
09.11.2008	36.25	27.87	66	4.8	57.2	89.8	-30.9	Mediterranean Sea